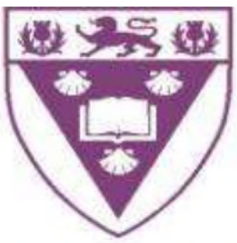

RHODES UNIVERSITY

Grahamstown • 6140 • South Africa

Characterization of the distribution of Platinum Group Elements in Sulphide Ores within the Merensky Reef at Modikwa and Two Rivers Platinum Mines, Eastern Bushveld Complex, South Africa

By

Nosibulelo Julie Zilibokwe

A thesis submitted in partial fulfillment of the requirements for the degree of

MASTER OF SCIENCE
(Economic Geology)

MSc Exploration Geology Programme
Geology Department
Rhodes University
P.O. Box 94
Grahamstown 6140
South Africa

April 2017

Acknowledgements

I would like to thank ***Almighty God*** for keeping me healthy and energetic from the start until the end of this journey.

This thesis is dedicated to my mother ***Dorothy Zilibokwe***, thank you mama-D for providing me with a sound education.

I would like to express my appreciation to my supervisor ***Dr Napoleon Q. Hammond***, now at the University of Limpopo, for your valuable professional guidance, advice and constructive suggestions during the planning and development of this dissertation. Thank you for believing in me Doc.

I remain indebted to my manager ***Dr Stewart Foya*** at the Council for Geoscience, thank you for permitting me to carry out my studies and for also taking time out of your busy schedule to attend to my queries. You provided great personal guidance, encouragement and support throughout this journey. My gratitude is boundless and I thank you for making this all possible.

Special gratitude to my co-supervisor ***Prof. R.E. "Jock" Harmer*** in the Geology Department at Rhodes University, for your advice, guidance and valuable support during the writing of this dissertation.

Furthermore, I wish to thank the staff of the Geology Department at Rhodes for warmly welcoming me whenever I had any questions or queries. I would especially like to thank ***Mrs Ashley Goddard*** for your unconditional support and excellent administrative performance. In addition, I would like to thank the many ***lecturers*** who took the time to teach our class about their geological specialities and the staff at the mines across South Africa we were exposed to.

Many thanks to the geological teams at Modikwa and Two Rivers Platinum Mines, in particular, ***Mr N. Machumele and Mr J. Khumalo*** for your assistance and warm welcome during the mine visits. This thesis would not have been possible without project data and drill-core samples supplied by Anglo Platinum and African Rainbow Minerals/Impala.

I would also like to sincerely thank ***Mr Abdul Kenan*** from the Council for Geoscience, the funniest advisor who is always ready to assist, I have learnt several things from you. Thank you for your assistance in the drawing of the grade profiles. Your tremendous support, timely help and advice have been extremely valuable to me and I am indebted to you.

NwaNdwandwe (Valerie Nxumalo) from the Council for Geoscience, words cannot convey my full appreciation for the interest, involvement, support and selfless help extended by you during this research, you have greatly motivated me as a mentor.

I cannot forget to thank my ***classmates*** who made this two-year journey unforgettable. It was fun to study with you guys.

I greatly acknowledge the ***Mining Qualification Authority*** (MQA), the ***Council for Geoscience*** in collaboration with the ***Department of Science and Technology*** (DST) for funding my studies.

I wish to extend my sincere thanks to the Council for Geoscience Laboratory staff, ***Mr N. Nxokwana (MK)*** and ***Mr L. Maema,*** without those thin sections this thesis would not have been possible.

Many thanks to ***Dr Gelu Costin*** for your critical input during the microprobe analyses. The use of the Jeol JXA 8230 Superprobe instrument, sponsored by ***NRF/NEP*** Grant 40113 (UID 74464) is kindly acknowledged.

I wish to humbly thank ***Mr T. Mothupi*** from Mintek for your warm welcome and advice on the Mineral Liberation Analyser (MLA) data presentation, together with ***Mr J. Chiliza*** for conducting the assay analyses.

I have no words to thank my ***entire family*** and ***relatives*** for your love, care, prayers and encouraging words that facilitated me achieving my goals.

To all my ***dearest friends, colleagues and well-wishers*** who I have not named above, you have been my pillar of strength and your best wishes greatly encouraged me during this research. Thank you all for the different roles you have played throughout this journey, (Yes You!).

Declaration

I, Nosibulelo Julie Zilibokwe, declare that this dissertation is my own work. It is being submitted for the Degree of Master of Science at Rhodes University, Grahamstown. It has not been submitted before for any degree or examination at any other University.

Signature of Candidate…Nosibulelo Julie Zilibokwe……

Date: ……th day of April 2017……

Place…Silverton……. Pretoria……...

Abstract

The distribution of the platinum group element (PGE), in the Merensky Reef was characterized by, first determining the occurrence of the platinum group minerals (PGM), then by establishing the PGE concentration in the base metal sulphides (BMS) associated with the PGE mineralization in the Merensky Reef from selected borehole intersections, at the Two Rivers (TRP) and Modikwa Platinum Mines in the Eastern Bushveld Complex. A mineral liberation analyser (MLA) was then used to identify the PGM phases; their silicate and base metal associations; and their grain size distribution. Electron microprobe quantitative analysis and mapping were then used to determine the compositional variation of the PGM and the PGE elemental distribution in the BMS, respectively. The study showed that the BMS including pyrrhotite, pentlandite, and chalcopyrite were the principal sulphides, where pyrrhotite was most prominent with minor quantities of pyrite. Orthopyroxene, clinopyroxene and plagioclase were the most abundant primary silicate minerals identified, while secondary silicates identified included talc, serpentine and amphibole. Platinum group minerals showed three distinct groups with respect to the mineralogical association with the PGE; (i) BMS association; (ii) chromite association; and (iii) silicate association. Of the BMS, chalcopyrite showed the most dominant association with the PGMs. All samples from both mines exhibited a wide range of PGMs, including maslovite, braggite, cooperate, laurite and PGE alloys such as ferroplatinum as well as other unidentified platinum and palladium sulphides, arsenides and bismuthides, while gold was present as electrum. The PGMs ranged in size from less than a micron to about 125 microns with an average of 20 microns. The close association of PGM with BMS along the margins of sulphides indicates that the PGMs were derived from the sulphide melt.

PGE distribution in the sulphides at Modikwa showed pentlandite contained the highest concentrations of palladium (up to 379 ppm) and chalcopyrite hosting the highest rhodium concentrations (up to 793 ppm). Samples from Two Rivers revealed pentlandite as the principal host to both palladium and rhodium, with concentrations reaching up to 695 and 930 ppm, respectively. Magnetite at both Modikwa and Two Rivers showed significant rhodium content, reaching up to 982 and 930 ppm, respectively.

The pyrrhotite compared to other sulphides contained all the elements found in the platinum group (PPGE), namely, platinum, palladium and rhodium, with all the platinum identified found in the pyrrhotite. The concentrations for the iridium group (IPGE) namely, iridium, osmium, and ruthenium were below the detection limit.

The PGE mineralization in the stratigraphy varied within each mine. The mineralization revealed top loading in the central sector (Modikwa) and bottom loading in the southern sector (Two Rivers). The sequence of the Merensky Reef at the two sectors of the Eastern Bushveld Complex showed a remarkable similarity in their mineralogy suggesting that these two sectors were formed from the same liquid or formed simultaneously within a single magma chamber; however the PGE distribution within the stratigraphy may have been controlled by the presence of cumulate sulphides.

Keywords: Platinum group elements (PGE), Platinum group minerals (PGM), Merensky Reef, Bushveld Complex, Modikwa, Two Rivers.

List of Abbreviations

Amp	Amphibole
ARM	African Rainbow Minerals
ASSMANG	Associated Manganese Mines of South Africa Limited
ATP	Annual Technical Report
BCU	Bastard Cyclic Unit
Bio	Biotite
BMS	Base Metal Sulphides
BSE	Back Scattered Electron
Ccp	Chalcopyrite
CGS	Council for Geoscience
Chl	Chlorite
Chr	Chromite
Cpx	Clinopyroxene
CZ	Critical Zone
EPMA	Electron Probe Micro Analyzer
IPGE	Iridium (Ir), Osmium (Os) and Ruthenium (Ru)
IRUP	Iron Rich Ultramafic Pegmatite
JV	Joint Venture
LZ	Lower Zone
MZ	Main Zone
MaZ	Marginal Zone
MCU	Merensky Cyclic Unit
MLA	Mineral Liberation Analyzer
MPM	Modikwa Platinum Mine
MPX	Merensky Pyroxenite
Ol	Olivine

Opx	Orthopyroxene
OV	Onverwacht
PFP	Pegmatoidal Feldspathic Pyroxenite
PGE	Platinum Group Elements
PGM	Platinum Group Minerals
Phl	Phlogopite
Pn	Pentlandite
PPGE	Platinum (Pt), palladium (Pd) and rhodium (Rh)
PPL	Plane Polarized Light
RLS	Rustenburg Layered Suite
SEM-EDS	Scanning Electron Microscopy-Energy Dispersive Spectrometry
Srp	Serpentine
TRP	Two Rivers Platinum
UZ	Upper Zone

Table of Contents

List of Figures

List of Tables

1. Introduction and Literature Review

1.1 Background

The Bushveld Complex in the Republic of South Africa is the largest known intrusion on Earth, containing the world's most important platinum group element (PGE) reserves (Rose *et al.* 2011; Cawthorn 1999; Hulbert and Von Gruenewaldt 1982; Misra 2000; Willemse *et al.* 1969; Vermaak 1995; Von Gruenewaldt 1977, 1979). There are three PGE mineralised horizons currently mined for their PGE content in the Rustenburg Layered Suite of the Bushveld Complex specifically, the Upper Group-2 chromitite layer (UG-2), the Merensky Reef and the Platreef. The UG-2 and Merensky Reefs of the Critical Zone are in the Eastern and Western limbs of the Bushveld, while the Platreef is found in the Northern limb. Presently, there is no consensus as to whether the Platreef is of Critical or Main Zone affinity (McDonald *et al.* 2005). Each of these horizons has a distinctive associated ore mineralogy requiring differing approaches for metallurgical processing. For instance, the UG-2 ore has a high proportion of chromite and is low in nickel and copper sulphides relative to the Merensky Reef. The Platreef however, has a greater proportion of PGE sulphides than both the Merensky Reef and UG-2. In the Platreef, the platinum group mineralogy (PGM) differs and is more complex, as documented by Hutchinson and Kinnaird (2005), who identified secondary silicates along the margins of sulphides which rarely occurred within or enclosed in sulphides.

This study is based on the Modikwa and Two Rivers Platinum mines located in the Eastern limb of the Bushveld Complex. Both mines presently extract PGE from the UG-2 chromitite layer. Thus, the focus of the present study is on the Merensky Reef which is currently not being mined due to absence of an advanced geometallurgical model of the Merensky Reef. Studies of the Merensky Reef have concentrated primarily on the Western limb of the intrusion, where mining operations yield exposures over tens of kilometres along the strike (Crocket *et al.* 1976; Vermaak 1976; Kinloch and Peyerl 1990; Wilson *et al.* 1999; Barnes and Maier 2002; Wilson and Chunnett 2006). Several studies inclusive of Vermaak and Hendricks (1976), Mostert *et al.* (1982), Kinloch and Peyer (1990) and Schouwstra *et al.* (2000), have characterized the PGE mineralogy in the Merensky Reef. These studies have also rendered it possible to make quantitative comparisons of the PGE and PGM contents in the studied deposits, thus providing vital information to maximise beneficiation and extraction.

The PGM sector provides a unique resource comparative advantage for South Africa, in the global minerals market. However, presently, very little (<12%) of South Africa's primary PGM output is beneficiated annually to the final stage of the value chain, locally. Comprehensive mineralogical studies on PGM have provided a significant understanding of the distribution of the PGE in the sulphide ores and the geochemistry of their mineralization (Vermaak and Hendriks 1976; Cabri and Laflamme 1981). However continuous problems still arise regarding the importance of sulphide minerals in dissolving PGEs and the exact siting of these elements, due to difficulties associated with the direct determination of PGEs in sulphide minerals and the quantitative estimation of PGM. It is also not clear whether PGEs that occur primarily as PGM in the sulphide ores, are structurally bound or are nanoparticles in the major sulphides of nickel-copper-PGE deposits.

1.2 Purpose of the Study

South Africa faces increased competition in terms of attracting foreign direct investment to the minerals sector due to ore bodies becoming more complex in mineralogy and occurring deeper. These factors render the resulting ore more difficult to access and to process. The aim of this study is to characterize the PGE distribution in sulphide ores within the Merensky Reef at Modikwa and Two Rivers Platinum Mines of the Eastern Bushveld Complex in South Africa, to:

- Improve the knowledge of the genetic processes that formed the mineralization of the Merensky Reef and to understand the link between PGE distribution and sulphide mineralization;
- Provide information that can be used to predict and explain the behaviour of the ore mineralogy in the Merensky Reef to assist in modifying current mineral processing methods and plant design for improved recovery.

For this study, four drill cores from the Critical Zone of the Rustenburg Layered Suite (RLS) were logged and sampled. These four drill cores show the mineralised portion of the Merensky Reef in the Eastern Bushveld Complex. Two of these four drill cores were obtained from the central sector of the Eastern Bushveld Complex at Modikwa Platinum Mine (OV 777, OV 778) and the other two drill cores originated from the southern sector of the Eastern Bushveld Complex at Two Rivers Platinum Mine (TRP 260, TRP 271).

1.3 Overview of the Bushveld Complex

The Bushveld Complex was emplaced at approximately 2.05 Ga in an essentially intraplate setting and currently covers an area of ca. 65.000 km^2, with a thickness of 5-10 km (Walraven *et al.* 1990; Eales and Cawthorn 1996; Cawthorn *et al.* 2006b). The Complex is exposed in five locations referred to as limbs (Figure 1.1). These are known as the Western, Eastern, Far western southern and Potgietersrus and/or Northern limbs. There are four groups of rocks that are found here: (1) the Rusternburg Layered Suite (RLS) which is the largest mafic layered complex (2) the Lebowa Granite Suite (3) the Rashoop Granophyre Suite which overlays the RLS and (4) the siliceous rocks of the Rooiberg Group (SACS 1980; Hatton and Schweitzer 1995).

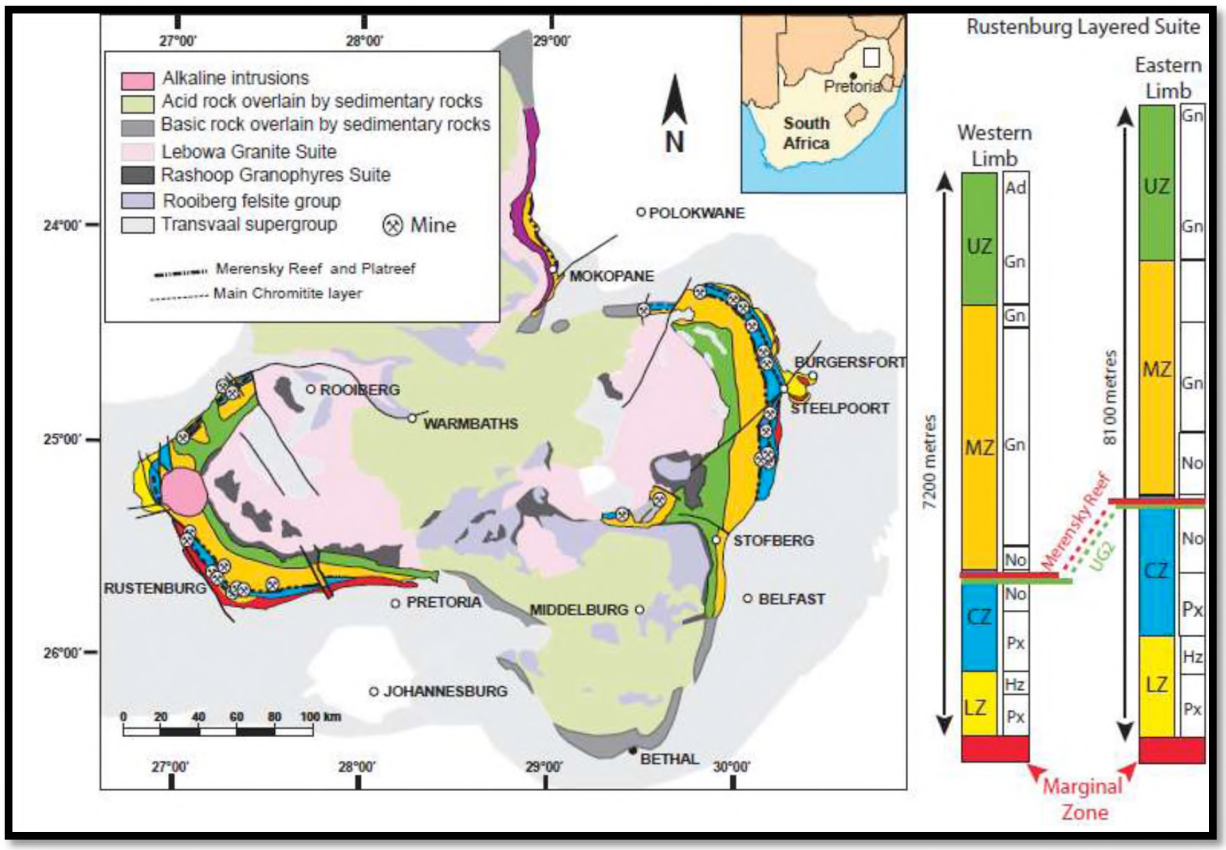

Figure 1.1: Simplified geological map of the Bushveld Complex (South Africa) and stratigraphy of the Rustenburg Layered Suite (Barnes 2015). Geological map is adapted from Von Gruenewaldt (1979) and stratigraphy for the Eastern and Western limbs is modified in accordance with Cawthorn *et al.* (2005). LZ Lower Zone; CZ Critical Zone; MZ Main Zone; UZ Upper Zone; Px pyroxenite; Hz harzburgite; No Norite; Gn gabbronorite; AD Apatite Diorite.

The Western limb extends from near Thabazimbi to the north of Pretoria. The Eastern limb outcrops from Stoffberg to Chuniespoort and is 200 km long (Eales and Cawthorn 1996).

The eroded Far western limb, which is known to be less prominent when compared to the other limbs, extends to the border of Botswana. The Northern limb is partially hidden beneath younger rocks (Eales and Cawthorn 1996) and consists of a slightly different succession.

The South eastern or Bethal limb is only identified based on a high gravity, and is known only from bore core information (Eales and Cawthorn 1996).

1.4 The Rustenburg Layered Suite (RLS)

The *RLS* is segregated into five main zones, specifically, the Marginal Zone (MZ), the Main Zone (MZ), the Critical Zone (CZ), the Upper Zone (UZ) and the Lower Zone (LZ) (Kruger 1990), dated at 2054.4 ± 2.8 Ma, uranium/lead zircon age (Harmer and Armstrong 2000).

The *Upper Zone* is well layered with a thickness of about 2000 to 2800 m of cyclic units of 24 magnetite layers, gabbronorites, anorthosites and diorites (Barnes and Maier 2002).

The *Main Zone* is a thick sequence of norite and gabbronorite, with minor anorthosite and pyroxenite layers, even though there is a lack of olivine and chromitite (Cawthorn *et al.* 2006b). The Main Zone is > 3000 m thick and does not show such spectacular layering as the Critical Zone, however modally layered rock packages can be identified (Molyneux 1974, Mitchell 1990, Nex *et al.* 1998 and 2002).

The *Critical Zone* is divided into a Lower and an Upper Critical Zone, containing vast deposits of chromite. The Upper Critical Zone at the base is defined by the appearance of cumulus plagioclase, except in the Eastern and more so in the Western limb (Teigler *et al.* 1992). The UG-1 and UG-2 occur directly above the Critical Zone (the UG-3 is restricted to the Eastern limb of the Complex) underlain by the top two cyclic units which are the Merensky Reef and the Bastard Reef (Cawthorn *et al.* 2002b). The Lower Critical Zone comprises of up to seven chromitite layers known as the Lower Groups (LG1-LG7) and the Middle Groups contain four chromitite layers (MG1-MG4) located at the top of the Lower Critical Zone and at the base of the Upper Critical Zone. The Merensky Reef dips to the centre of the Complex at an angle of 9-27° (Du Plessis and Kleywecht 1987; Von Gruenewaldt *et al.* 1990). The PGE grade of the Merensky Reef is remarkably uniform and ranges from 5.6-9.2 g/t 4E in the Western limb to 4.9-5.9 g/t 4E in the Eastern limb (Cawthorn *et al.* 2002a) and the relative proportions of the different PGEs are virtually constant. The highest PGE grades tend to be found within the two thin chromitite layers of the Merensky Reef, with lower grades in between them (Cawthorn 1999).

Grades in the Eastern limb are significantly lower than in the Western limb, at 2-3 g/t platinum, which is the reason the Merensky Reef, in the east, was considered uneconomical for 20 years (Naldrett *et al.* 2015).

The *UG-3* occurs 10 m above the UG-2 chromitite seam. UG-3 unit, which occurs about 365 m below the Merensky Reef, includes several thin chromitite layers and thin harzburgite layers (Eales and Cawthorn 1996). It forms part of the strata and therefore strikes and dips the same way as the UG-2 reef. The UG-3 seam has an average thickness of 22 cm. This chromitite seam only appears in the Eastern limb of the Bushveld Complex (Eales and Cawthorn 1996).

The *UG-2* is considered as the largest PGE resource on Earth (Vermaak 1985; 1995). UG-2 represents only one lithological unit and dips to the centre of the Complex at an angle of between 10-26 ° (Cawthorn *et al.* 2002b). The UG-2 has a PGE grade between 4.8-6.5 g/t and 4.5-8.0 g/t PGE on average in the Western and Eastern Bushveld, respectively (Cawthorn *et al.* 2002a). The UG-2 chromitite ranges from 60-120 cm. Grades that are usually quoted by mining companies for platinum, palladium, rhodium and gold, 4E average 5 g/t, with some suggestion that the thinner the layer the higher the grade (Cawthorn 2015). The distribution of the grade within the layer is not uniform. Mining widths at the Atok, Marula and Modikwa mines are thinner than the mines in the south, namely Two Rivers (Cawthorn 2015). The Platreef is in the Northern limb of the Bushveld Complex and comprises of feldspathic pyroxenite with PGE and BMS mineralization (Van der Merwe 1976). The Platreef is associated with the Critical Zone (Wagner 1929; White 1994) however; Van der Merwe (1978) regarded the Platreef as the base of the Main Zone. It hosts significant PGE content but differs from the UG-2 and Merensky Reef concerning the PGE grade and the platinum/palladium ratio.

The *Platreef* typically contains 1-2 g/t over many meters while the platinum/palladium ratio is approximately 1:1 (Kinnaird *et al.* 2005). In some cases, as at the open pit operations of Sandsloot, higher grades occur at the base, whereas to the north (Overysel), mineralization may occur higher in the layer (White 1994). Copper and nickel, which are higher than in the Merensky Reef positively correlate with sulphur, but the PGEs do not (White 1994).

The *Lower Zone* is divided into the lower pyroxenite, harzburgite and upper pyroxenite subzones, all with less than 1 % chromite (Cawthorn *et al.* 2006b). The thickness of the Lower Zone reaches 1300 m (Cawthorn *et al.* 2002b).

The *Marginal Zone* comprises medium-grained unlayered rocks, which are primarily norite with variable amounts of accessory clinopyroxene, quartz, biotite and hornblende (Cawthorn *et al.* 2006b). Quartz and biotite reveal the assimilation of shale (Cawthorn *et al.* 2002b). The rocks of the Marginal Zone may reach up to 800 m in thickness and may represent multiple magmatic intrusions of magma (Cawthorn *et al.* 2006b).

In all these deposits, PGM is extremely diverse and complicated (Cawthorn *et al.* 2002a). Such information is crucial for the efficient extraction of the ore minerals.

The *Lebowa Granite Suite* consists of different types of granites. It comprises a series of sheeted intrusions between 1.5-3.5 km in thickness (De Beer *et al.* 1987; Molyneux and Klinkert 1987; Klemann and Twist 1989). These granites underlay the mainly felsic volcanics of the Rooiberg Group and generally consist of alkali feldspar granites with iron-rich ferromagnesian minerals.

The *Rooiberg Group* occurs mainly above the Rustenburg Layered Suite (RLS) and can be divided into several formations. The bulk of the succession comprises siliceous volcanic rocks with sandstone and shale intercalations. The Rooiberg Group has been dated at 2057.3 ± 3.8 Ma, uranium/lead zircon age; (Harmer and Armstrong 2000).

The *Rashoop Granophyre Suite* represents the acid phase of the Bushveld Complex (Cawthorn *et al.* 2006b). The rocks of the Bushveld Complex intrude the sedimentary strata of the Transvaal Supergroup and at present are buried under a younger sedimentary cover, which is partly removed by erosion (Cheney and Twist 1991).

The *RLS of the Eastern limb* is an arcuate body that is exposed on the surface for 220 km (Van der Merwe 2007). It is well exposed in the area between Stoffberg and Burgersfort (Sharpe and Hulbert 1985). The geological structures that occur in the Eastern limb subdivide the RLS into three sectors namely, (1) the Western sector (2) Central sector and (3) the Southern sector. These geological features include associations of domes and faults, which commonly occur in the floor rocks of the intrusion. In the south, the Steelpoort pericline along with the associated Steelpoort fault separates the Southern sector from the Central sector. In the north, the Katkloof anticline and the up-faulted Fortdraai fold structure, together with the associated Wonderkop fault system, separate the Central from the Western sector (Von Gruenewaldt *et al.* 1990; Rose *et al.* 2011).

Mining operations along with detailed mapping, especially, of the Critical Zone have shown that there are changes in the lateral facies within a few km, which take place across the Steelpoort fault (Von Gruenewaldt *et al.* 1990).

The Rustenburg Layered Suite in the Western Bushveld is like the formerly described RLS in the Eastern limb, as it is also divided into sectors. The Western limb consists of a North-western sector or segment and a South-western sector that are separated by the Pilanesberg Alkaline Intrusion (Naldrett *et al.* 2008).

1.4.1 *The Merensky Reef in the Rustenburg Layered Suite*

The Merensky Reef which was discovered in 1924 by Dr Hans Merensky is one of the PGE-rich layers of the Bushveld Complex and, after the UG-2 chromitite, the second largest PGE reserves in the world (Cawthorn, 1999). Although the Merensky Reef is generally regarded as a uniform reef type, large variations occur in reef thickness, reef composition and in the position of mineralization (Schouwstra *et al.* 2000). Variations in reef thickness, composition and mineralization are described by the term "Merensky Reef facies". The Merensky Cyclic Unit (MCU) occurs in the upper layer of the Upper Critical Zone which is in turn overlain by the Bastard Cyclic Unit (BCU). Naldrett *et al.* (2009) regarded the BCU to be similar in several ways to the Merensky Cyclic Unit, but both units have less abundant sulphides and lower PGE tenors at their base (based on the work done in the Western limb). The BCU is in turn overlain with the Giant Mottled Anorthosite (GMA) of the lower subzone of the Main Zone, in the same way as the Eastern limb. The reef thickness varies from as thin as 4 cm to as thick as 4 m (Lee, 1996). Seismic surveys conducted by du Plessis and Kleywegt (1987) show that, reflectors that correlate the position of the Merensky Reef can be traced continuously up to 50 km down from the outcrop and up to 6 km deep below the surface (Lee 1996).

1.4.2 *Stratigraphy of the Merensky Reef*

Generally, the Merensky Reef has a sheet-like geometry (Schwellnus *et al.* 1976) that is para-conformable to the underlying or footwall cumulates (Lee 1996). The Merensky Reef package is composed of a pegmatoidal feldspathic pyroxenite, which, in places is replaced by a pegmatoidal feldspathic harzburgite at the base. One or two (occasionally more) chromitite stringers, reaching up to 2 cm in thickness distinguish the upper and lower bounds of the reef. The hanging wall of the reef comprises of feldspathic pyroxenite or norite, as presented in Figure 1.2 below. The reef is usually 1.5-3.5 m thick (Osbahr *et al.* 2013).

Mitchell and Scoon (2007) reported the stratigraphic succession for the interval between the base of the Merensky Reef and the top of the UG-2 to be 410 m, of which 80 % is composed of anorthosite, leuconorite and gabbronorite.

The Merensky Reef in the Eastern Bushveld has recently been documented by Wilson *et al.* (2005) and Mitchell and Scoon (2007) who show that it differs markedly from the Western Bushveld, and has defined a new facies type called "wide reef facies" for this area.

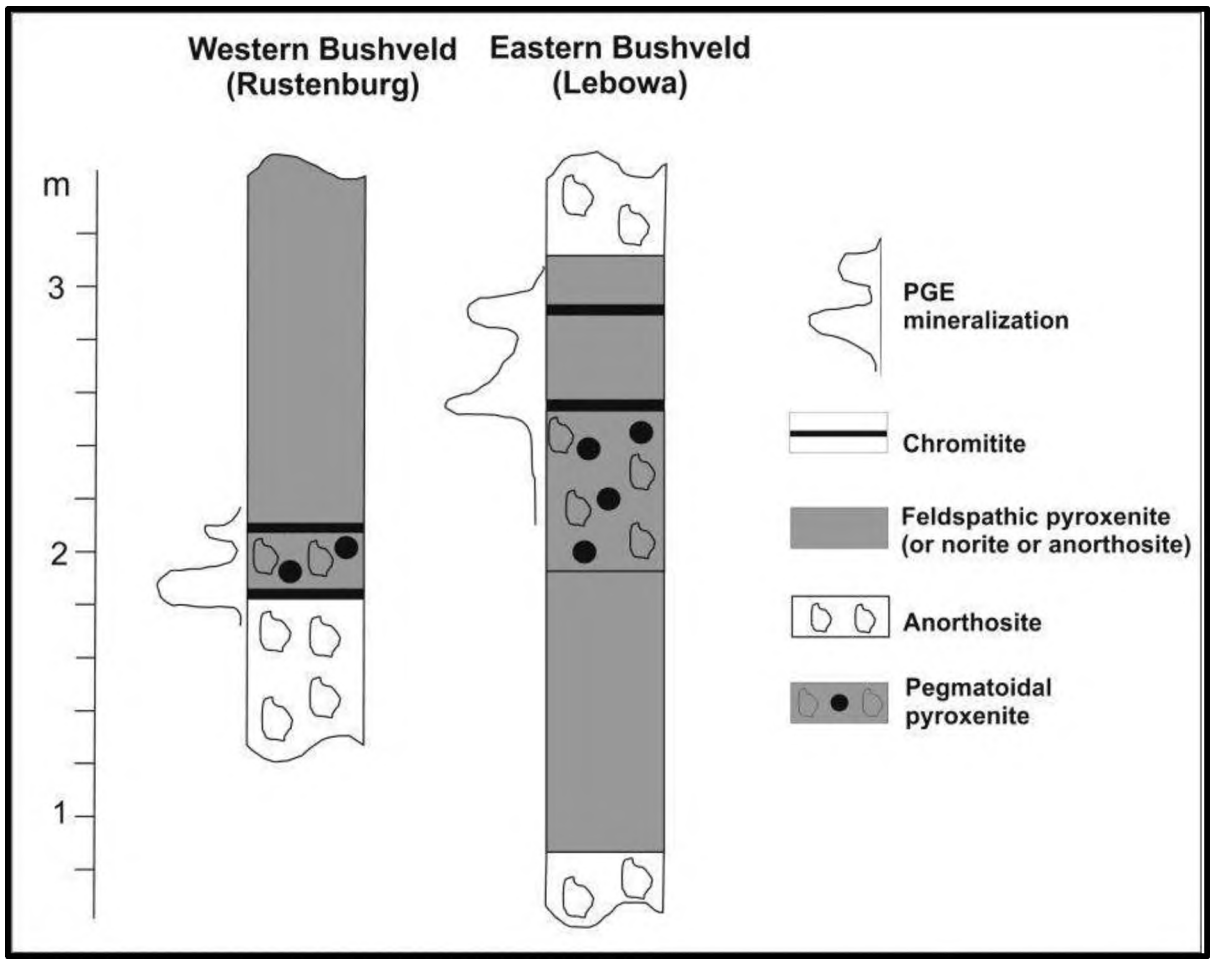

Figure 1.2: Schematic showing the distribution of rock units and mineralization in the Merensky Reef of the Western Bushveld (Rusternburg location) after Vermaak (1976), and in the Eastern Bushveld (Lebowa mine) after Schwellnus *et al.* (1976), modified after Naldrett (1989).

1.5 Platinum group Elements (PGE)

The PGE include six metals; platinum, palladium, rhodium, osmium, iridium, and ruthenium. They can be divided into light PGE, including ruthenium, rhodium and palladium and heavy PGE, including osmium, iridium and platinum. The light elements have only half of the density of the heavy PGE (Buchanan 1988).

The PGE based on their coherent behaviour during magmatic processes, can further be divided into the Platinum Group (PPGE) consisting of palladium, platinum and rhodium and the Iridium Group (IPGE), consisting of osmium, iridium, and ruthenium (Mungall 2005; Barnes *et al.* 1985).

The elements of the two subgroups (i.e. PPGE and IPGE) have different melting points, ranging between 1552 and 1966 °C for the PPGE Group and between 2310 and 3045 °C for the IPGE Group (Osbahr *et al.* 2013). The PGE prefer to form metallic bonds with iron, copper and nickel. In addition, they share a tendency with copper and silver to favour the formation of covalent bonds with sulphur. This behaviour gives the PGE a siderophile and chalcophile character, respectively (Mungall 2005). Besides the high melting points, PGE are known for their chemical inertness and for their ability to catalyse chemical reactions (Brenan 2008), thus, PGEs are in high industrial demand in the automotive industry.

1.6 Introduction to Magmatic Sulphide Ore Deposits

Certain aspects must be considered in view of the genesis of PGE bearing magmatic sulphide deposits; for example, how sulphide saturation is achieved in the host magma leading to the formation and separation of an immiscible sulphide liquid in which the chalcophile elements partition as documented by Naldrett (2010). The work of Naldrett (1989a) and (2004) documented four critical processes in the formation of magmatic nickel-copper (PGE) sulphide deposits; firstly, the partial melting of the mantle results into a metal bearing, mafic-ultramafic parental magma. It then separates from the solid residue, rises through the asthenospheric and lithospheric mantle, intruding into the crust and erupting on the surface. Secondly, as magma interacts with the wall rocks it loses heat, forming contaminated/hybrid magma, which incorporates crustal sulphur and resulting in the segregation of an immiscible sulphide liquid. Thirdly, the sulphide melt interacts with silicate magma, increasing the tenors of ore metals, extremely for chalcophile elements and lastly, the metal rich sulphide liquid accumulates in sufficient quantities to form an economic deposit.

Deposits were further divided into two major groups; (1) those that primarily are recognised for their nickel and copper and are mostly sulphide rich > 10 % and (2) those that are valued primarily for their PGE and tend to be sulphide poor (< 5 % sulphides) (Cabri 1981; Maier 2005).

Three important intrusions which are mostly known for their PGE resources in the world are; the Bushveld Complex, the Great Dyke and the Stillwater. These intrusions according to Naldrett (2010) crystallized from different types of magma, (i) an unusually high silicon dioxide (SiO_2), magnesium oxide (MgO) and chromium (Cr) and low aluminium oxide (Al_2O_3) type known as the U-type, which were emplaced at an early phase and then (ii) a normal tholeiitic-type magma known as the T-type that is later emplaced.

The T-type magmas are all richer in olivine and feldspar than the U-type and are characterized by a much lower chromitite content. The PGE are concentrated in layers close to the level at which primary crystallization changes from one magma type to another. U-type magma is understood as a PGE-rich; komatitic magma that has interacted to variable degrees with the crust, becoming SiO_2 enriched (Naldrett 2010).

Platinum group elements may possibly bond together as PGE alloys with base metals (e.g. Ni, Cu and Fe) and with semimetals (e.g. As, Bi, Sb, Se, and Te) to form a PGM (Knight 2014). Platinum group elements may also occur as trace elements in solid solution in BMS (Naldrett 2004). Irrespective of which form they occur, common economic PGE occurrences are often linked to magmatic sulphide ore deposits. Hence, understanding the genesis of these types of deposits requires the knowledge of the physical and chemical processes involved. Pressure, temperature, composition and oxidation state of the magma are important factors controlling the solubility of iron sulphide in magmas and therefore potentially affecting the point at which sulphide saturation is achieved (Arndt *et al.* 2005). The sulphur content required for sulphide saturation (commonly known as sulphur content of silicate magma in equilibrium with sulphide-rich liquid at the point of sulphur saturation (SCSS) can vary according to changes in the factors previously mentioned. Cawthorn (2010) stated that oxygen fugacity changes may influence the oxide mineral stability. Processes that are likely to produce sudden fluctuations in oxidation state within large volumes of magma need to be recognized. Pressure changes create an appealing mechanism for producing laterally continuous layers as pressure would be transmitted throughout the entire chamber Cawthorn (2010). At this stage of the research it appears that for a deposit to form, mantle derived magma must comprise sufficient ore metals and essentially be capable of being directed to sulphide saturation.

1.7 Sulphide Liquid Fractionation and Partitioning of PGE

Experimental investigations conducted by numerous authors (e.g. Mungall *et al.* 2005; Barnes and Pritchard 1993; Naldrett 2004; Barnes *et al.* 1997, 2001; Peregoedova *et al.* 2004; Li *et al.* 1996) revealed that sulphide liquid fractionation is mainly responsible for the distribution of the PGE. These studies indicated that at high temperatures, <1000 °C, a monosulphide solid solution (MSS) and a copper rich residual liquid were formed due to the separation of an iron-nickel-copper sulphide liquid from a silicate magma. The PGE partition into the (iron, nickel, and copper) sulphide liquid with a partition coefficient in the range of 10^2-10^5, rather than into a basaltic melt (Bezmen *et al.* 1994). The sulphide liquid differentiates as they cool (Hawley, 1965; Naldrett *et al.* 1982).

The MSS occurring at an approximate temperature of 1000 °C, crystallises first from the sulphide liquid, leaving a copper rich residual liquid. This copper rich residual liquid crystallises to form an intermediate solid solution (ISS) at 900 °C.

As temperatures fall below 650 °C, MSS re-crystallizes to form pyrrhotite and pentlandite, whereas ISS re-crystallises to form chalcopyrite (Kullerud *et al.* 1969; Barnes *et al.* 1997; Holwell and McDonald 2010; Ballhaus *et al.* 2001). According to Barnes *et al.* (2008), after the rocks have cooled, the locations of the PGE and other chalcophile elements originally collected by the sulphide liquid are no longer apparent. Possible explanations include their presence in the BMS minerals in solid solution or their exsolution as PGM in BMS.

Fleet *et al.* (1993) used experiments to determine how PGE and gold behave in terms of partitioning between MSS and a sulphide liquid consisting of iron-nickel-copper at temperatures ranging from 1000-1040 °C. Bulk compositions and PGE concentrations of typical magmatic sulphides associated with mafic and ultramafic systems were used. They found that gold, platinum and palladium were incompatible with MSS and would therefore remain in the sulphide liquid during MSS crystallization whereas osmium, iridium, ruthenium (the IPGE) and rhodium are compatible with MSS (Knight 2014).

Ballhaus *et al.* (2001) showed that platinum and palladium are incompatible with MSS having partition coefficients of less than 0.1 (MSS/sulphide liquid) whereas iridium and ruthenium are compatible with MSS having partition coefficients between 3 and 10. Further experiments by Li *et al.* (1996) produced similar results as platinum, palladium and copper were incompatible with MSS whereas iridium and rhodium were compatible with MSS.

Mungall *et al.* (2005) reported correlative results that copper, platinum, palladium and gold are all strongly incompatible with MSS whereas iridium and rhodium are strongly compatible.

The incompatibility of copper in MSS clarifies how after the crystallization of MSS, the residual sulphide liquid is copper rich and how chalcopyrite is the sulphide phase to re-crystallize from ISS. Nickel partitions into MSS, but is not strongly compatible, having a partition coefficient of approximately 1 (Barnes *et al.* 1997), and during exsolution at lower temperatures forms pentlandite with iron and sulphur. Accordingly, pyrrhotite and pentlandite ought to be enriched in iridium, ruthenium, osmium, and rhodium and chalcopyrite in platinum, palladium, gold and silver, however, this effect was not observed in previous studies of different nickel-copper-PGE deposits (Godel *et al.* 2007; Dare *et al.* 2010; Barnes *et al.* 2006). There seem to be variations in precious metals and PGE in different sulphide phases due to fractionation of the sulphide liquid containing these elements. Additional studies by Peregoedova (1998) indicate that palladium and platinum are not only incompatible with MSS, but are also incompatible with ISS.

Furthermore, Helmy *et al.* (2007) studied the effects of tellurium on the partition coefficients of platinum and palladium in MSS, and found that platinum also revealed strong affinity with semimetals to form PGM than palladium.

Therefore, with limited semimetals available, excess palladium would be accommodated by pentlandite rather than competing with platinum to form a PGM with the semimetals (Helmy *et al.* 2007). Arsenic behaviour is more complex and dependant on the proportions of platinum and palladium present (Helmy 2010). If platinum is dominant, sperrylite may crystallise, whereas if palladium is dominant, an immiscible palladium-arsenic liquid may separate from the sulphide melt; both these processes occur early before the crystallisation of MSS.

On the other hand, Campbell and Naldrett (1979) suggested that sulphides that formed from very large volume of magma (Large R) would have low copper/platinum ratios, reflecting the effect of the high partition coefficient for platinum into sulphide. Therefore, with less volume of magma (Small R), the effect of depleting the magma in platinum becomes dominant and higher copper/platinum values are predicted (Campbell and Naldrett 1979). They defined the R factor as the ratio of the mass of the silicate magma over that of the sulphide liquid and assume that the sulphide liquid equilibrated in bulk with the magma and was later removed.

Naldredtt *et al.* 2004 expressed the effect of ratio of magma to sulphide through the R factor approach:

$Yi = [D_i * C_{oi} * (R+1)]/(R+Di)$,

Where Yi, is the final concentration of metal I in the sulphide melt; R is the ratio of the mass of silicate magma to the mass of sulphide, and Coi referes to the original concentration of metal I in the silicate magama before reaction with sulphides commenced.

It appears that the presence of different semimetals changes how different PGE behave which directly affects the type of PGM that may form.

1.8 Models for the origin of the Merensky Reef

Several models have been proposed to ascertain the origin of the Merensky Reef, these are summarised as follows:

Supporters of the "Downers" school of thought (e.g. Campbell *et al.* 1983; Campbell and Barnes 1984; Naldrett 1989) envisage PGE mineralization to have occurred via the collection of noble metals in the sulphide melt that segregated in response to the mixing of compositionally contrasting magmas (Maier and Barnes 1999). The sulphide melt is thought to have formed in the overlying magma pile and then settled to the floor of the chamber due to density differences (Mathez 1995).

Naldrett and Von Gruenewaldt (1989) demonstrated qualitatively how existing sulphur solubility data supports the magma mixing hypothesis, improving the availability of sulphur solubility data over time. Mixing of the two magmas, T and U-type compositions could produce sulphide immiscibility has been however been disputed extensively (Cawthorn 2002; Li *et al.* 2001).

Li and Ripley (2005; 2009) based on a modification of their prior 2001 for sulphur solubility demonstrated that, an extensive range of quantities in the mixing of these magma types can progress to sulphide immiscibility, given that both magmas are close to sulphide saturation during the period of mixing.

Contradictions arising from this model include the association of PGE with "pegmatoids" and chomitites (Mathez 1995) along with the petrographic evidence that petrogenesis may have involved volatiles (Boudreau *et al.* 1986; Ballhaus and Stumpfl 1986; Scoon and de Klerk 1987; Nicholson and Mathez 1991). This resulted in the proposal of the so named "Uppers" model which involved magmatic fluids.

Cawthorn *et al.* (2002) proposed that the PGE mineralization originated by the footwall successions. Supporters of the "Uppers" model believe that an upward infiltration process of volatile-rich fluid was responsible for the transport and precipitation of the PGE from the footwall (Vermaak 1976; Boudreau and Meurer 1999; Boudreau and McCallum 1992).

A third school of thought combines both the "Uppers" theory and the "Downers" theory by Wilmore *et al.* (2000). Models in this school of thought suggest that the PGE were scavenged from the footwall by a fluid that subsequently reacted with the magma at the crystal-magma interface to produce a primary sulphide precipitate.

Further, Cameron (1982) suggested that injection of new magma triggered the formation of the Merensky Reef. The new magma might have been enriched in sulphur or mixing with the residual magma and might have caused a change in the oxygen (fo_2) and sulphur (fs_2) fugacity. The decrease in the solubilty of sulphides in the melt is due to a change in total pressure. Cawthorn (2010) highlighted three events of magma emplacement in the Merensky Reef; (i) each of the events produced variable reactions with the erosion of the footwall; (ii) this then caused recrystillization of pyroxenite into pegmatitic pyroxenite and finally, (iii) the magma produced a chromitite layer followed by pyroxenite with each chromitite layer associated with mineralization of sulphide liquid carrying PGEs.

Furthermore, the Upper Critical zone contains cycles of chromitite, pyroxenite, norite and anorthosite. The Merensky Reef pyroxenite is where most of the mineralization is focused. Cyclic units were initially defined by Jackson (1970), where he suggested that chromite-olivine and olivine-orthopyroxene cycles are the product of differentiation. For both scientific and economic reasons, there have been numerous studies on the Merensky Reef, with most of these studies interpreting the Critical-Main zone boundary to invoke two separate magmas to distinguish between the zones, however, the PGE enrichment is generally poorly understood.

Contrary to two magma mixing, Kruger (1992) and Hatton (1989) argue that the mineral assemblages were not in equilibrium therefore did not form from a mixed magma but rather crystals from both magma layers variably accumulated together at the base of the chamber to form a mixed cumulate.

Seabrook *et al.* (2005) proposed a model about the development of the Merensky and Bastard Units and suggested that the orthopyroxene in the Merensky and Bastard pyroxenite units originated from the Critical Zone magma and the interstitial plagioclase was derived from the Main Zone magma. Seabrook *et al.* (2005) elaborated further in this model that the Main Zone magma is intruded which elevates the residual Critical Zone magma. Orthopyroxene and plagioclase crystals settle from the Critical Zone magma to form the Merensky Reef. The Main Zone magma crystallises norite and then anorthosite of the Merensky Cyclic Unit.
The Critical Zone magma crystallises a second pulse of orthopyroxene, which forms the Bastard pyroxenite with either Main Zone interstitial plagioclase or cumulus plagioclase from the Critical Zone.

1.9 Geometallurgy

Geometallurgy is a multi-disciplinary, applied science integrating mining, geology and metallurgy to assess the processing needs of an ore body (Beniscelli 2011; Lotter 2011; Philander and Rozendaal 2011). It integrates the principles of material characterization and process mineralogy. Process mineralogy is the use of mineralogical techniques to understanding and solving problems experienced during the process of separating valuable minerals from gangue or waste (Petruk 2000). Different minerals hosting the same metal type may respond differently to various processing techniques. There have been several studies on the PGMs in various ore bodies, which are vital to maximise beneficiation and extraction.

While individual minerals can be documented, estimating relative abundances, their association and their liberation characteristics can be challenging due to their small sizes and scarcity (Cawthorn 2015). PGEs are known to occur as fine inclusions within BMS or as intergrowths between BMS and gangue contacts surface, which aid in liberation during the grinding process. Wiese *et al.* (2006) interpreted the role of reagents in the flotation of platinum bearing Merensky ores and concluded that the diverse BMS in the Merensky Reef react distinctively to the operating conditions and to various reagents and operating conditions. The PGEs are recovered by flotation and to maximise PGE recovery, the recovery of all the BMS needs to be optimised.

Reagents are added to achieve distinct specific roles that that can influence the pulp chemistry and improve the differentiation in mineral surface hydrophobicity to promote and simplify the separation. Furthermore, Pillay *et al.* (2011) reported that the key mineralogical factors controlling the separation are the texture of the sulphides, grain size, particle density and particle shape.

Generally, in the Merensky Reef, the liberation size is coarse with most operations choosing a grind size between (P_{80}) 75 and 150 microns. The presence of talc can cause significant process difficulties (SGS 2002). Hence geometallurgy seeks to provide mineralogical information of an ore to determine the causes of the different responses of minerals to various metallurgical processes to ensure the employment of appropriate metallurgical techniques for optimal mineral beneficiation. Mineralogical measurements involve the quantitative mineralogical characterization of the ore to determine mineral textures, mineral associations, mineral grain size distribution (Fandrich *et al.* 2007).

2 Study Area

2.1 Location and History of the Mines

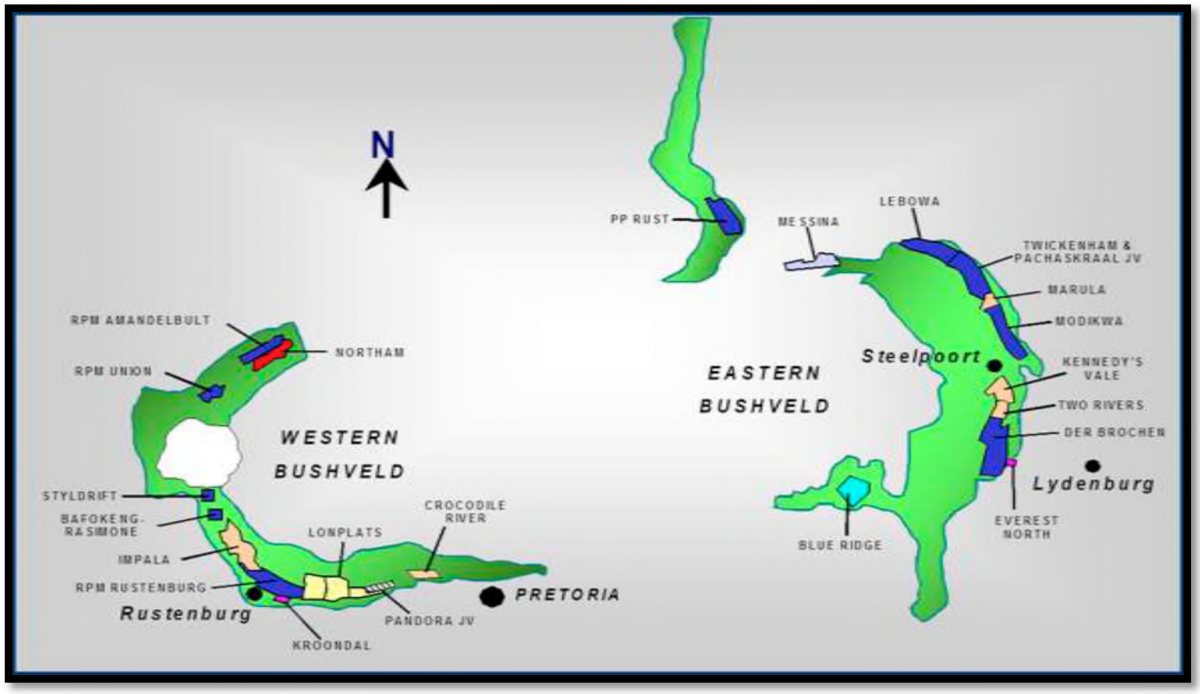

Figure 2.1: Map of the Bushveld Complex showing location of the Platinum mines in the Bushveld Complex (Adapted from CGS ATP Report, 2014).

2.1.1 *The Modikwa Platinum Mine (MPM)*

The Modikwa Platinum Mine is an independently managed 50:50 Joint Venture (JV), between African Rainbow Minerals (ARM) Mining Consortium Limited and Rustenburg Platinum Mines Limited. The mine is situated on the boundary of the Mpumalanga and Limpopo provinces approximately 25 km west of the town, Burgersfort, forming part of the Eastern limb of the Bushveld Complex. Modikwa Mine operates under a mining right covering a total area of 140 km^2. The mineral lease area covers the 28.4 km of strike length on the farms Driekop 253 KT, Maandagshoek 254 KT, Heindreksplaas 281 KT, Onverwacht 292 KT and Winterveld 293 KT. Platiniferous reefs identified within the area are the Merensky Reef and the UG-2 Reef and the current study area is located within the farm, Onverwacht 292 KT.

The Modikwa Platinum Mine infrastructure consists of two major decline shafts, namely; the North Shaft and the South Shaft, three adits on the Onverwacht Hill and a concentrator. The mine operates as an underground mine and exploits UG-2 exclusively from the surface to 450 m underground.

The life of mine (LoM) at the current rate of production may extend to 2087. In September 2011, the mine acquired the prospecting right for a portion of the Doornbosch, an adjoining property from Randgold and Exploration Company Limited (Mining-technology 2013). The Modikwa Plant was then commissioned in August 2002 and the borehole locations are tabulated below.

Table 2.1: Borehole coordinates for Modikwa

	Coordinates	
	X	Y
OV 777	28257	89845
OV 778	27892	90068

2.1.2 *Two Rivers Platinum Mine (TRP)*

Two Rivers Platinum Mine is located approximately 25 km south west of the town of Steelpoort, Mpumalanga within the farm Dwarsriver 372 KT. Dwarsriver 372 KT is bordered by the farms Kalkfontein 367 KT in the west, Tweefontein 360 KT in the north, De Grootboom 373 KT in the east, with the farm Richmond 370 KT flanking the southern boundary while the farm Thorncliffe 374 KT flanks the south-eastern border (TRP Trial Mining Report, 2003). The main decline is approximated at a latitude of 25° 59′ 00″ S and a longitude of 30° 05′ 00″ E.

Dwarsriver 372 KT was successively acquired by Goldfields, South Africa from 1970 and prospecting was carried out on the Merensky Reef, the UG-2 and the LG-6 chromitite (TRP Trial Mining Report 2003). Associated Manganese Mines of South Africa Limited (ASSMANG) acquired the farm, Dwarsriver 372 KT, in 1998 and primarily targeted the LG-6 chromitite layer for its chromium content. In 2005, a JV was pronounced between ARM and Impala Platinum (ARM 2007). TRP is also an underground mine targeting UG-2 chromitite for its PGE mineralization. At TRP, ARM has a 55 % stake in the JV while the remainder of the stake is held by Impala Platinum. The project is operated by ARM and the plant was officially commissioned in 2006 (ARM 2007). Early exploration records of development and production from the Eastern limb of the Bushveld Complex date to the early 1920's and borehole locations are tabulated below.

Table 2.2: Borehole coordinates for Two Rivers

	Coordinates	
	X	Y
TRP 260	93155	27628
TRP 271	92708	27592

Both the Modikwa and the TRP target the UG-2 chromitite for its PGE mineralization, with proposed plans are to exploit the Merensky Reef. The current metallurgical plant is designed to recover the PGE with UG-2 characteristics. Provided the ore deportment and mineralogy of the Merensky Reef differs from the UG-2 currently mined at the two mines under investigation, the findings of this study may be used to predict and remedy the problems with the current plant and before a new treatment plant is proposed or prematurely deployed.

2.2 The Geology of the Study Area

2.2.1 *The Merensky Reef in the Central Sector*

The limits of the Central sector are demarcated by major faults and basement domes (Scoon and Mitchell 2004b) with the layered cumulates forming a sequence about 9 km thick (SACS 1980). The Merensky Reef in the Central sector belongs to facies described as 'wide reef facies' (Mitchell and Scoon 2007a). In these facies, PGE mineralization is largely contained within a relatively thick succession of medium-grained non-pegmatoidal feldspathic pyroxenite, bounded top and bottom thin chromitite stringers (Mitchell and Scoon 2004a). The Lower Critical Zone is dominated by feldspathic orthopyroxenite with minor dunite and harzburgite (Cameron 1980) and contains only intercumulus plagioclase. The overlying Upper Critical Zone is dominated by norite and anorthosite (i.e. plagioclase cumulates) with subordinate feldspathic orthopyroxenite and minor amounts of feldspathic harzburgite (Cameron 1982). Chromitite layers are restricted to the Lower Critical and Upper Critical Zones (Hatton and von Gruenewaldt 1987). The two main PGE ore bodies (i.e. Merensky and UG-2 Reefs) occur in the Upper Critical Zone. The Merensky Reef Unit in the Central sector includes the Merensky Reef, which consists of a basal layer of medium-grained feldspathic orthopyroxenite (from 2-5 m) and a thick spotted-mottled anorthosite (from 5-8 m) thick. Although the occurrence of the Merensky Reef and the Dunite Pipes is known, insufficient data exists to quantify any resources contained therein.

At other sites, especially in the Western Bushveld Complex, the Merensky Reef is found at the base of the orthopyroxenite layer that forms the lower most part of the Merensky Reef Unit (Mitchell and Scoon 2007a). Schwellnus *et al.* (1976) also documented the occurrence of the Merensky Reef in the Central sector of the Eastern Bushveld Complex particularly that of the Atok section which was the only active mine in the Eastern limb until recently.

The deep footwall consists of a pyroxenite overlain by a pegmatitic pyroxenite up to 1 m thick. Mitchell and Scoon (2007) described the Merensky Reef within the Winnaarshoek property, close to the south of the Atok Mine, as similar to other occurrences of the Merensky Reef in view of the PGE mineralization. The PGE mineralization occurs within an interval bounded by two chromitite stringers. A key difference of the Merensky Reef in the Winnaarshoek property, however, is that the chromitite stringers are separated by a medium-grained (instead of the usual pegmatiodal) feldspathic orthopyroxenite (Mitchell and Scoon 2007). At Marula mine, the Merensky Reef is yet to be exploited (Scoon and Mitchell 2004), but is similar in terms of thickness and PGE distribution to the western mine.

A significant feature of the Merensky Reef Unit and its associated rocks in the Central sector is the relative absence of the discordant, late-stage Iron Rich Ultramafic Pegmatite (IRUP) bodies that are common in the other parts of the Bushveld (Viljoen and Scoon 1985). IRUPs, as proposed by Viljoen and Scoon (1985), is a term used to describe replacement bodies believed to be post-cumulus in nature and being composed of iron-rich olivine, clinopyroxene, ilmenite and titanium-magnetite with accessory BMS and being barren of precious metal mineralization.

The richest mineralization constitutes an upper reef, a feature colloquially referred to as "top loaded" as most facies of the Merensky Reef contain the highest PGE grades in association with the upper chromitite stringer (Viljoen and Schurmann 1998). Minor PGE mineralization may extend into the underlying pegmatoid but most of the other pegmatoid are weakly mineralised. The Central sector differs from the Western limb, where the reef zone in many areas is dominated by pegmatoidal assemblages (Wilson and Chunnett 2006).

In contrast to the south of the Steelpoort Lineament, the Merensky Reef in the Central sector has similarities with that seen at the Rusternburg Platinum Mine (Wagner 1929), hence in each limb, there are considerable facies variations, but between the Eastern and the Western limbs, similarities can be recognised.

The UG-2 chromitite exists at Modikwa Platinum Mine as a layer that is characterised by a regular thickness of 60 cm. The three thickest chromitite layers overlie the top of the main seam. The UG-2 comprises of pyroxenites, norites and anorthosites. Randomly distributed potholes of various sizes categorise the North shaft region while lesser potholes categorise the South shaft. The area is extremely disrupted by faulting. Several IRUPs and Replacement Pegmatoids have been observed particularly at the Onverwacht hill area.

2.2.2 *The Merensky Reef in the Southern Sector*

Fine-to-medium-grained dolerite dykes associated with the Steelpoort fault, trending sub-parallel to the north, north east direction, are also present within the Dwarsriver 372 KT property. Based on a limited number of exploratory geological core logs, there are areas where the dolerite dykes partially or wholly replace the Merensky Reef or UG-2 chromitite. The Steelpoort fault also affects the lithology as the sequences found in the Southern sector are somewhat different to those of the Central sector (TRP Trial Mining Report 2003). PGE mineralization occurs within both the Merensky Reef and the UG-2 chromitite horizons.

The Merensky pyroxenite sub-crops occur along a north-south strike on the western slopes of small Dwarsriver valley. Previous studies of the Merensky Reef in the study area reveal that it is similar in many aspects to the western Platinum facies of the Western limb (TRP Trial Mining Report 2003). The Merensky Reef at TRP is classified into four facies types based on thickness of the Merensky pyroxenite and the PGE mineralization style (Rose *et al.* 2011). The reef facies are explained as follows:

Reef facies (1) is characterized by bimodal PGE mineralization, where the mineralization is directly associated with the upper and basal chromitite stringers. The Western Bushveld analogue of this reef facies is the "Western Platinum Facies". Reef Facies (2) has no direct analogue in the Western Bushveld, with the closest possible analogue being the "Marikana facies" of the Western Platinum/Karee Mine Boundary. The PGE mineralization occurs throughout the "Merensky Pyroxenite" and is not intimately associated with the chromite mineralization. Reef facies (3) is also known as the "thick reef", with the Merensky pyroxenite for this reef facies type being greater than 3 m but averaging 4.85 m. This reef is however, restricted to the southern portion of the TRP property.

The mineralization of the PGE is localized at three distinct peaks, with the upper and lower mineralization peaks associated with the upper and basal chromites respectively, while the third peak is located within the Merensky pyroxenite and is not associated with chromite mineralization (TRP Trial Mining Report 2003). Reef facies (4) also known as the thin reef, the Merensky pyroxenite for this facies type is usually less than 1 m thick; with the average thickness being 0.9 m. The upper chromitite stringer and its associated mineralization are generally absent.

Usually the pegmatoidal feldspathic pyroxenite is restricted to the base of the normal pyroxenite, although in places the pegmatoidal feldspathic pyroxenite caps the normal pyroxenite and may also occur sandwiched between the normal pyroxenite. In the event the pegmatoidal feldspathic pyroxenite is sandwiched by the normal pyroxenite, it is usually restricted to either the upper or the lower reaches of the normal pyroxenite (Rose *et al.* 2011).

According to the limited information sourced from exploratory drill cores, the pegmatoidal feldspathic pyroxenite ranges in thickness from less than 10 cm to above 40 cm. Further, the Merensky Reef in this area is occasionally affected by circular replacements or IRUPs (Scoon and Mitchell 2004).

These replacement bodies are typically restricted to the Upper Critical and Main Zones and are rare in the Lower Critical and Lower Zones, with their distribution being controlled by structural features.

To be precise, they commonly occur in distributed areas marked by extensive faulting and post-Bushveld dykes (Viljoen and Scoon 1985). The limited borehole data sourced revealed there are occasions where the Merensky and UG-2 are partially or wholly replaced by dolerite dykes.

The UG-2

Three different types of reef are well-defined at Two Rivers. These are; the 'normal reef' with a leading chromitite layer; a 'split reef' characterised by an internal pyroxenite/norite lens within the leading chromitite layer; and lastly the 'multiple split reef' with several pyroxenite/norite lenses occurring within the leading chromitite layer. The southern portion of the mining area is mainly dominated by the multiple split reef.

2.3 Previous Work

2.3.1 *Platinum Group Minerals and Platinum Group Elements in the Merensky Reef*

The general aspects of the mining and beneficiation of South African PGE ores minerals, which include the Merensky Reef, were reviewed by Cramer (2001) and by Merkle and McKenzie (2002). Most of the work done on the Merensky Reef specifically the efforts of Vermaak and Hendricks (1976), Kinloch (1982) and Kingston and El-Dosuky (1982) focussed on the Western limb, due to better infrastructure; (primarily the availability of water and human resources) as opposed to the Eastern limb (Cawthorn *et al.* 2002). The seminal work of Vermaak and Hendricks (1976) on PGM within the Merensky Reef showed that the PGM are generally associated with three assemblages; (i) BMS associations (ii) chromite associations and (iii) silicate associations; with the majority of the commonly observed PGMs in the Bushveld Complex being: laurite, platinum-iron alloys, platinum-palladium sulphides and sperrylite with lesser rhodium sulphides (Lee 1996), as well as antimonides and tellurides (Maier and Barnes 1999).

The strong association of PGM with BMS has led some researchers like Osbahr *et al.* (2013), Ballhaus and Ryan (1995), Godel *et al.* (2007) and Ballhaus and Sylvester (2000) to establish the amount of PGE occurring in the BMS of the Merensky Reef. It was found that pentlandite contained the highest amount of PGE ranging from 500 to 1750 ppm PGE (Godel *et al.* 2007; Ballhaus and Ryan 1995; Osbahr *et al.* 2013).

Pyrrhotite contained 10 to 40 ppm PGE (Godel *et al.* 2007; Ballhaus and Sylvester 2000). Chalcopyrite contained the lowest amount of PGE in solid solution with 4 to 10 ppm PGE (Godel *et al.* 2007). Of the PGE, platinum was found to mostly occur as discrete PGM and does not partition into BMS, whereas palladium, rhodium, ruthenium, iridium and osmium were found to be present in more significant amounts in the BMS (Osbahr *et al.* 2013; Ballhaus and Sylvester 2000; Godel *et al.* 2007). The platinum:palladium ratio is up to 5 in the Merensky Reef (Cousins and Kinloch 1976; Hey 1999). Barnes and Maier (2002a) studied the PGE, sulphur, nickel and copper concentrations in the Merensky Reef at Impala Platinum Mines in the Western Bushveld and concluded that in addition to the collection of the PGE by sulphide liquid, some of the PGMs solidified and settled onto the chromitite layer before the BMS fluid infiltrated the cumulate pile.

Recently, the evaluation of PGM has been carried out using a technique known as automated scanning electron microscopy with energy dispersive spectrometry (SEM-EDS) image-based analysis (e.g. Gu 2003; Hoal *et al.* 2009; Chetty *et al.* 2009).

Rose *et al.* (2011) documented the Merensky Reef and pointed out that the maximum PGM contents are usually associated with PGE in the Merensky Reef, and are closely associated with the chromitite stringers. The BMS including pentlandite, pyrrhotite, chalcopyrite and minor pyrite occur interstitially with the silicates and chromites (Lee 1996). The BMS and PGE correlate with each other in the mineralised portion of the reef (Lee 1983). In most of the Merensky Reef facies the economic PGE mineralization is concentrated in the pegmatoidal feldspathic pyroxenite with the highest concentrations in the range of the chromitite stringers (Lee 1996). Depending on the location of the maximum PGE concentration, the mineralization is referred to as "top loaded" if the maximum PGE concentration is in the range of the upper chromitite layer and as "bottom loaded" if the mineralization is in the range of the lower chromitite stringer (Osbarh *et al.* 2013). If not, then it exhibits a more complex distribution. The PGEs occur as sulphides, arsenides, tellurides, bismothotellurides and alloys.

The PGMs identified include sulphides: cooperite (PtS), braggite (PtNiPdS), and laurite (RuS); telluride: moncheite ($PtTe_2$); bismuthotellurides: (PtBiTeFe); maslovite (PtTeBi); arsenides: sperrylite ($PtAs_2$); antimonides: stibiopalladinite (PdSb) and geversite (PbSb) and ferroalloy (PtFe). Gold occurs as an electrum and as a rare compound, AuBiPdTe (Brynard *et al.* 1976; Viljoen *et al.* 2012). Sperrylite is the most abundant PGM in this area (Brynard *et al.* 1976). In general, it has been noted that the PGMs in the Merensky Reef show closer associations with BMS (Schwellnuss *et al.* 1976; Vermaak and Hendriks, 1976; Prichard *et al.* 2004).

However, PGMs also occur along the sulphide grain boundaries or included in primary and secondary silicates (Cawthorn *et al.* 2002). The primary mineral assemblage of the Merensky Reef is orthopyroxene, plagioclase feldspar, clinopyroxene and olivine, and localized concentrations of chromitite occurr in thin stringers (Schouwstra *et al.* 2000). A variety of secondary silicates and alteration minerals also occur in minimal to trace amounts such as amphibole, mica, chlorite, talc, serpentine, calcite and magnetite (Schouwstra *et al.* 2000; Li *et al.* 2004).

2.3.2 *Platinum Group Minerals and Platinum Group Elements in the UG-2*

McLaren and De Villiers (1982) state that the UG-2 Reef consists primarily of chromite (60-90 %), orthopyroxene (5-25 %) and plagioclase (5-15 %), with secondary or accessory minerals also forming part of the UG-2 reef.

Based on the mineralogical investigation by Penberthy *et al.* (2000), the most commonly found PGM group in the UG-2 are PGE sulphide mineral chromitites such as laurite, cooperite, malanite and braggite. Other resources reveal non-sulphidic minerals, such as antimonides, arsenides, bismuthides, tellurides and alloys. Common substitutions are identified for some of the PGM minerals by Vermaak (1976). McLaren and De Villiers (1982) reported that PGMs occur as discrete grain sizes ranging between 1 and 4 microns and associated with BMS (33-85 %), along grain boundaries (6-57 %), in silicates (2-29 %) and in chromite (<12 %).

2.3.2.1 High PGE in Chromite

The model of sulphide control on PGE enrichment is problematic when applied to the chromitite layers because of the high PGE to sulphide ratio (Hiemstra 1985; 1986). It has been suggested that greater proportions of sulphide originally existed, but that the sulphide has been oxidised by reactions with chromite (Naldrett and Lehmann 1987). Scoon and Teigler (1994) suggested that the precipitation of chromite induces sulphide saturation within an evolving magma. Scoon and Mitchell (2007) also suggested that controls on PGE mineralization are essentially primary magmatic as they ascribed the presence of chromite to magma mixing due to repeated replenishment.

Determinations by Barnes and Maier (2002) on the PGE paradox were that; (1) the affinity of chromitites to bond with PGEs rather than silicate rocks could arise as the conditions favouring chromite crystallisation also favour PGM crystallisation (2) the PGE enrichment in chromitite layers is due to the interaction between trapped sulphides liquid and chromitite resulting in loss of sulphur from the sulphide liquid.

During reheating the sulphides may have reacted with chromites leading to low sulphur contents in the sulphide liquid while some of the fractionated liquid is compressed from the chromitite during the period of compaction.

3 Methodology

3.1 Borehole Core Logging

Four boreholes intersections, two each from the Modikwa and TRP Mines were used for the study. Logging of cores from the boreholes was done in detail to identify the lithologies of the Merensky Reef, its immediate hanging wall and footwall. The logging involved a visual inspection of the core to ensure that a proper quantitative rock description is carried out. Observations of colour, grain size and texture, nature of contacts, primary mineralogy and the presence of structural features were noted. Examination of the hand specimens was done both visually and under hand lense magnification. The presence or absence of core losses was recorded as well. Four boreholes were drilled for the exploration of PGEs resident in the two farms Onverwacht 292 KT and Dwarsriver 372 KT and all intersected the Merensky Reef seam of the Critical Zone.

3.2 Sampling

Core samples were split into half and quarter cores (Figure 3.1) and then labelled and bagged. The samples were taken from the economically mineralised part of the reef (within the range of chromitite stringers) 20 cm above the top chromitite stringer and 30 cm below the bottom chromitite stringer and sulphidised zones. Details of the depths at which sampling took place were recorded. A total of 41 samples were sent to the Council for Geoscience (CGS) laboratory for the preparation of polished thin sections and stubs. The sample list attached as Appendix A.

Figure 3.1: Quarter core, corresponding thin section and stub.

3.3 Laboratory Analyses

3.3.1 *Conventional Optical Microscopy*

A petrographic microscope, Olympus BX43 with a dedicated camera was utilized in conjunction with the Stream Essentials software package. Polished thin sections were viewed under transmitted light for the characterisation of mineral assemblages and phases, textural relations as well as gangue silicate associations to the ore minerals. The round polished stubs (approximately 24 mm in diameter) were observed under reflected light for oxides and opaque minerals such as associated sulphides. Image were taken using the camera attached to the microscope to produce photographic images (Figure 3.2). Aspects such as crystal habit, morphology and texture were noted in opaque minerals.

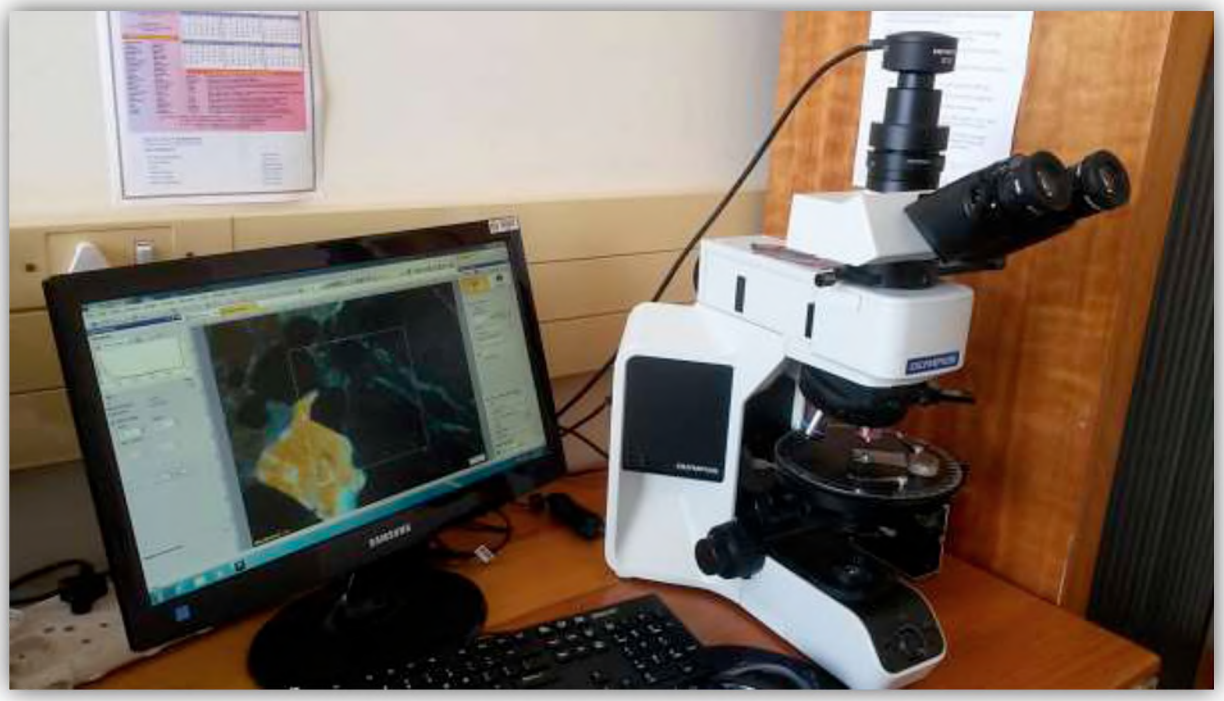

Figure 3.2: Zeiss Conventional Optical Microscopy used during the study.

3.3.2 *Scanning Electron Microscopy-Energy Dispersive Spectrometry (SEM-EDS)*

A secondary electron microscopy study was carried out on a Leica Stereoscan 440 SEM, linked to an OXFORD INCA (Energy Dispersive Spectrometry) EDS shown in Figure 3.3. The data acquisition was performed at the Council for Geoscience laboratory to characterize the PGM. All specimens were polished and coated with carbon to provide a conductive surface for optimum imaging and X-ray micro analysis. Mineral chemistry then was determined using spot analyses at a beam setting of 20 kV accelerating voltage.

This technique was used to characterize the PGM phases and their preliminary elemental composition to confirm the homogeneity of the minerals prior to electron microprobe analyses. Results on the back scattered images with corresponding spectra of the PGM identified are attached in Appendix FI and Appendix FII.

Figure 3.3: Leica Stereoscan 440 SEM linked to an OXFORD INCA EDS. The system consists of digital scanning electron microscope and three major subsystems the Fisons Keyex energy dispersive X-ray analysis system, the Finson LT7400 Cryo Transfer System and the Oxford Monochromator Cathodoluminescent system.

3.3.3 *Electron Probe Micro Analyzer (EPMA)*

Quantitative analysis and mineral chemistry were carried out using a Jeol JXA 8230 Superprobe machine equipped with four wavelength dispersive spectrometers (WDS) (Figure 3.4) in the Department of Geology at Rhodes University. An acceleration voltage of 15 kV, a probe current of 20 nA and a counting time of 10 seconds on peak and a 5 second on background, and a beam size spot < 1 micron were employed for quantitative and PGE concentrations analysis. The ZAF matrix correction method was employed for quantification. The polished stubs were sputtered with a graphite layer to enable electrical conductivity. Natural standards were used for measuring the characteristic X-rays. PGM grains sizes and their association with BMS may result in mixed spectra which may possibly bring complications to the data, causing some of the results to be considered poor. Some results may be disregarded/ignored as these are unreliable.

This is applicable to anything below 95 % in total, for the EPMA data and as a result only acceptable values are discussed in this study (for all totals see Table 3 in Appendix BII).

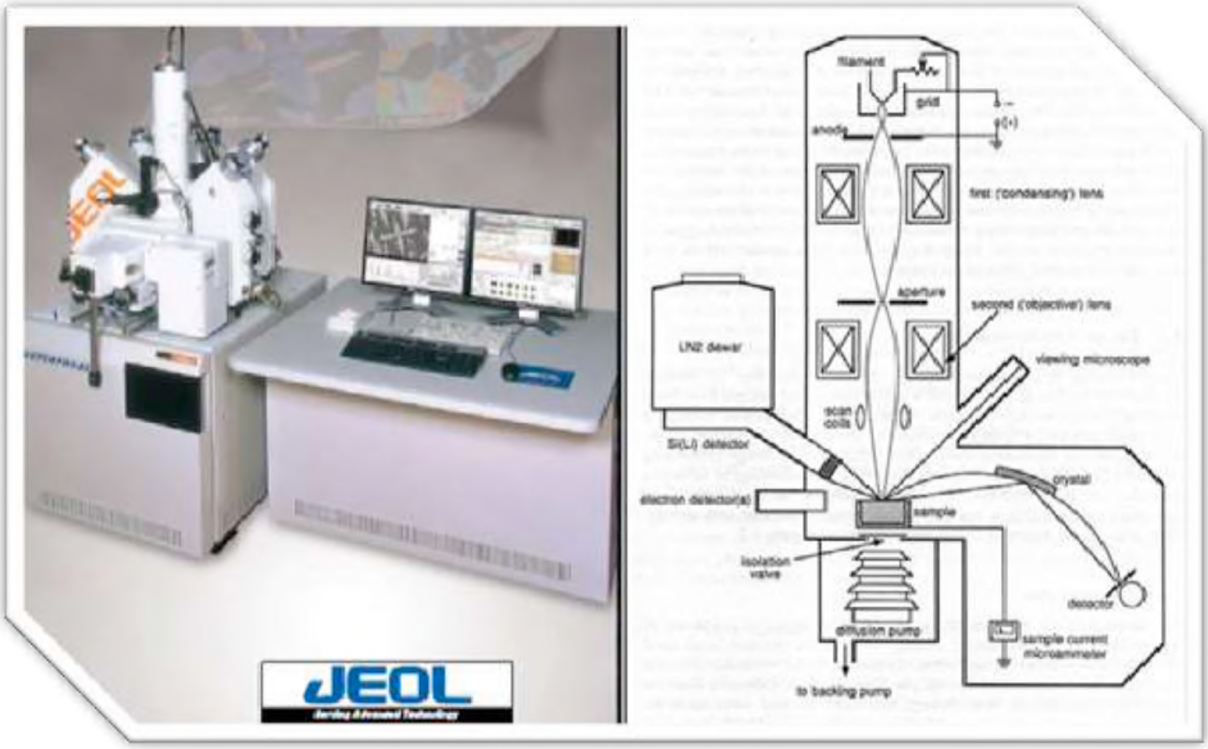

Figure 3.4: Photographic image of the Jeol JXA 8230 Superprobe Analyzer used for point analyses. The probe consists of a filament at the top, sample stage, deflecting crystal and detector (Jeolusa.com).

The EPMA was used to determine the distribution of PGE and other trace elements within sulphides by elemental mapping. Trace element analysis on sulphide ores was undertaken to determine the quantitative composition of the PGE (including platinum, palladium, rhodium, ruthenium, iridium and osmium) which are known to occur in trace amounts specifically on micron scale sizes, in the Bushveld Complex ores. During the quantification process, a beam was pointed toward bright appearing particles and the reflection thereof is captured by a detector which reports the quantity of the elements by comparing to the calibrated natural standards used. The quantities of the major elements in the specific particle are reported in mass percentages. An in-built camera is utilized to capture the images of the sample view. The counting time for PGEs (platinum, palladium, rhodium, ruthenium, iridium and osmium) was set to 100 seconds on peak and 50 seconds on each background. The overlap corrections were applied, and are shown in Table 3.1 below.

Table 3.1:EPMA Overlap Corrections Applied

Element	K-value
Os (Mα) – Pt (Mα)	1.7355
Ru (Lα) – Pt (Mα)	0.9524
Pt (Mα) - Ir (Mα)	0.3635
Os (Mα) – Ir (Mα)	0.198
Ir (Mα) – Os (Mα)	0.322
Pd (Lα) – Ru (Lα)	0.287
Os (Mα) – Ru (Lα)	0.258
Os (Mα) – Fe (Kα)	0.675
Ru (Lα) – Fe (Kα)	0.05
Rh (Lα) – Ru (Lα)	0.212
Pd (Lα) – Rh (Lα)	0.485
Os (Mα) – Rh (Lα)	0.334
Ru (Lα) – Ni (Kα)	0.236

Small backgrounds were chosen for platinum, palladium, rhodium, ruthenium, iridium and osmium to avoid overlaps between secondary peaks and backgrounds. Nickel, sulphur, iron and copper were analysed within the trace element runs (but with lower counting times) set at 4 seconds per peak and 3 seconds on each background to optimize the effect of matrix correction (PRZ) on the trace elements. The standards used for quantification were: S (pyrite), Fe (pyrite), Cu (chalcopyrite), Ni (pentlandite), Rh (rhodium metal), Pd (palladium metal), Pt (platinum metal), Os (osmium metal), Ir (iridium metal), and Ru (ruthenium metal).

3.3.4 *Mineral Liberation Analyser (MLA)*

FEI's electron microscope-based Mineral Liberation Analyzer (Figure 3.5), is designed to provide the quantitative analysis of mineral and material samples. It is used to examine fine grained mineral textures to determine the abundance of various mineral types and other parameters of metallurgical significance. The MLA incorporates the technologies of SEM and Energy Dispersive X-Ray Analysis. Similar to micro probe and SEM, MLA also uses back scattered electron intensity where minerals with a high density (high atomic mass), like the PGM and gold, appear as bright particles under the electron beam relative to lower density minerals like silicates. It is also possible to determine metallurgical parameters such as particle liberation, mineral association and grain size distribution which is critical to the efficient separation of ores and waste. The strength of the MLA is in its ability to detect and analyse tiny grains present which SEM and EPMA cannot detect.

In MLA, minerals are considered to be associated with each other when they share grain boundaries. The higher the degree of grain boundary shared between two minerals, the greater the degree of association between them. It utilises a software which automatically determines this association. Free surface refers to the perimeter of the particle that is exposed and/or the perimeter that does not share a boundary with any other mineral.

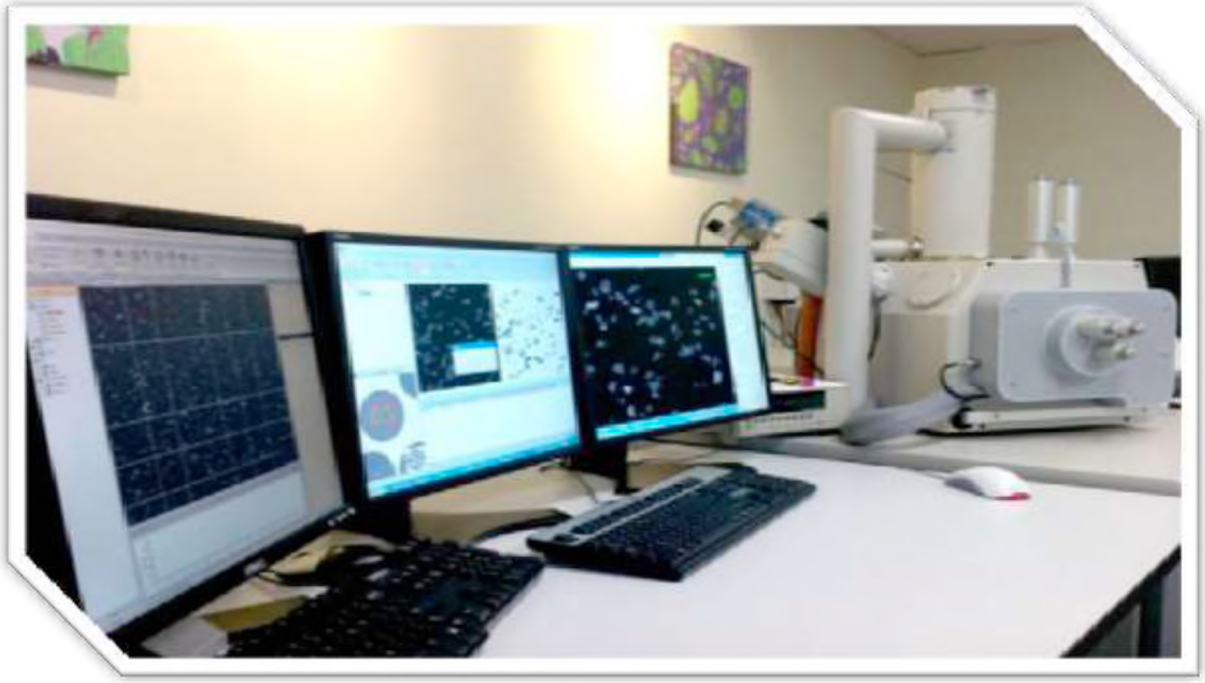

Figure 3.5: Photographic image of the Mineral Liberation Analyzer (MLA). Product components include automated electron-beam analysis system based on FEI Quanta SEM (W or FEG source), Custom software combines BSE and EDS X-ray detection Multiple EDS detectors for accurate high-speed data acquisition (Adapted from MLA user guide provided at Mintek).

During MLA examination, a software sub-module (XBSE_Std) is used which is designed to aid in the recognition of all mineral species present, through the construction of a mineral reference library in which each entry is numbered successively (e.g. mineral1, mineral2). The operator allocates names to each mineral species encountered, or sub-grouping the minerals accordingly. A standard SPL-DZ measurement mode is performed where bright particles are located and mapped on a regular grid system. The resulting output includes a mineral map of each bright particle, as well as the surrounding associated phases. All analyses were conducted at 15 X magnifications and at a selected maximum particle size of 8 micron. Final data processing was performed using data view software (Gu 2003). For the present study, the MLA was used to determine the nature of minerals closely associated to the PGMs and the PGM grain size distribution.

The smaller PGM sizes obtained and their close association with BMS brings complexity in the data that, causes the overlapping in the EDS spectrum obtained for that particular PGM. The mixture of spectrums brings confusion in data interpretation as experienced in other techniques, namely SEM and EPMA, used including the MLA. And so this led to the generation of PGE sulphide group as it becomes difficult to detect whether the phases were the PGM base metal sulphide phases or were as a consequence of the mixture in the EDS spectrum. For example, overlap of the electron beam interaction between the occurrences of michenerite (PdBiTe) in or close to pentlandite $(Ni, Fe)_9 S_8$ will result in a mixed spectrum of (PdBiTeNiFeS).

With the aid of all the techniques mentioned above and a better understanding of the mechanism of mineralization, this information can be incorporated developing a geometallurgical model. In examining the PGE associated with the Merensky Reef at the two mines, no geochemistry studies were undertaken for PGE in this study. Extensive work has previously been done on the PGE chemistry by several researchers namely Junge *et al.* (2014) Rose *et al.* (2011) and Osbahr (2013).

3.3.5 *Fire Assay*

Fire assay measurements were carried out at Mintek's Analytical Services Division (ASD). Determination of the PGE suite was carried out using the nickel sulphide collection fire assay method. Two nickel sulphide fluxes were used, specifically, the Merensky Reef flux and UG-2 special flux to accommodate the varying chromite contents in the samples. The samples were then analysed for six PGEs (platinum, palladium, rhodium, ruthenium and iridium). The presence of osmium could not be analysed as the Mintek laboratory is unaccredited for the analysis for osmium. The method comprised of pulverizing the quarter drill cores which had a length of about 15-25 cm. Appropriate amounts of sample were weighed out on an analytical balance, mixed with a nickel sulphide flux to a homogeneous state and loaded into a fusion furnace at 1100 °C to 1200 °C for 50 minutes. The nickel sulphide serves as a collector for PGEs, by process called cuppelation. PGEs are separated from the collector in a cuppel. A cuppel is typically a ceramic porous shallow cup. The lead alloy is heated and as it melts the lead is oxidised and absorbed into the cuppel, this process continues until all the lead is drawn out, leaving a small bead containing only precious metals.

To complete the separation from the collector the beads are weighed then subjected to leaching, precipitation and filtration processes to separate the PGEs which are then dissolved in an aqua regia and further analysed by Inductively Coupled Plasma Mass Spectrometry (ICP-MS) to determine the concentrations of platinum, palladium, rhodium, iridium, ruthenium and gold in the solution. ICP-MS is a trace technique that analyses samples at a low part-per-billion (ppb) range. The instrumentation, ICP-MS, was optimized and calibrated using calibration standards ranging from 1 ppm to 50 ppm. The uniqueness of this technique lies in the fact that it utilises the naturally occurring isotopes of all analysable elements to correctly determine the concentration of an analyte. The technique is especially suited for environmental and water analyses, soils and ores for trace and ultra-trace elements. Figure 3.6 shows the laboratory furnaces used for high temperature assays.

Figure 3.6: Fire assay-high temperature laboratory furnaces.

4 Sample Description and Petrography

4.1 General Summary of Rocks and Minerals Encountered in the Merensky Reef

Samples for this study were taken from only the economic, mineralised part of the reef, Merensky Reef pyroxenite, within the chromitite stringers; therefore, other rock lithologies such as norite, anorthosite, gabbronorite and harzburgite were not sampled, but are summarized below as they were encountered during core logging.

Pyroxenite: There are two types of pyroxenite that commonly appear in the Merensky Reef sequence; (1) normal feldspathic pyroxenite and (2) pegmatoidal feldspathic pyroxenite. Mineralogically, the two units are alike; but only differ in their grain sizes, where orthopyroxene grains vary between 3-5 mm in the feldspathic pyroxenite and up to a few cm in pegmatoidal feldspathic pyroxenite. In all four investigated drill cores, clinopyroxene commonly occurs as inclusions in orthopyroxene and rarely as a matrix mineral. Plagioclase normally occurs as an interstitial mineral. The base metal sulphides mostly occur in the feldspathic pyroxenite and pegmatoidal feldspathic pyroxenite. The chromite grains occur as disseminated grains and are commonly associated with micas, where visible they range between 2-3 mm in grain sizes.

Anorthosite: Anorthosite is well-defined by the size of the plagioclase present in the unit, with sizes ranging from 2 to 3 cm. In the anorthosite unit the plagioclase amount ranges between 80 to 100 vol % containing up to about 20 vol % of pyroxene, principally orthopyroxene.

Norite and Gabbronorite: Contains 60-67 vol % of orthopyroxene and to approximately 35 vol % of plagioclase with comparable grain sizes as in the feldspathic pyroxenite. Minor constituents of biotite, rutile and olivine are commonly encountered. The primary phases present in gabbronorite are clinopyroxene, orthopyroxene and some plagioclase. In some cases plagioclase predominates over pyroxene in gabbronorite.

Harzburgite: The pyroxene content in this unit is up to 65 vol %, with the amount of olivine reaching up to 20 vol % and about 10 vol % of plagioclase. Grain sizes of olivine and plagioclase can reach up to 5 mm while pyroxene reaches up to 1 cm. The olivine grains are usually or partly replaced by serpentine minerals. Disseminated sulphides, chromite and biotite are common.

Chromitite: Occur as thin layers, known as stringers, at the top and bottom of the Merensky Reef pyroxenite sequence.

It also occurs disseminated throughout the Merensky Reef units. The chromitite stringers consist of about 95 vol % chromite. Idiomorphic to hypidiomorphic chromite grains range between 100-200 microns in size. The chromite grains are embedded in a matrix of plagioclase with minor pyroxene and biotite. Magnetite, rutile and sulphides occasionally occur as inclusions in chromites.

4.1.1 *Sample Description*

The samples examined originate from four drill cores of the Merensky Reef in the Eastern Bushveld Complex; two of the four boreholes originated from Modikwa Platinum Mine in the central sector (OV 777 and OV 778) while the other two (TRP 260 and TRP 271) was obtained from TRP Mine in the southern sector. The Merensky Reef is typically made up of the normal pyroxenite, which is the dominant pyroxenite occurring within the Merensky. The normal pyroxenite at both Modikwa and Two Rivers is comparable to that described by Cawthorn and Boerst (2006) as consisting of up to 80 vol % orthopyroxene, occurring as a subhedral to polygonal grains with interstitial plagioclase. Clinopyroxene and orthopyroxene grains appeared medium-grained, ranging between 2 to 3 mm in the normal pyroxenite (Cawthorn and Boerst 2006).

The two drill cores from Two Rivers (TRP 260 and TRP 271) showed the most dominant lithology found in the immediate hanging wall of the Merensky Reef (i.e. the spotted anorthosite). The investigated cores also demonstrated a normal Merensky Reef profile which is generally considered as a 1 m feldspathic pyroxenite sequence underlain by an anorthosite and bounded by top and bottom chromitite stringers or bands (Brynard *et al.* 1976; Davey 1992). The TRP drill cores showed high grade mineralization distributed around the chromitite stringers within the pyroxenite. The pyroxene grains appeared medium grained with average sizes of about 2 mm. The grain sizes of the orthopyroxene range between 2 and 6 mm. The anorthosite in this unit showed colour variations of white to cream-white and light grey to pinkish grey. The core log profile displayed a sharp contact between the Merensky Reef pyroxenite and the hanging wall spotted anorthosite. A zone of transition between the two lithologies occurs over a few cm, comprised of norite. This norite also revealed colour variations of light to dark grey instantaneously revealing a greenish tint which is thought to be chlorite.

In the Modikwa drill cores, the normal pyroxenite overlies the top chromitite stringer as seen in Figure 4.3. The top chromitite stringer either caps the Merensky Reef pyroxenite or is towards the upper parts of the normal pyroxenite within the Merensky Reef.

The top chromitite stringer is thinner than the bottom chromitite stringer (Figure 4.2). The lithological succession of the drilled core OV 778 from Modikwa showed leuconorite as the hanging wall succession underlain by a few cm of anorthosite, which then gradually transitioned into a chloritized norite showing a green tint (Figure 4.1). The chloritized norite showed orthopyroxene grains ranging from 2-3 mm in size. The anorthosite which is a regional marker, persistent throughout the Central sector was observed during field studies occurring at the base of the Merensky Reef and later grades into being pegmatoidal. Interstitial plagioclase and micas (such as biotite) were also present. The pyroxenite marked the footwall which later graded into a pegmatitic pyroxenite. Drill core OV 777 showed a pegmatoidal feldspathic pyroxenite that occurred directly between the basal chromitite stringer. This pegmatoidal feldspathic pyroxenite where developed it occurs sandwiched between the pyroxenite package and is not well developed (only about 3 cm thick) and is also barren.

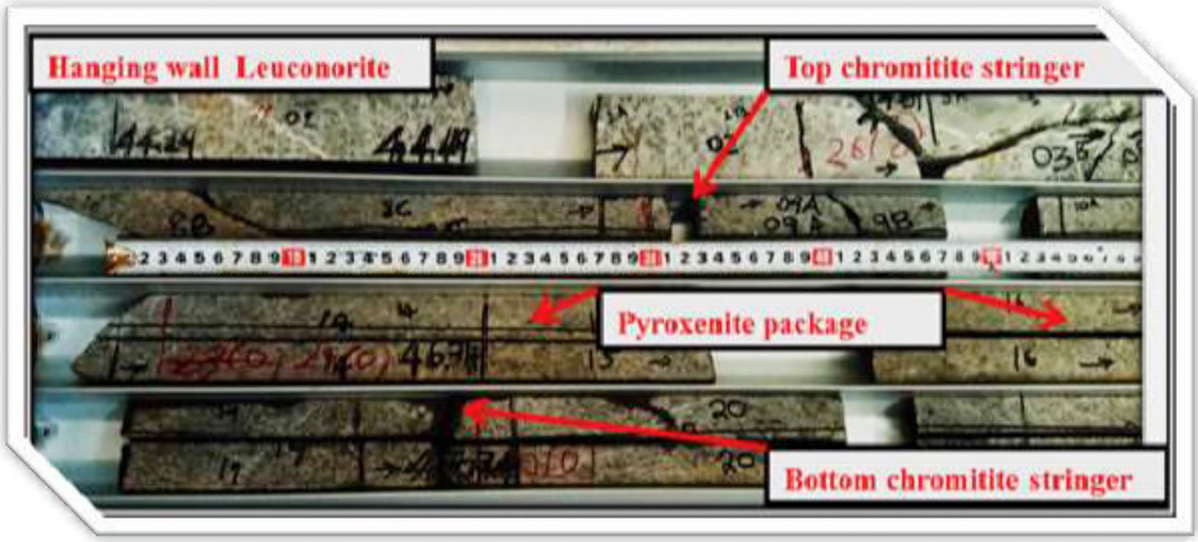

Figure 4.1: Drilled borehole core from farm Onverwacht 292 KT, OV 778.

In the two mines (Modikwa and Two Rivers), the BMS typically pentlandite (Pn), pyrrhotite Po), chalcopyrite (Ccp), and minor pyrite (Py) occur within the pyroxenite unit. The norite and anorthosite units are almost barren of the base metal sulphides. Disseminated sulphides occur throughout the Merensky Reef sequence.

The BMS occur as coarse-grained irregular granular aggregates. In places, pentlandite show exsolution flames in pyrrhotite, or as coarse-grained granular aggregates intimately intergrown only with pyrrhotite.

PGM occur as accessory minerals. In the Central sector of the Eastern limb, the section under investigation on the farm Onverwacht at the Modikwa showed the Merensky Reef has similarities with the Rustenburg wide reef facies in the Western limb of the Complex. In the Rustenburg wide reef facies, pegmatitic pyroxenite occurs usually in the footwall succession of the main mineralization, but is poorly mineralised as was the case at Modikwa. The mineralization at Lebowa mine (also known as Atok) together with that at Winnaarshoek has similarities to the mineralization at Modikwa in that, the main mineralization occurs in the pyroxenite between the two layers of chromitite that lie above the pegmatitic pyroxenite (footwall). In the Southern sector of the Eastern limb, the Merensky Reef in the farm Dwarsriver at Two Rivers display similar features corresponding to the Marikana facies of the Western limb of the Bushveld Complex, which also lacks the basal pegmatoidal pyroxenite (Rose *et al.* 2011). In all four drill core samples of this study, the Merensky Reef displays the most common mineralization pattern and is not disrupted by potholes, discordant bodies such as iron-rich-ultramafic pegmatoid, magnesian dunite pipe, faults and dykes. The highest PGE grades are intimately associated with the chromitite stringers.

4.2 **Ore Microscopy and Petrography**

The petrographic examination was undertaken in order to identify the textural variation and mineralogy associated with the ore. Ore microscopy and petrography are important tools for characterizing the ore mineralogy in terms of mineral association and textural relationships and variations. These powerful techniques are extensively utilised to provide parameters of exploration, production planning and for the improvement of process plant designs. Photomicrographs were taken from certain areas on the thin sections and on the ore mounts for description. These photomicrographs showed the Merensky Reef pyroxenite viewed under plane polarized light (PPL) and crossed polarized light (XPL). The work of MacKenzi *et al.* (1982) was used as a reference for mineral identification and the determination of igneous rocks and their textures, while the Table by Spry and Gedlinske (1987) was used as a reference for the determination of common opaque minerals.

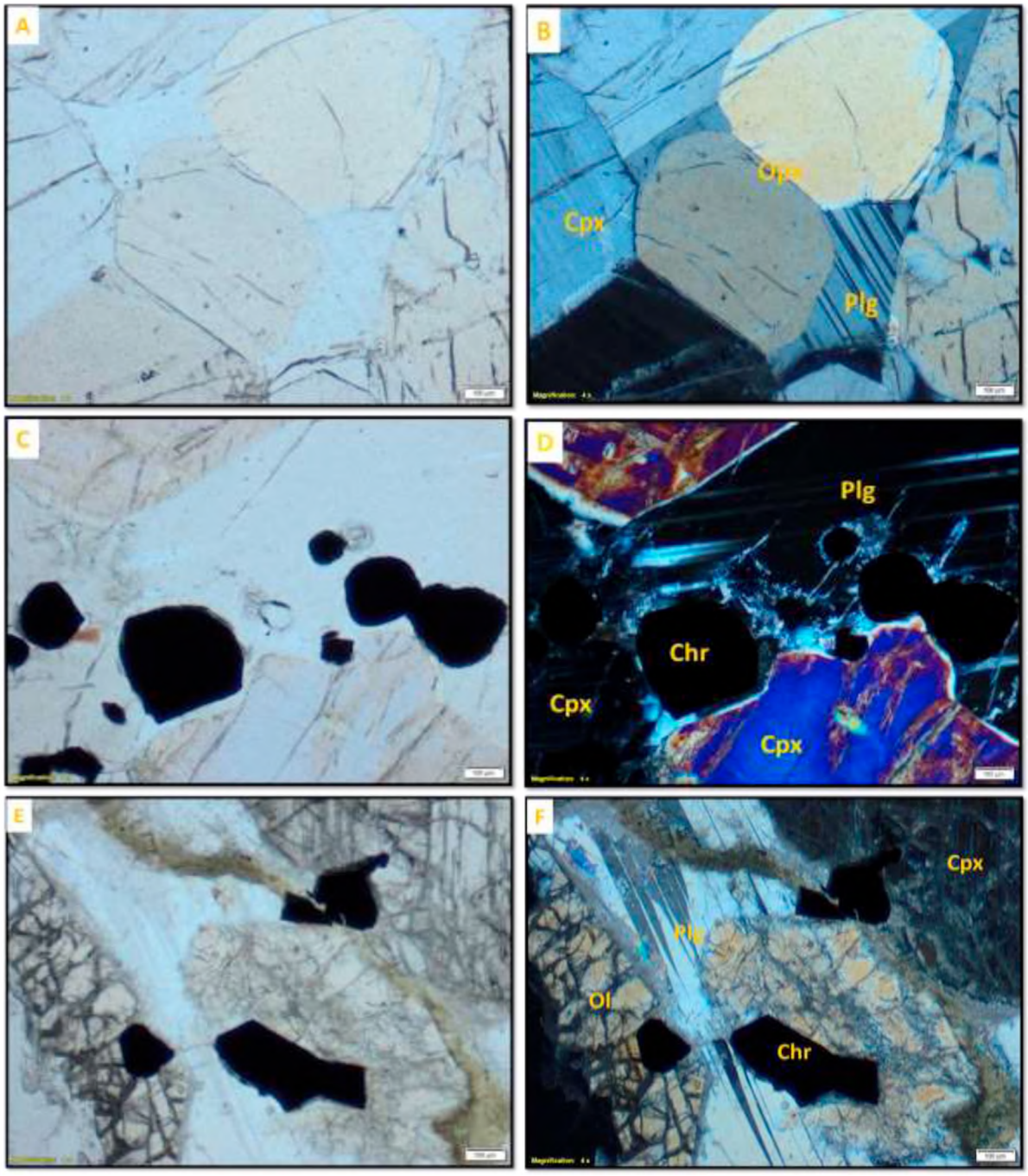

Figure 4.2: Photomicrographs of polished thin sections of selected samples taken from various boreholes of the Merensky Reef pyroxenite. Images are viewed under PPL and XPL. (A and B) show interconnected medium to coarse grained sub-hedral to euherdal phenocrysts of orthopyroxene (Opx) and clinopyroxene (Cpx). Plagioclase (Plg) is characterized by its strong parallel sets of albite twins. (C and D) show interstitial Plg in the chromitite stringer, note fine sericitisation of plagioclase. (E and F) show elongated olivine phenocrysts encountered in the feldspathic pyroxenite unit, note blebby Cpx microcrysts in Plg. (Drill core OV 777, Modikwa).

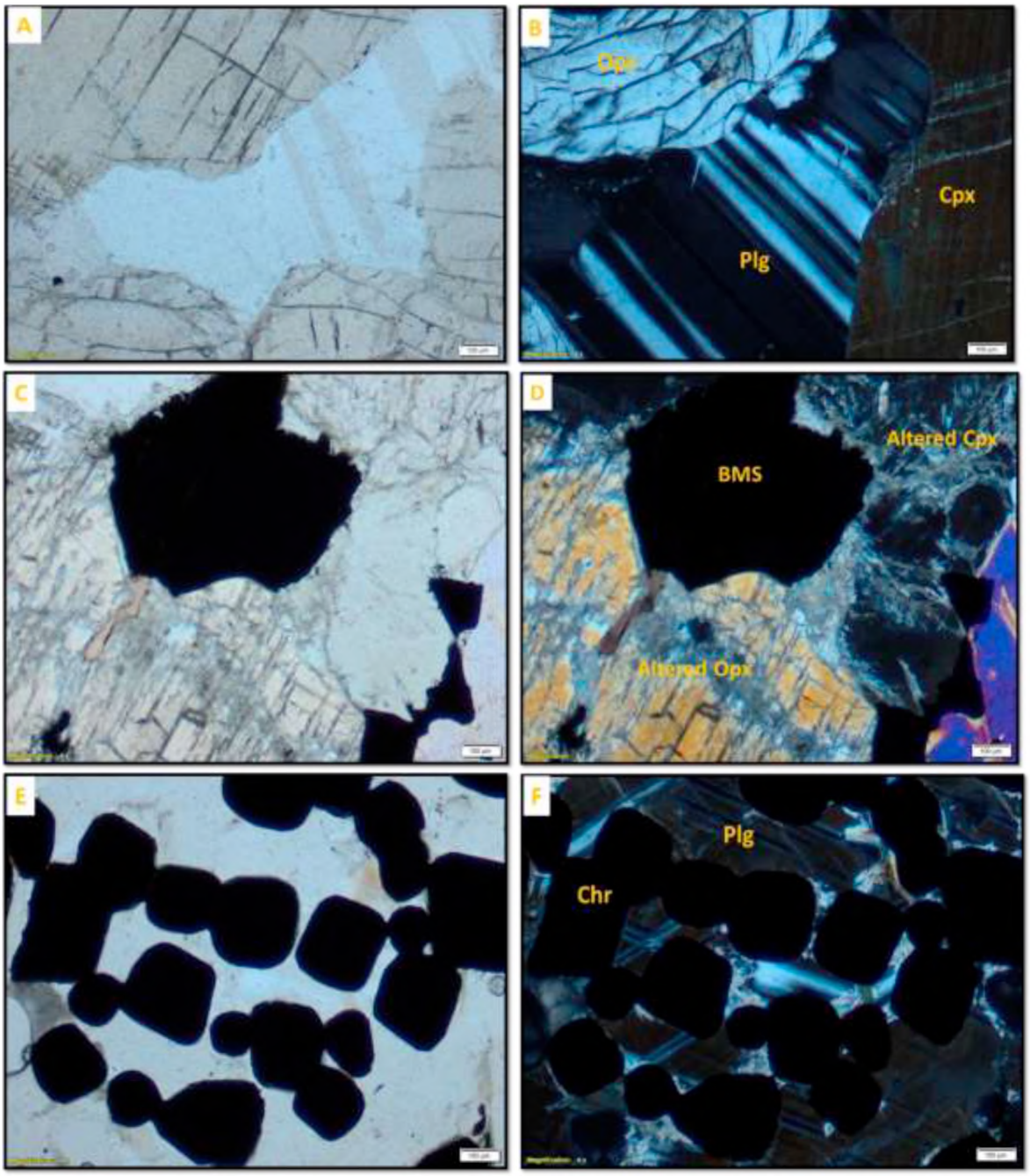

Figure 4.3: Photomicrographs of polished thin sections of selected samples from various boreholes of the Merensky Reef pyroxenite. Images are viewed under PPL and XPL. (A and B) are showing coarse grained anherdal phenocrysts of orthopyroxene (Opx), clinopyroxene (Cpx) and plagioclase (Plg). (C and D) show intensely altered Opx and Cpx phenocrysts accompanied by sericite. Base metal sulphides (BMS) are filling up the interstitial spaces. (E and F) display Plg hosting disseminated chromite (Chr), the grains do not exhibits a preferred orientation but are scattered throughout the section (Drill core OV 777, Modikwa).

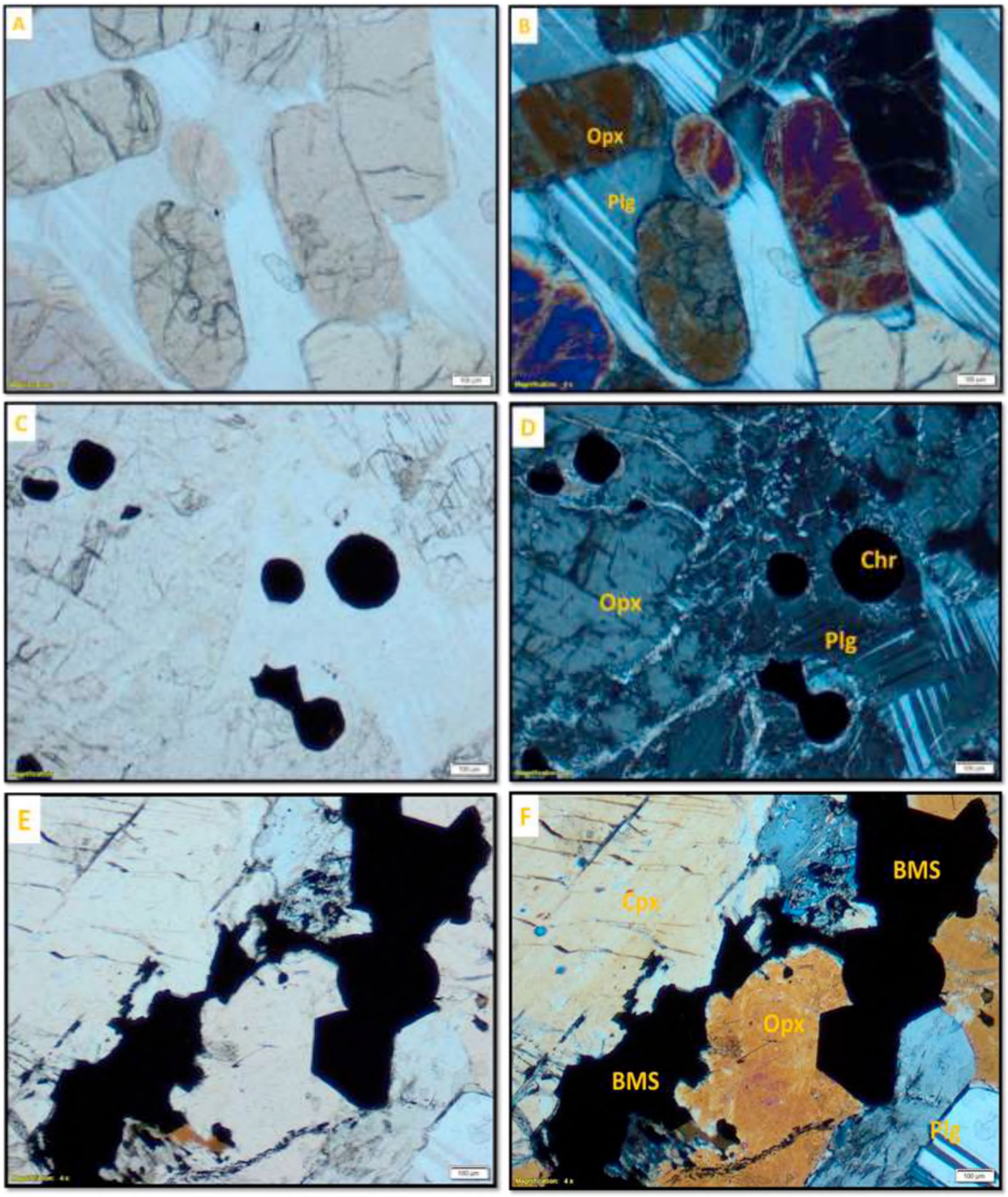

Figure 4.4: Photomicrographs of polished thin sections of selected samples from various boreholes of the Merensky Reef pyroxenite. Images are viewed under PPL and XPL. (A and B) are showing medium to coarse grained sub-herdal phenocrysts of orthopyroxene (Opx) in plagioclase (Plg) groundmass. (C and D) show chromite grains are scattered locally, exhibiting a round compact shape, sericite tend to fill up the microfractures. (E and F) display Cpx, Opx and Plg accompanied by anhedral crystals of base metal sulphides (BMS) and disseminated euherdal chromite grains. (Drill core OV 778, Modikwa).

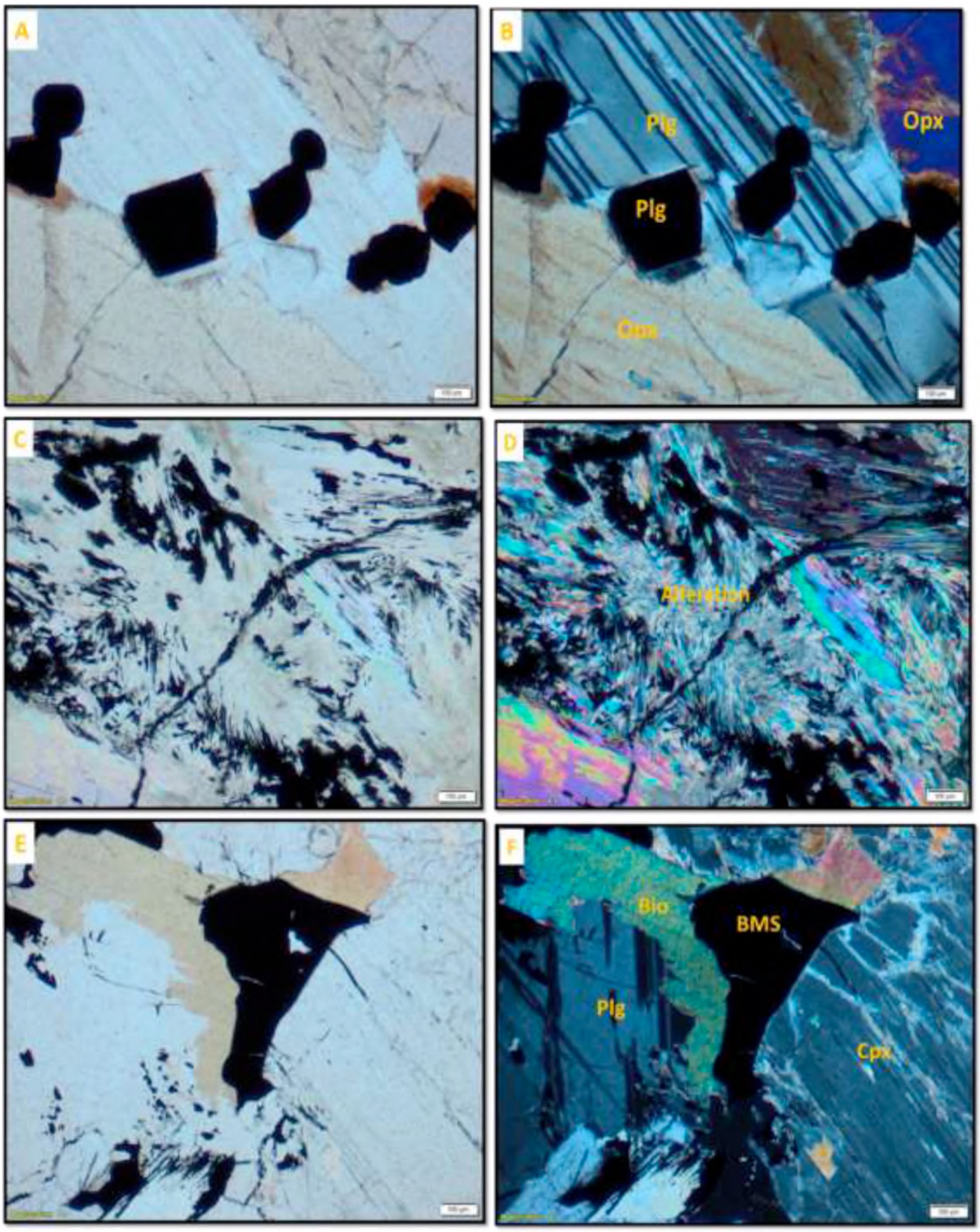

Figure 4.5: Photomicrographs taken from polished thin sections of selected samples from various boreholes of the Merensky Reef pyroxenite. Images are viewed under PPL and XPL. (A and B) shows Euhedral and rounded chromite grains hosted in plagioclase (Plg) matrix. (C and D) show highly altered zone that appears to have undergone low-grade metamorphism with muscivite, chlorite, talc, glaucophane and secondary BMS and oxides. The zone also composes of secondary oxide and base metal sulphides (BMS) minerals. (E and F) show a large phonecryst of clinopyroxene (Cpx), plagioclase (Plg) and biotite (Bio) in association with base metal sulphides (BMS). (Drill core OV 778, Modikwa).

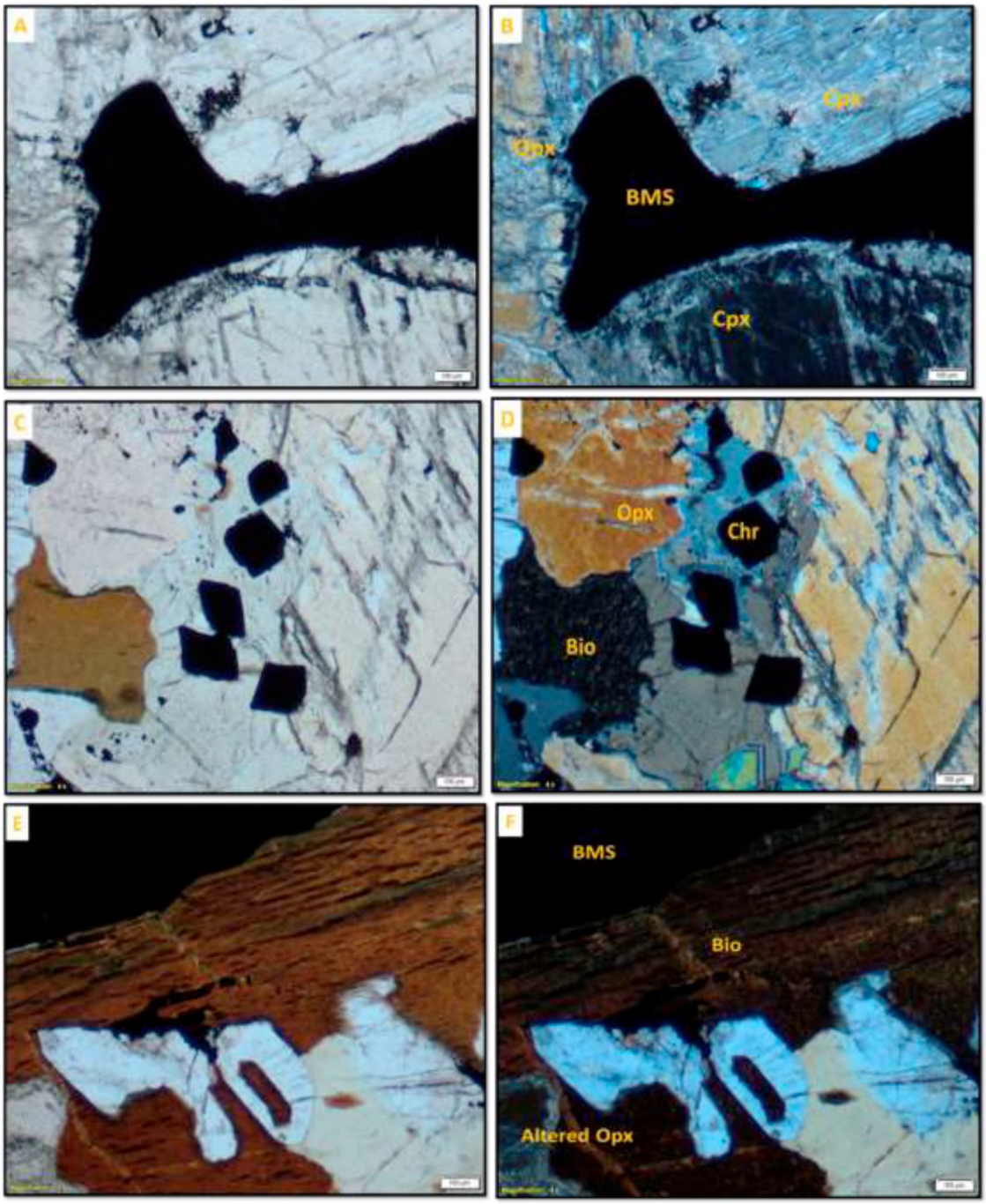

Figure 4.6: Photomicrographs taken from polished thin sections of selected samples from various boreholes of the Merensky Reef pyroxenite. Images are viewed under PPL and XPL. (A and B) show intensely altered phenocrysts of both orthopyroxene (Opx) and clinopyroxene (Cpx) accompanied by anhedral granular crystal of base metal sulphides (BMS) with a fish-like structure. Note sericite as a result of alteration of plagioclase. (C and D) show disseminated euhedral chromite grains hosted sub-ophitically in both Cpx and Opx phenocrysts. (E and F) display elongated to tabular flake of biotite (Bio) (Drill core TRP 260, Two Rivers).

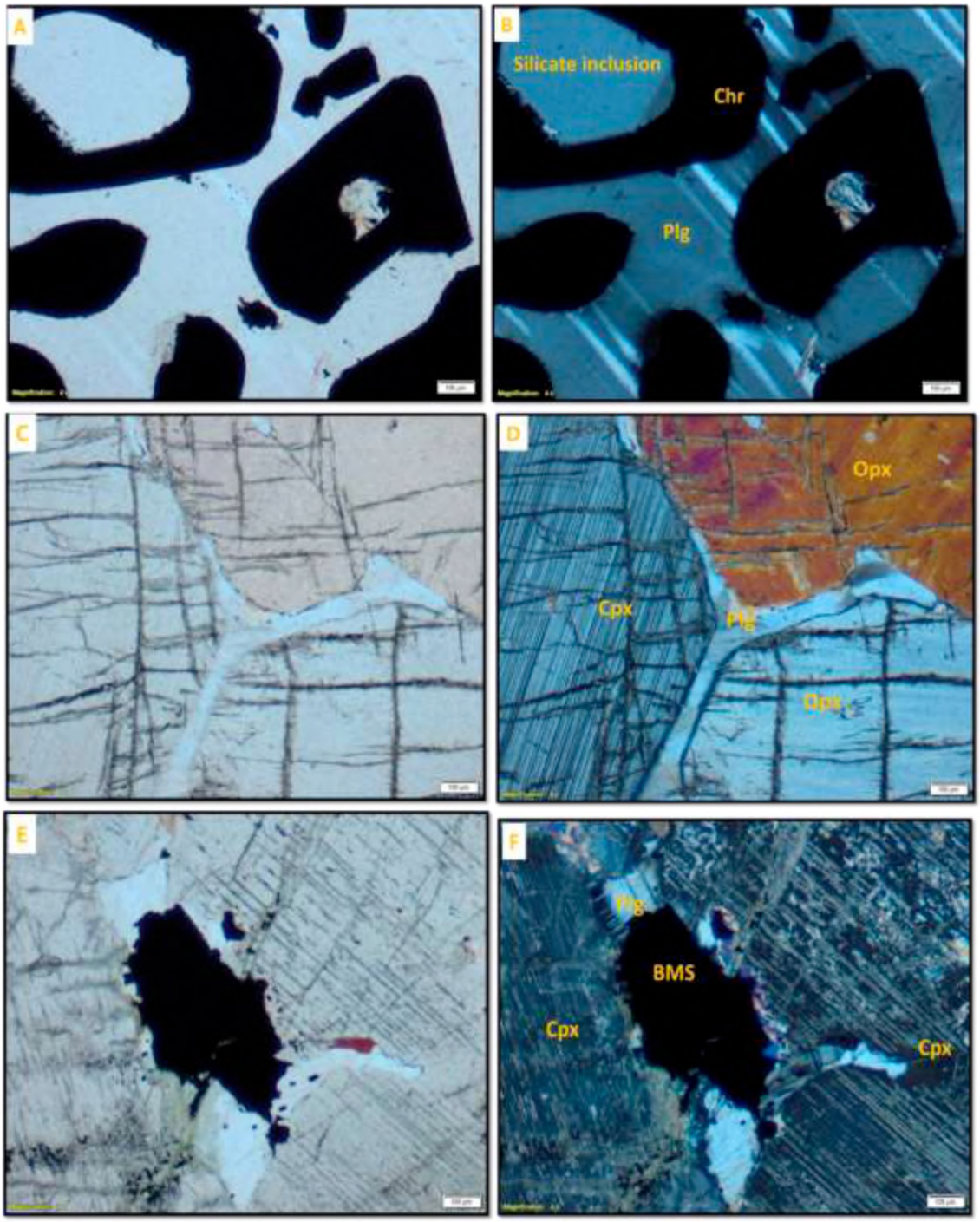

Figure 4.7: Photomicrographs taken from polished thin sections of selected samples from various boreholes of the Merensky Reef pyroxenite. Images are viewed under PPL and XPL. (A and B) show interstitial (Plg) hosting chromite (Chr) grains, inclusions of Plg inside Chr may suggest that the Chr is late in paragenetic sequence. (C and D) show medium to coarse grained sub-hedral to euhedral phenocrysts of clinopyroxene (Cpx) and orthopyroxene occurring interstitially with Plg. (E and F) display partially altered clinopyroxene phenocrysts, base metal sulphides display a well-developed triple point junction with Cpx (Drill core TRP 260, Two Rivers).

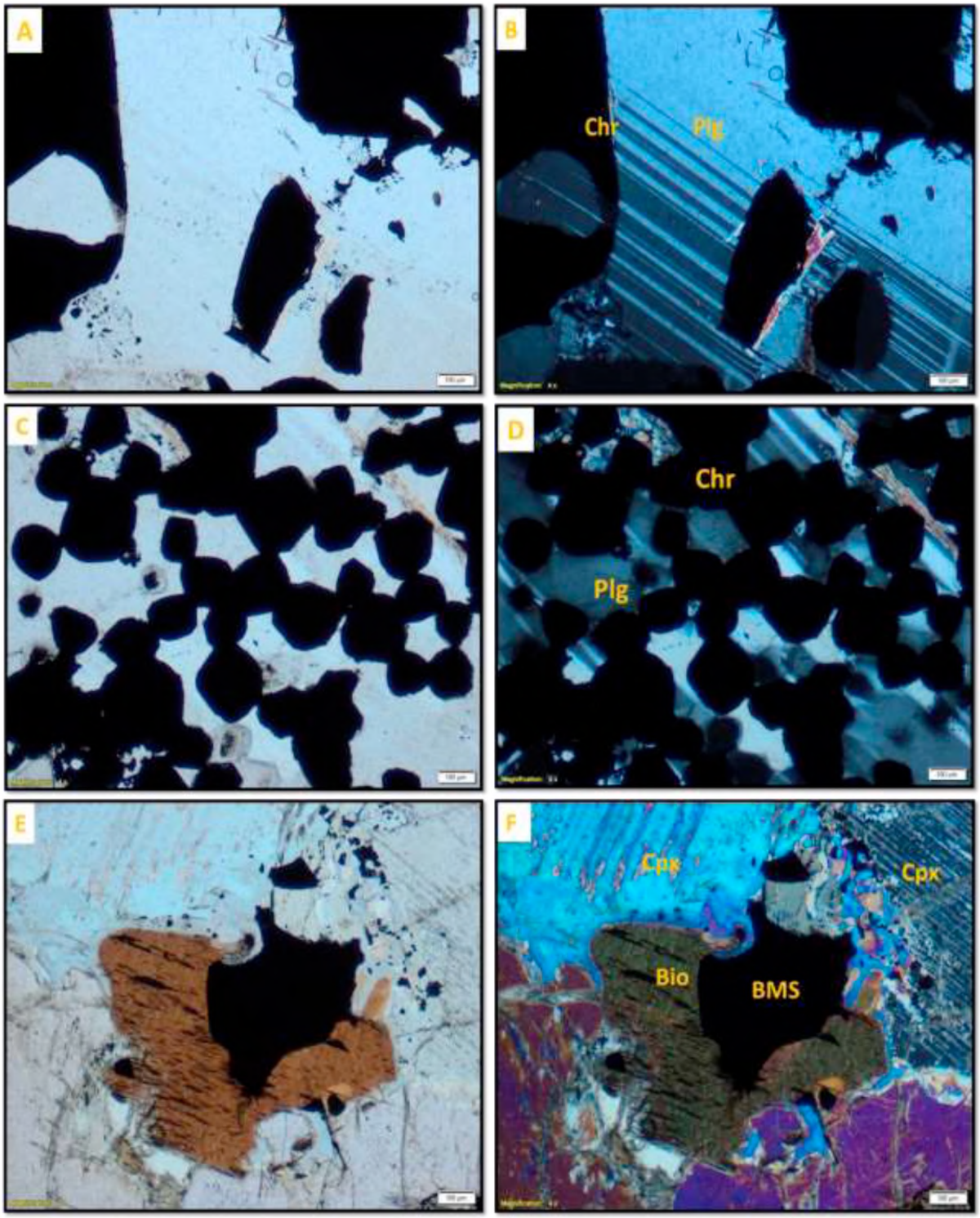

Figure 4.8: Photomicrographs taken from polished thin sections of selected samples from various boreholes of the Merensky Reef pyroxenite. Images are viewed under PPL and XPL. (A and B) show widespread albite twinning in plagioclase (Plg) hosting chromite (Chr) grains, note biotite along Chr margins. (C and D) display Plg hosting disseminated chromite (Chr), the grains do not exhibit a preferred orientation but are scattered throughout the section. (E and F) display partially altered clinopyroxene (Cpx) phenocrysts with biotite (Bio) occurring associated with anhedral base metal sulphide (BMS) (Drill core TRP 271, Two Rivers).

4.2.1 *Petrography*

Generally, in the four investigated drill cores, the BMS mineralization occur either distributed widely throughout the pyroxenite units (Figures 4.6 A and B; 4.3 C and D; 4.8 E and F) or within or adjacent to the chromitite stringers (Figures 4.4 E and F; 4.8 C and D). Orthopyroxene (Opx) crystals accumulate in loose sometimes tight mutual contact and an intercumulus liquid of plagioclase fills the interstices (Figures 4.2 A and B, 4.4 A and B). Poikilitic plagioclase grain appear enclosing euhedral or sometimes subhedral to elongated orthopyroxene grains (Figures 4.7 C and D; 4.4 A and B). In places orthopyroxene and clinopyroxene (Cpx) occur at irregular intervals exhibiting sub-rounded sometimes rounded to euhedral grains. Elongate grains of orthopyroxene are commonly noted, particularly at Modikwa (Figures 4.7 C and D; 4.4 A and B). The clinopyroxene occasionally occurs both as an intercumulus and cumulus phase while in places it occurs as a minor component (Figures 4.7 E and F). Given that the pyroxenite unit had encountered persistent alteration, orthopyroxene grains are replaced along cracks by BMS and sometimes by amphibole and/or serpentine in places. Another type of alteration present includes sericitisation, where the interstitial plagioclase is replaced by fine grained sericite (Figures 4.2 C and D; 4.3 E and F). Clinopyroxene and orthopyroxene show similar morphology, particularly under plane polarized light (Figures 4.2 A and B and 4.7 C and D). However, clinopyroxene commonly shows exsolution lamellae of orthopyroxene (Figure 4.7 C and D). It was also encountered as inclusions and as blebs or exsolution lamellae within the orthopyroxene. Biotite was observed as tabular flakes at varying grain sizes and is commonly associated with BMS (Figures 4.7 E and F and 4.8 E and F) and relatively more abundant in samples from the TRP compared to Modikwa.

In the pegmatoidal feldspathic pyroxenite unit in samples from Modikwa, olivine occurs commonly elongated to amoeboid in crystal shape with orthopyroxene (Figure 4.2 E and F). In places olivine is observed exiting a rounded morphology and is commonly fractured. Pegmatoidal feldspathic pyroxenite occurs just below the top chromitite stringer in the normal pyroxenite, but is not well developed (Figure 4.2 E and F), note that the pegmatoidal is only present in Modikwa drill cores OV 777. The selected thin sections show olivine in the process of being replaced by serpentine with cracks filled in by secondary BMS. Chromite grains are disseminated within pyroxenes (Figures 4.6 C and D; 4.3 E and F) and the intercumulus plagioclase (Figures 4.5 A and B; 4.8 A, B, C and D). Disseminated chromite grains do not exhibit a preferred orientation but are scattered throughout the section.

The chromite grains occur mostly as euhedral, rounded to sub-rounded morphology and commonly rimmed by mica, mostly biotite and/or muscovite (Figures 4.2 C and D; 4.8 C and D). Clusters of chromite grains exhibit a triple point junction in places, which is characteristic of the thicker layers according to Eales and Reynolds (1986). In a similar manner, the BMS display a well-developed triple point junction with clinopyroxene (Figure 4.7 E and F). In most cases recrystallization causes the coalescing grain boundaries to form into triple point junction observed from these crystals. Inclusions of plagioclase in chromite were also noted and may suggest that chromite is late in paragenetic sequence. Increased plagioclase contents were observed in the range of chromitite stringers however decrease in plagioclase content below and above chromitite stringers (Figures 4.5 E and F; 4.8 E and F). The top chromitite stringers (approximately 4-5 mm thick with an average of 2 mm) are much thinner (Figures 4.5 C and D; 4.6 C and D) and not well developed compared to the bottom chromitite stringers (Figures 4.3 E and F; 4.8 C and D). Altered silicates observed include serpentine, talc, amphibole, and in places, a mixture of fine netted mass of randomly oriented muscovite and chlorite microphenocrysts. Quartz and magnetite were observed at minor amounts.

4.2.1.1 Comparison between Modikwa and Two Rivers

There are two types of pyroxenite units that occur in the Merensky Reef sequence; the normal pyroxenite and pegmatiodal feldspathic pyroxenite. Mineralogically, the two units are alike; but only differ in their grain sizes (e.g. orthopyroxene grains vary between 3-5 mm in the feldspathic pyroxenite and up to a few cm in pegmatoidal feldspathic pyroxenite).

The studied drill cores (TRP 260 and TRP 271) from Two Rivers reveal similar characteristics to the drill cores of Modikwa (OV 777 and OV 778) in regard to the texture and mineralogy of the Merensky Reef pyroxenite sequence. The two locations show some variation in silicate phases present. The orthopyroxene appear as a cumulus phase while plagioclase appear as intercumulus phases. Clinopyroxene mostly appear as blebs or inclusions within the orthopyroxene at both mines. In both mines, Modikwa and TRP, the two chromitite stringers, top and bottom, are present and located within the normal pyroxenite. Chromite grains are more often rimmed by mica, biotite and/or muscovite. However, sericite was observed along chromite grain boundaries while in places a mixture of fine netted mass of randomly oriented muscovite and chlorite microphenocrysts were identified pointing to alteration processes.

In all four studied drill cores an occurrence of the interstial plagioclase is common. The association of chromite with plagioclase and pyroxene members occur in three main forms; (1) interstitial plagioclase occurring as inclusions in chromite (2) chromite occur as inclusions in the orthopyroxene and (3) chromite scattered though out the pyroxene unit and in association with BMS. The BMS often occur interstitial to the orthopyroxene grains and sometimes in association with chromite. In some places they were observed replacing plagioclase while in other places appeared filling up the cracks in the orthopyroxene but commonly disseminated throughout the Merensky pyroxenite. The olivine shows a noteworthy elongated amoeboidal texture and also showed a strong preference for the pegmatiodal pyroxenite unit which is only identified in drill core OV 777 from Modikwa and literally absent in drill cores from TRP.

Altered silicates were recorded occurring as minor to trace amounts and include serpentine, talc, amphibole, mica and chlorite. The two Reefs (Modikwa and TRP) generally appear to be highly affected by alteration of silicates. The Winnaarshoek facies occurring in the Central sector of the Eastern Bushveld suggest more passive formations and lower temperatures.

4.2.2 ***Ore Mineralogy***

The BMS at Modikwa and Two Rivers Platinum mines include chalcopyrite (Ccp), pentlandite (Pn), pyrrhotite (Po) and minor pyrite (Py). They show a variety of grains sizes and occur as medium to coarse grained crystals. The petrographic results revealed that BMS occur in both the normal pyroxenite and pegmatoidal feldspathic pyroxenite units. The BMS occur in immediate contact with the interstitial silicates and often associated with mica and disseminated chromites, in places. Broadly, BMS appear as; large multi-mineralic sulphides with blebs (up to several mm), smaller mono-mineralic sulphides with blebs and also as disseminated sulphides. The sulphide blebs consist of minerals pyrrhotite, chalcopyrite and pentlandite and generally showing irregular shapes and variable complex patterns of replacement textures.

4.2.2.1 Textural relationship

Silicates and BMS

It is observed that the only characteristic that the gangue minerals have in common is their association with sulphides. Features observed include extinction and deformation twins in

the plagioclase and as well as indented faces between the orthopyroxene grain boundaries. These features are suggestive of the movement of grains and plastic deformation through the period of compaction. The association of plagioclase with biotite could be related to post compaction crystallization. The orthopyroxene is the most dominant silicate in the two Reefs, and reveals coarser grain sizes forming interconnected grain to grain boundaries in places. Orthopyroxene grains do not form interlocking crystals with BMS; therefore minerals are likely to show good liberation if milled finely enough. In places orthopyroxene shows alteration into fine grained talc aggregates. The replacement orientation occurs adjacent to the contacts between silicate and sulphides grains. The petrographic observations suggest that sulphides and associated PGM formed after primary silicates, where sulphides liquid would infiltrate into the silicate crystal slurry filling up the accessible interstial spaces. The textural relationship between the minerals exhibit a genetic relationship between BMS and PGMs was observed.

Base Metal Sulphides

Pentlandite (Ni, Fe)$_9$ S$_8$: Occurs as a fine to medium grained light yellow cream exhibiting various shapes of elongated, irregular to euhedral crystals. There are two types of pentlandite observed; (1) the coarse grained pentlandite, granular in texture, intimately intergrown with chalcopyrite and pyrrhotite, this main type is present in Figures 4.9; 4.10 C and D. (2) pentlandite occurs as exsolution flames in pyrrhotite and chalcopyrite, this type is occasionally observed in Figure 4.19 E and F. The pentlandite tends to occur as a multi-mineralic sulphide as observed in Figures 4.9 C; 4.10 A, B and C. Pentlandite also occurs as irregular; anhedral to euhedral sometimes rounded crystals (Figures 4.9; 4.10 A, B C), revealing textures of intergrowths, particularly in pyrrhotite (Figure 4.10 A, C) and marginally in chalcopyrite (Figure 4.10 B). In some places it has been observed to fill the interstices between chromite grain boundaries (Figures 4.9 D and E; 4.10 E). Pentlandite occurs as relatively granular crystals (Figure 4.9 A, B and D) with minor inclusions and microfractures. The abundance of pentlandite is more than that of chalcopyrite.

Chalcopyrite (Cu FeS$_2$): Occurs mostly as fine to medium grained yellow anhedral crystals often intergrown with pentlandite (Figure 4.10 A, B, C and D) and pyrrhotite (Figure 4.9 A and B) or frequently as single residual grains associated with chromite grains (Figures 4.9 B and 4.10). The amount of iron content varies. Chalcopyrite often occurs as fine grained

monomineral (Figure 4.10 F) or as multi-mineralic sulphide blebs and or overgrowths (Figure 4.10 A-D). It often exhibits complex textures of replacement preferentially along margins of either pyrrhotite or pentlandite (Figures 4.9 A and C).

Pyrrhotite (FeS-$Fe_{1-x}S$): Pyrrhotite occurs as coarse grained granular pinkish brown crystals oftenly associated with pentlandite and chalcopyrite. Pyrrhotite is the most abundant sulphide type within both Modikwa and TRP. It also shows successive replacement by pentlandite as shown in Figure 4.9 B. Pyrrhotite appears to host other sulphides however it also occur as blebs together with chalcopyrite in pentlandite. Silica inclusions are abundant in pyrrhotite grains indicating growth outward in all directions. Successive recrystallisation was noted where pentlandite grains occur included within pyrrhotite but mineral grain sizes are not the same.

Pyrite (FeS_2): It occurs intimately with pentlandite, chalcopyrite and pyrrhotite. Pyrite is highly stoichiometric and forms a minor component of the sulphides.

Oxides

Magnetite

Magnetite is present in the pyroxenite unit in variably minor quantities as anhedral to skeletal crystals dispersed throughout and replacing BMS in places. A possibility for magnetite formation could involve processes such as oxidation and desulfurization of the primary sulphides.

Chromite

Chromite often occurs as dark grey euhedral and rounded to sub-rounded grains in aggregates associated with BMS, with pentlandite, commonly filling up the interstices in between grain boundaries (Figures 4.9 D and E; 4.10 E). Chromite occurs regularly as disseminated grains in various shapes (Figure 4.10 A). In some places the euhedral grains reveal annealed texture of recrystallization within the plagioclase matrix.

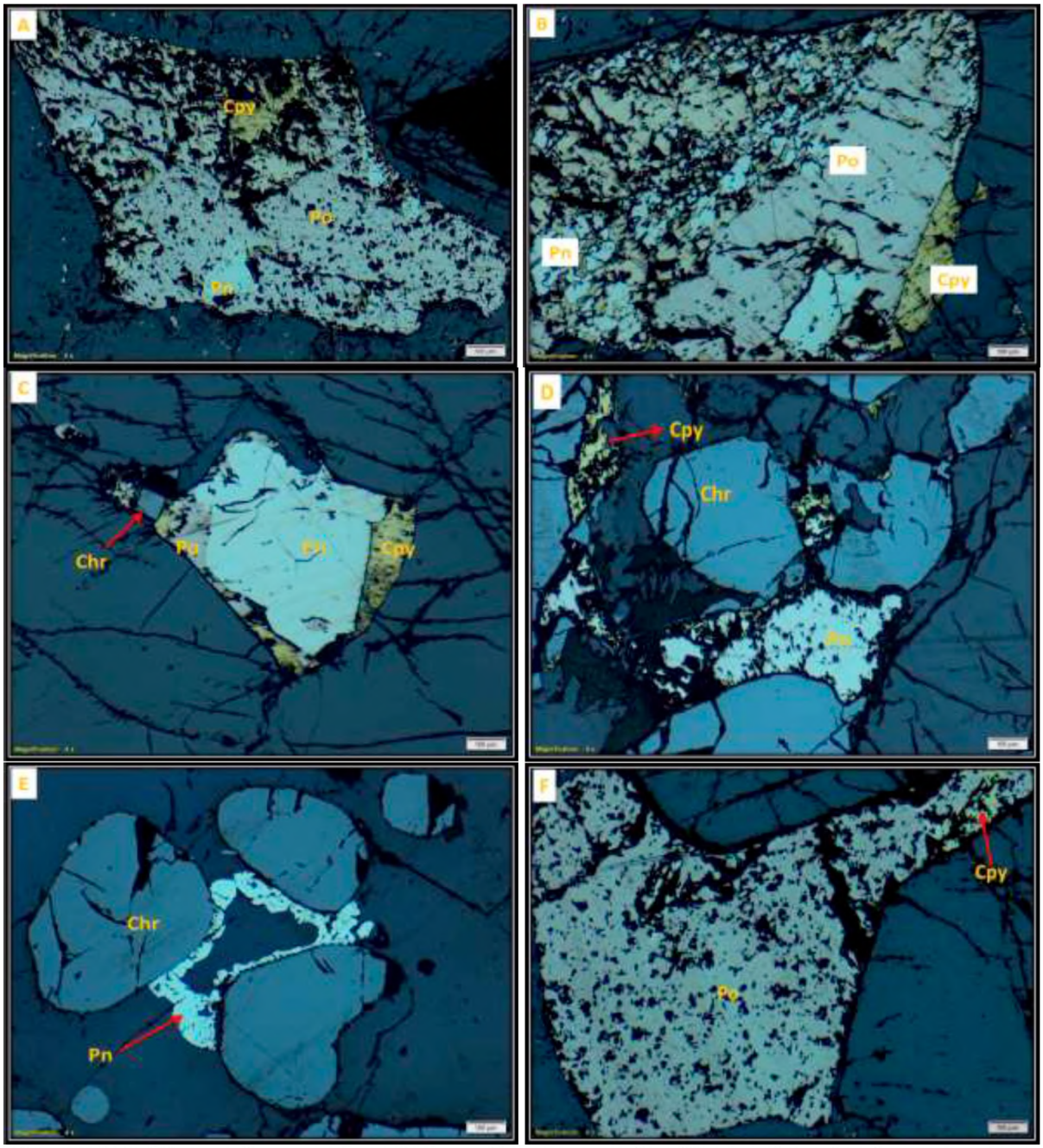

Figure 4.9: Photomicrographs of the selected samples illustrating the important ore characteristics of the Merensky Reef pyroxenite. Images are viewed under reflected light (RL). Image (A) shows anhedral to euhedral derfomed granular grain of pyrrhotite (Po, darker grey to brownish pink) appearing invaded by chalcopyrite (Ccp, yellow). Image (B) show an intensely deformed aggregate of pyrrhotite with pentlandite (Pn, lighter yellow to creamish-white) phases and well-developed overgrowths of chalcopyrite. Image (C) shows an aggregate of coarse-grained pentlandite showing patterns of marginal replacement by chalcopyrite. Image (D) shows a top chromitite stringer in association pentlandite and chalcopyrite. Image (E) shows pentlandite exhibiting triple point junction. Image (F) show a coarse grained granular grain of pyrrhotite with blebs of chalcopyrite. Note the multiple inclusion of earlier formed silica in sulphides. It appears that the inclusions were incorporated and stretched as the pyrrhotite matrix flowed under pressure. (Drill core TRP 260 and 271, Two Rivers).

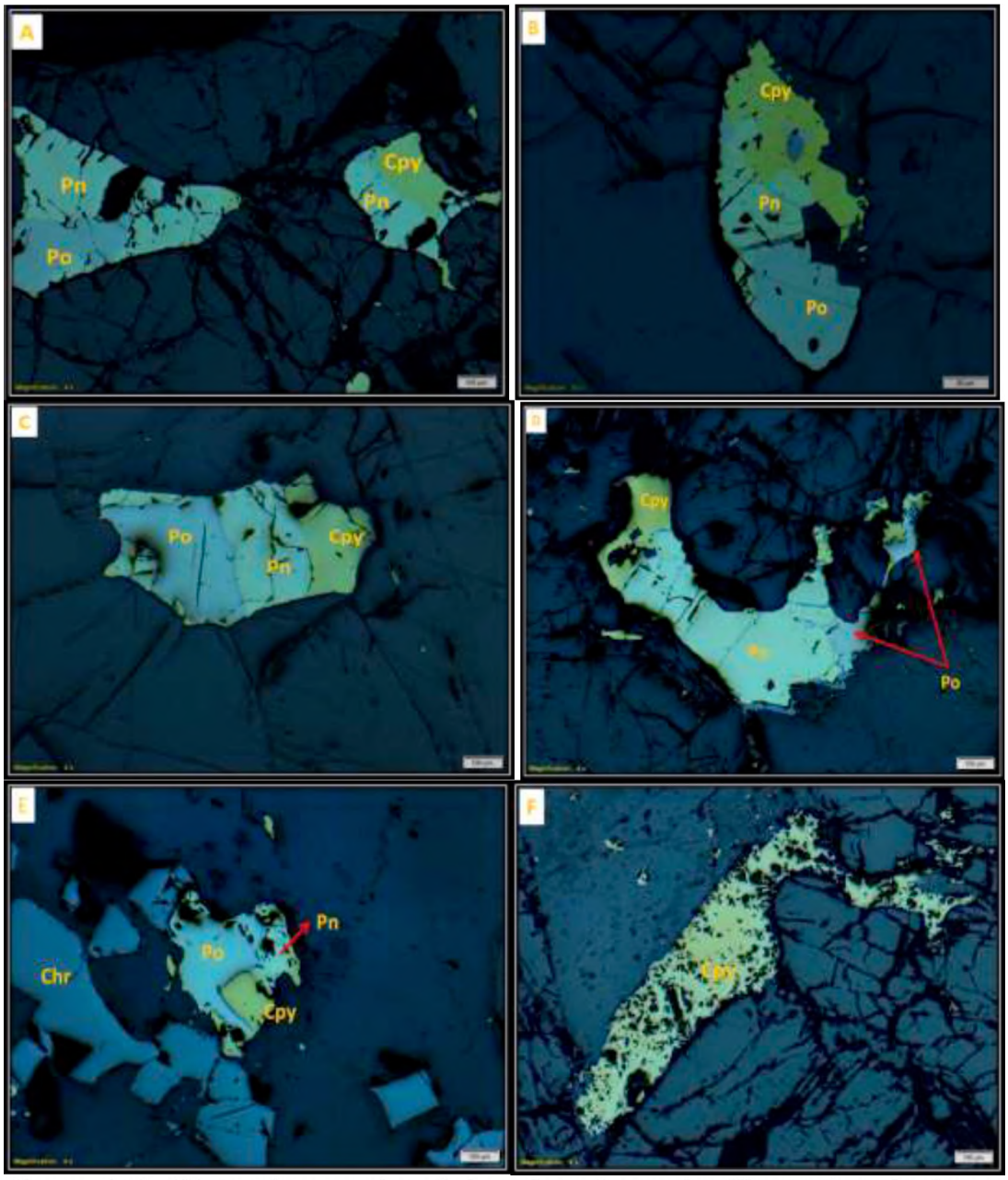

Figure 4.10: Photomicrographs of the selected samples illustrating the important ore characteristics of the Merensky Reef pyroxenite. Images are viewed under reflected light (RL). Image (A) shows anhedral pentlandite (Pn, light yellow to creamish yellow) in the process of being replaced by pyrrhotite (Po, darker grey to brownish pink) and by chalcopyrite (Ccp, yellow). Image (B) shows pentlandite in the process of being reaplced by both ptrrhotite and chalcopyrite. Image (C) shows a medium grained intergrown of pyrrhotite and chalcopyrite with pentlandite. Image (D) shows pentilandite with flame-like exsolutions of chalcopyrite. Image (E) shows a bottom chromitite stringer in association with an aggregate of sulphides composing of pyrrhotite, pentlandite and chalcopyrite. Image (F) show an elongated grain of chalcopyrite multiple inclusions of which appear to have been incorporated during crystal growth. (Drill core OV 777 and 778, Modikwa).

4.2.2.2 Comparison between BMS at Modikwa and Two Rivers

The petrography for both Modikwa and Two Rivers showed that the BMS occur in immediate contact with the silicates or closer to the disseminated chromite grains in places. Commonly they also occur associated with orthopyroxene, clinopyroxene and within the interstitial plagioclase or dispersed in the pyroxenite unit. In a few cases the sulphides appear to fill up the interstices between chromite grains pointing to injection of a later phase (Figures 4.9 D and E; 4.10 E). Generally the two Reef types highlighted a broad range of sulphide textures and grain sizes and though not every case, pyrrhotite has been observed to be more abundant than pentlandite which is more abundant than chalcopyrite.

The principal difference between the four studied drilled cores is the grain size distribution of sulphide ores, which appeared coarser in the TRP samples relative to those taken from Modikwa. Craig (2001) suggested that the finer grain sizes tend to form under low temperature conditions while larger crystals form under higher temperature conditions. In places; samples showed magnetite association in minor proportions to the BMS at both Modikwa and TRP.

The type of intergrowth predicts liberation of particles after milling and crushing. For example in Figure 4.10 C, D and E grains appear locked in whereas in Figure 4.9 A and B pentlandite grains appear included within the pyrrhotite thus separation may be difficult to achieve. At Modikwa liberation is likely to be moderate to good as most minerals show straight common boundaries are commonly locked. At TRP the contact boundaries between grains appear more complicated with interpenetration. In cases where complex patterns of replacement textures like intergrowths and exsolutions of chalcopyrite in pyrrhotite, liberation will be extremely difficult unless fine milling is undertaken. Replacement textures appear to commonly progress along fractures and grain boundaries, and penetrating along these locations of weaknesses. In Figure 4.9 B, pyrrhotite is been coated by an intergranular rim/overgrowths of chalcopyrite, and in this case poor liberation is predicted. In some places there is no evidence of replacement textures between sulphide grain boundaries suggesting that grains crystallized most probably at the same time (mutual replacement).

In general at TRP pyrrhotite is coarser compared to other sulphides (pentlandite and chalcopyrite) while at Modikwa pentlandite appears to be the coarsest.

The different sulphide grain sizes observed in this study could be related to the interconnectivity of interstitial spaces between pyroxene and plagioclase leading to different sulphide grain sizes. Multiple inclusions of other unknown opaque minerals and earlier formed silicates in BMS are abundant at TRP and slightly reduced at Modikwa.

It appears that the inclusions were incorporated and stretched during crystal growth. Most of the sulphides occur as multi-mineralic crystals, with majority of the crystals appearing invaded by further events that resulted in changing their crystal shape and dissolved the crystals in places to form cavities. Additionally, grains also appear fractured while in places, some grains were observed revealing textures of near complete replacement.

Table 4.1: Summary of the commonly occurring minerals in the Merensky Reef at Two Rivers and Modiwa Platinum Mines

	Minerals	Two Rivers			Modikwa		
		Abundance	Crystal shape	Mode of occurrence	Abundance	Crystal shape	Mode of occurrence
Primary Silicates	Orthopyroxene	Major	Round, euhedral to subhedral	Closely packed or sometimes dispersed	Major	Elongated, round, euhedral to subhedral	Closely packed or sometimes dispersed
	Clinopyroxene	Major	Anhedral	Contain exsolution lamellae of orthopyroxene	Major	Anhedral sometimes large	Contain exsolution lamellae of orthopyroxene
	Plagioclase	Major	Elongated to irregular laths	Interstitial	Major	Elongated to irregular laths	Interstitial
	Olivine	Minor	Elongated granular masses or rounded grains	Fractured & exhibiting replacement textures	Minor	Granular masses or rounded grains	Fractured and revealing replacement textures
Secondary /Alteration Silicates	Serpentine	Minor-trace	Flat and tabular crystals	Isolated or as in fillings in orthopyroxene cracks	Minor-trace	Veins and tabular	Isolated or as in fillings in orthopyroxene cracks
	Amphibole	Minor-trace	subhedral to anhedral masses/ fibrous	Commonly replacing orthopyroxene	Minor-trace	subhedral to anhedral/ fibrous	Commonly replacing orthopyroxene
	Chlorite	Minor-trace	Thin netted	Randomly oriented microphenocrysts	Minor-trace	Thin netted	Randomly oriented microphenocrysts
	Mica*	Minor	Fine netted microphenocrysts	Tabular or flaky	Minor-trace	Fine netted microphenocrysts	Tabular or flaky
	Sericite	Minor	Fine microcrystalline	Fine microcrystalline commonly replacing plagioclase	Minor	Fine microcrystalline	Fine microcrystalline commonly replacing plagioclase
	Clay (Talc)	Minor-trace	Fine phenocrysts	Locally scattered & appear similar to mica	Minor	Fine grained	Occur as aggregates
Oxides	Chromite	Minor	Euhedral, round to subrounded	Disseminated and Masive	Minor	Euhedral, round to subrounded	Disseminated and Masive[2]
	Magnetite	Minor-trace	anhedral to euhedral	Associated with sulphides	Minor-trace	anhedral to euhedral	Associated with sulphides
Base Metal Sulphides	Pyrrhotite	Minor	anhedral to euhedral & granular	Hosting other sulphides, with abundant silica inclusions	Minor	anhedral to euhedral granular	A host of other sulphides, with abundant silica inclusions
	Pentlandite	Minor-trace	Anhedral, euhedral to subhedral	Occurs as overgrowths/ intergrowths within pyrrhotite	Minor-trace	Anhedral, euhedral to subhedral	Occurs as blebs/overgrowths and orintergrowths within pyrrhotite
	Chalcopyrite	Minor-trace	Anhedral to subhedral	Occurs as blebs/overgrowths in pyrrhotite and pentlandite	Minor-trace	Anhedral to subhedral	Occurs as blebs/overgrowths in pyrrhotite and pentlandite
	Pyrite	Trace	Euhedral	Not common	Trace	Euhedral	Not common

[1] Muscovite and biotite
[2] Bottom Chromitite stringer

4.3 Paragenesis

Paragenesis is the successive order of formation of a group of associated minerals within a particular deposit in terms of when they formed. This is a principal feature associated with identification and textural characterization of minerals in ore deposits (Craig 1994).

Ores such as BMS oxidise in situ, and therefore paragenesis in terms of degree of oxidation is relevant for mineral beneficiation and extraction. For example, if ores are oxidised, the oxide mineral may rim or coat the outer sulphide grain boundary, hindering flotation.

However, sulphide ores are amenable to floatation. Additionally, mixed ores require double treatment either using oxide float or sulphide float, or both leaching and flotation.

The ore microscopy studies revealed numerous complex textures at varying degrees of oxidation as a function of changing temperatures. It is also unlikely that only one texture observed can provide enough evidence about paragenesis, all the observed textures are therefore important particularly for liberation purposes. From the textural associations observed in the Merensky Reef at both Modikwa and TRP, it can be inferred that, orthopyroxene, olivine and plagioclase crystals formed earlier than BMS. Most descriptions of the Merensky Reef refer to orthopyroxene a cumulus mineral while plagioclase is intercumulus (commonly up to 30 %). This is supported by observations in Figures 4.2 A and B; 4.6 A and B where plagioclase and/or orthopyroxene crystals accumulate in loose mutual contact and an intercumulus liquid fills the interstices (plagioclase in this case). This would therefore suggest that the interstitial plagioclase observed in these studies indicates that orthopyroxene formed earlier than plagioclase. Additionally, othopyroxene crystals exhibit euhedral shapes and appear to have grown unobstructed due to early growth within magma. However, the textural observations alone are inconclusive as the extensive textural annealing occurred in these rocks. As observed in Figures 4.3 A and B; 4.5 A and B, where plagioclase appears cumulus, it could be possible that plagioclase grains originally existed. The sequence of deposition shown by these gangue minerals suggests that they formed during the period of crystallization of Merensky Reef. The orthopyroxene can be easily liberated since crystals habit does not reveal any interlocking patterns and mostly occur as single grains. Moreover, the work of Seabrook *et al.* (2005), documented that the presence of cumulus plagioclase with a Critical Zone signature in the pyroxenites suggests that plagioclase sank with orthopyroxene as composite mineral clusters.

Alteration of silicates was noted in this study, including minerals like serpentine, which is most likely an alteration product of olivine, although, could possibly be of orthopyroxene. Talc is common alteration product of orthopyroxene occurring mostly along the rims of orthopyroxenes and occur as talc-aggregate in selected samples from Modikwa.

The presence of talc has been reported as the most problematic as it can cause significant process difficulties (Penberthy 1999).

Amphibole crystals where observed appear as medium subhedral crystals suggesting either to be an early secondary mineral or representing completely replaced orthopyroxene. Chloritisation of minerals such as biotite and clinopyroxene was noted and is thought to be as a result of metasomatism, forming in a variety of styles under different conditions. Chloritisation is commonly associated with low-temperature metamorphism, while formation of muscovite/sericite could be as result of hydrolysis of feldspars.

In most cases sulphides are rimmed and replaced by the alteration silicates and such replacements are thought to have formed by the reaction of sulphides with aqueous fluids which can be deuteric, which Li *et al.* (2004) and Crocket *et al.* (1976) suggested to be the result of interaction with hydrothermal fluids. The sulphide liquid appear to have infiltrated in the primary silicates and filled in the interstitial spaces accessible as observed in Figures 4.7 E and F; 4.3 C and D and as result are thought to have crystallised in the order of:

pyrrhotite > pentlandite> chalcopyrite and > pyrite later.

From ore microscopy study (Figures 4.9; 4.10), the BMS commonly occur as two mutually interpenetrating grains and more likely indicate simultaneous crystallisation. Disseminated crystals of sulphides occur in some of the samples and would be difficult to liberate given the closely packed nature of the grains, in comparison to coarser particle grain easily liberated due sizes.

Chemical remobilization and reprecipitation of sulphides appear as a paragenetically late feature as indicated by the formation of secondary BMS veinlets that crosscut the pyroxenite (Figure 4.4 E and F) and/or talc in the zone of alteration (Figure 4.5 C and D). Minerals hosted in cross cutting veins are thought to have formed during post-magmatic hydrothermally-induced alteration (Smith *et al.* 2013).

In some of the selected samples from both Modikwa and Two Rivers, the presence of magnetite was observed in places associated with fluid ingress of which might suggest recrystalization.- No recrystallization maybe due to deformation, but fluid ingress will likely result in alteration. Hence magnetite may be due to alteration.

The paragenetic relationship between magnetite and BMS is not clear, in some instances, magnetite appear to be replacing BMS while there is no evidence of replacement textures between the two grain boundaries, suggesting that grains crystallized most probably at the same time. This could most probably mean that there were two generations of magnetites, one later than the other.

Disseminated chromite grains occur throughout the Merensky Reef pyroxenite in all the four studied drilled cores as observed in Figures 4.4 C and D; 4.6 C and D; 4.8 C and D; 4.9 E and F. Top and bottom chromitite stringers occur interstially with plagioclase or sometimes orthopyroxene, these observations could suggest that chromite formed early and was subsequently enclosed in these minerals.

Cawthorn and Boerst (2006) proposed that the chromite in composite orthopyroxene could have grown by a reaction of primary orthopyroxene and superheated liquid, in which case the chromite would be a secondary mineral after the primary silicates.

However, if chromite was formed and later trapped within orthopyroxene during recrystallization, the timing of crystallisation of chromite relative to the orthopyroxene is difficult to determine. Some of the chromite grains are rimmed by biotite suggesting some reaction involving fluid at the contact between orthopyroxene and chromite.

The processes that bring about these *replacement textures* include oxidation, dissolution, subsequent precipitation and solid state diffusion of the magnetite that shows no replacement textures could be due to solid state diffusion. Most sulphide grains show early stages of replacement, where much of the original parent mineral is still evident (Figure 4.9 A and B; 4.10 A, B, C and D) but as the process advances the primary minerals appear corroded, forming floats within the particle. *Advanced replacements* were noted and tend to consume the original structure leaving rounded to corroded remains with fractures showing no parallel alignment and resulting in boundaries between the replaced and the replacing mineral commonly appearing sharp, irregular or diffused. *Fracture infilling* was recorded in this study and is thought to be as a result of precipitation or injection of later phase, often during metamorphism.

Exsolutions occurring in BMS are certainly not easy to interpret as they often appeared very similar to replacement textures. Most sulphides observed reveal a diagnostic pattern/shape and form in disseminations and dispersions.

Cracks, inclusions and lamellae twins often showed preferred orientation of blebs either along the grain boundary or rather in the center of the grains. The sulphide ores revealed evidence of *deformation textures* due to minor pressure induced twinning. Deformation in BMS was identified by commonly observing linear features such as crystal faces, fractures, exsolution lamellae, veining and twinning. These features appeared to have been offset and as result are deformed (Figures 4.9; 4.10). Some of the selected samples, in places BMS appear to have subjected to intense deformation resulting in brecciation of the present ore mineral which in turn result in broken and shattered grains.

Recrystallisation of BMS was observed; where after initial formation, BMS could be subjected to repeated periods of slow cooling or prolonged periods of slow heating as a result of metamorphism. In cases such as in Figure 4.10 D, recrystallization causes the coalescing grain boundaries to form into triple point junctions.

These observations suggest that *PGM* occurring in sulphide would suggest that the PGE in the magma was collected by the sulphide liquid, whether in solution or later exsolving from the sulphide blebs, or as discrete PGM floating in the magma. PGM therefore formed either shortly before or concurrently with the sulphides (Li *et al.* 2004).

5 Results and Discussion

5.1 PGM Mineralogy

This chapter discusses the quantitative analyses of the PGM based on the EPMA, the PGM phase association and their grain size distribution from the MLA. In particular, it focuses on the BMS and associated PGMs that occur within the Merensky Reef pyroxenite package. A sub section presenting the trace element analysis including PGEs in BMS follows below, and subsequently presents the grade profiles which were drawn based on the assay data. Scanning electron microscopy (SEM) was also utilized for the identification of PGMs in conjunction with MLA and EPMA. SEM images obtained for PGMs are attached as Appendix FI and FII. Only EPMA images are used for illustrations of the PGMs in this chapter. Naming of PGMs was done per the order given in Cabri (1981; 2002).

The EPMA analyses were carried out on 41 samples obtained from a total of four drill cores, two from Modikwa and two from TRP Mines. The PGMs identified, were classified into five groups namely; PGE-tellurides, PGE-arsenides and sulphoarsenides, PGE-sulphides, gold (in the form of native gold and electrum), and other PGE alloys, e.g. platinum and palladium alloys and palladium-lead alloys, presented in Tables 5.1 and 5.2 below. Gold and electrum even though are not part of the PGEs, they were considered in the PGMs classification in this study. In terms of PGM association with the sulphides, a strong association exist between PGM and sulphides with the association of chalcopyrite being the most remarkable. Relative proportions of dominant PGMs differ between the two mines, with PGE (platinum and palladium) telluride and bismuthotellurides being the most dominant PGE group at both TRP (97 %) and Modikwa (85 %).

Table 5.1: PGM groups occurring in the Merensky Reef pyroxenite at Modikwa

PGE group	Chemical composition	Mineral name	Number of grains	
Gold			**OV 777**	**OV 778**
	AuAg	Electrum	9	12
PGE arsenides	PtAs	Sperrylite	4	71
	PtAsS	Platarsite	3	3
PGE bismuthotelluride and tellurides	PdBiTe	Michenerite	14	51
	PtPdBiTe	Unnamed	18	3
	PdBiFeTe	Michenerite	2	2
	PtTeBi	Maslovite	34	9
	$PtTe_2$	Monocheite	2	4
PGE base metal sulphides	PtPdSn	Braggite	10	1
	PtS	Cooperite	28	2
	RuS	Laurite	2	4
	PtPdS	Braggite	10	3
	PtRhCuS	?	1	1
Other PGE Alloys	PdSb	Stibiopalladinite	2	
	PtSn	?	5	
	PtPdSn	?	8	1
	PdSn	?	1	
	PtFe	Isoferroplatinum	8	3
Total			**160**	**170**

Table 5.2: PGM groups occurring in the Merensky Reef pyroxenite at Two Rivers

PGE group	Chemical composition	Mineral name	Number of grains	
Gold			**TRP 260**	**TRP 271**
	AuAg	Electrum	11	25
PGE arsenides	PtAs	Sperrylite	11	22
	PtAsS	Platarsite	3	1
PGE bismuthotelluride and tellurides	PdBiTe	Michenerite	9	27
	PtTeBi	Maslovite	32	71
	$PtTe_2$	Monocheite	4	4
	PtPdBiTe	?	16	29
PGE base metal sulphides	PtPdS	Braggite	52	12
	PtS	Cooperite	54	29
	RuS	Laurite	10	29
	PtRhCuS	?	31	6
Other PGE Alloys	PtAu	?		1
	PtFeTe	?		1
	PtPdSn	?	1	10
	PtSn	?	1	7
	PtSb	?		2
Total			**235**	**276**

5.1.1 *Platinum Group Mineral Association*

Using MLA, minerals are considered as associated with each other when they share grain boundaries. The higher the degree of grain boundary shared between two minerals, the greater the degree of association between them.

Sulphide association: The PGMs in the Merensky Reef at Modikwa and Two Rivers have strong associations with sulphides. Two modes of sulphide association with PGM occurrence were recognized with in this study; (1) PGM occurring enclosed in sulphides and (2) PGM occurring at the borders/margins of sulphides (this is the common occurrence observed for this study). Samples in drill core OV 777 from Modikwa showed dominant association of PGMs with chalcopyrite while samples in drill core OV 778 PGMs showed stronger association with pentlandite (Figure 5.1). In total, samples from the Modikwa boreholes exhibit stronger associations in decreasing order of pentlandite > chalcopyrite > pyrrhotite with pyrrhotite showing the least association with the PGMs at Modikwa (5.1 A and B). Samples from drill cores TRP 260 and TRP 271, showed similar trends as the Modikwa boreholes (Figure 5. 20 C and D), in terms of PGM association with sulphides. From the ore microscopy, SEM and MLA observations of sulphides, pyrrhotite is generally the coarsest, followed by pentlandite, chalcopyrite and pyrite. Coarser sulphides in this study were commonly associated with coarser PGM (these observations are discussed further in the following subsection on PGM distribution).

Silicate Association: The association of silicates was confirmed by petrography in Chapter 4. PGM in the Merensky Reef at both Modikwa and Two Rivers showed high association with pyroxene members (which includes both orthopyroxene and clinopyroxene). Plagioclase contents were decreased in drill cores OV 778 and TRP 260 while in drill cores OV 777 and TRP 271 the plagioclase contents showed an increase (Figure 5.1 A and D; B and C). From the two mines, the PGM association is more dominated by pyroxene followed by plagioclase.

The observations in this study revealed strong association of PGMs with primary silicates (pyroxene and plagioclase) which is hardly surprising, as these minerals occur in abundance within the Merensky Reef. The relationship of PGM with silicates could be related to the mechanical trapping of the PGM during the period of crystallisation of the silicates as suggested by Boissonnas and Omenetto (1998).

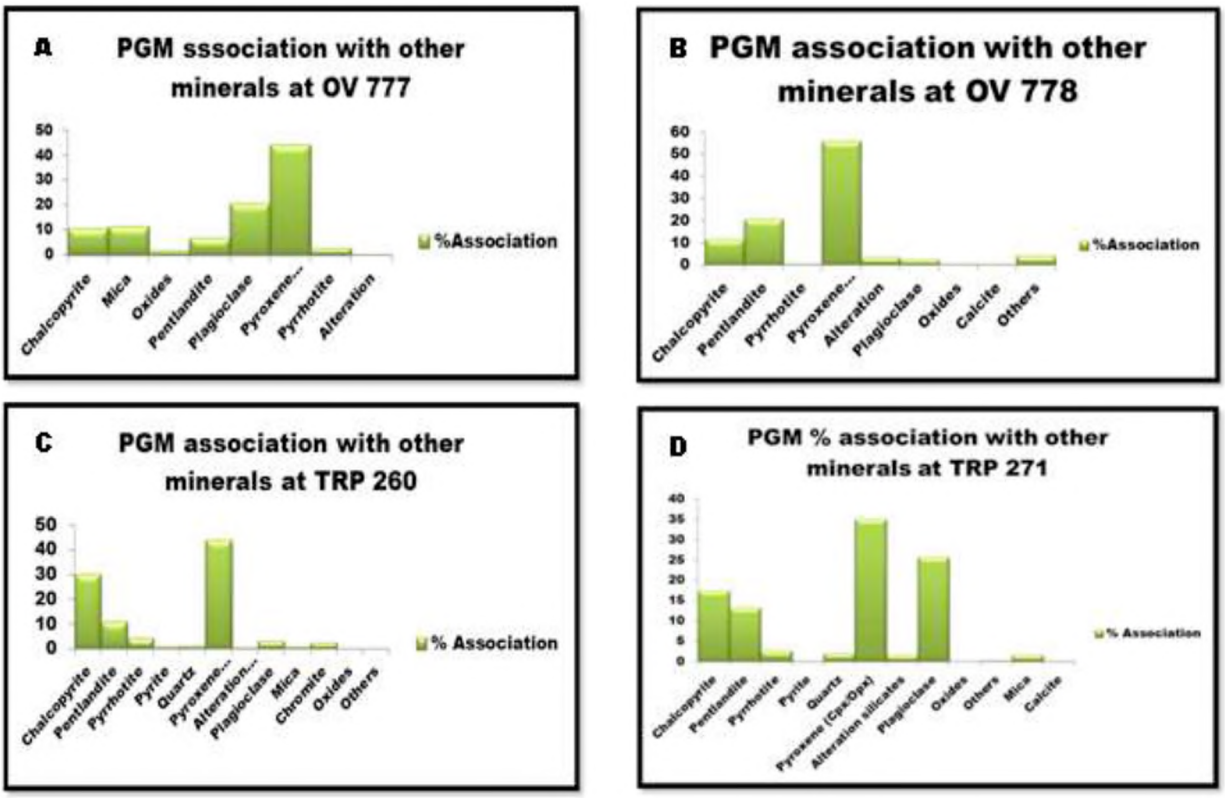

Figure 5.1: PGM association with other minerals at Modikwa (boreholes OV 777 and OV 778) and Two Rivers (boreholes TRP 260 and TRP 271) Platinum Mines.

Secondary/Alteration Silicate Association: PGMs show association with alteration silicates. The identified secondary silicates include; mica, chlorite, amphibole, talc and serpentine. As documented in the petrography section the coarse - to medium-grained subhedral to euhedral orthopyroxene crystals has altered to talc aggregates and amphiboles along fractures. Mica (which includes biotite and muscovite) showed increased contents in drill core OV 777 compared to the other three drill cores (OV 778, TRP 260 and 271). The occurrence of rims of secondary silicates around sulphides and PGMs is common as was also observed by Li *et al.* (2004). This predominance of alteration at the rims is most probably due to grain contacts between sulphides/PGM and silicates being pre-destined for fluid flow. The alteration of silicates with PGMS can also have significant influence on flotation performance as this could lead to poor floatability. However, talc-talc causes serious problem in flotations, please check from literature, amphibole and mica are the most floatable secondary products. After the milling process, the PGM recovery depends entirely on the associated mineral.

PGMs occurring along the sulphide rims in the alteration minerals which also in turn rimmed by sulphide, are probably due to higher resistance to alteration processes and will most probably be harder to recover. This could be related to their fine crystalline texture.

Oxides Association: The PGM association with oxides is generally low at both Modikwa and Two Rivers. These observations are not surprising as oxide minerals such as chromite are only encountered with in the two thin chromitite contacts which define the Merensky Reef. An association of chromite with some of the PGMs, mostly with PGE-sulphides was observed. Magnetite phases were also encountered but no conclusions could be made of its occurrence with PGM due to its occurrence as fine grain disseminations.

Other association: Galena appeared to be associated mostly with PGE-alloys (the percentage associations were low).

5.2 Platinum Group Mineral Distribution within the Merensky Reef at Modikwa

5.2.1 *PGE-tellurides and bismuthotellurides*

This group forms the most dominant PGMs encountered from the two investigated drill cores of Modikwa. The PGE-tellurides comprises minerals such as maslovite (PtBiTe) and michenerite (PdBiTe), which forms about 85 modals % at Modikwa. The PGE-tellurides at Modikwa exhibits various shapes; elongated, sub to euhedral shapes and ranging from 10 to 80 microns in grain sizes. This group occur in vein-like habit, which may possibly suggest that the PtTeBi has flowed/intruded into and filling up the silicate cracks following the same trend as that of the associated sulphides (Image 4 Appendix BI and Image 2-Sample OV 777-2, Appendix F1). A PGM grain identified as maslovite at Modikwa is shown in Figure 5.2 A below. The PGM exhibit an elongated worm-like shape and occur predominantly between BMS and silicates. It ranges in size reaches up to about 20 microns in length. The cross-cutting textural relationship between the maslovite and sulphides suggests possible displacement of the sulphides. The PGM composition varies widely as depicted in Table 5.3 below. PGM maslovite ranges in composition from (37-38 %) Pt, (37-40 %) Te and (19-20 %) Bi. The elemental qualitative map analysis revealed different sulphide phases associated with the PGM (Figure 5.2). The dominant sulphide assemblage in the sample is pyrrhotite. Rhodium and Bi in this PGM show irregular distribution along certain parts of the grain while platinum and tellurium distribution appear homogeneous (Figure 5.3).

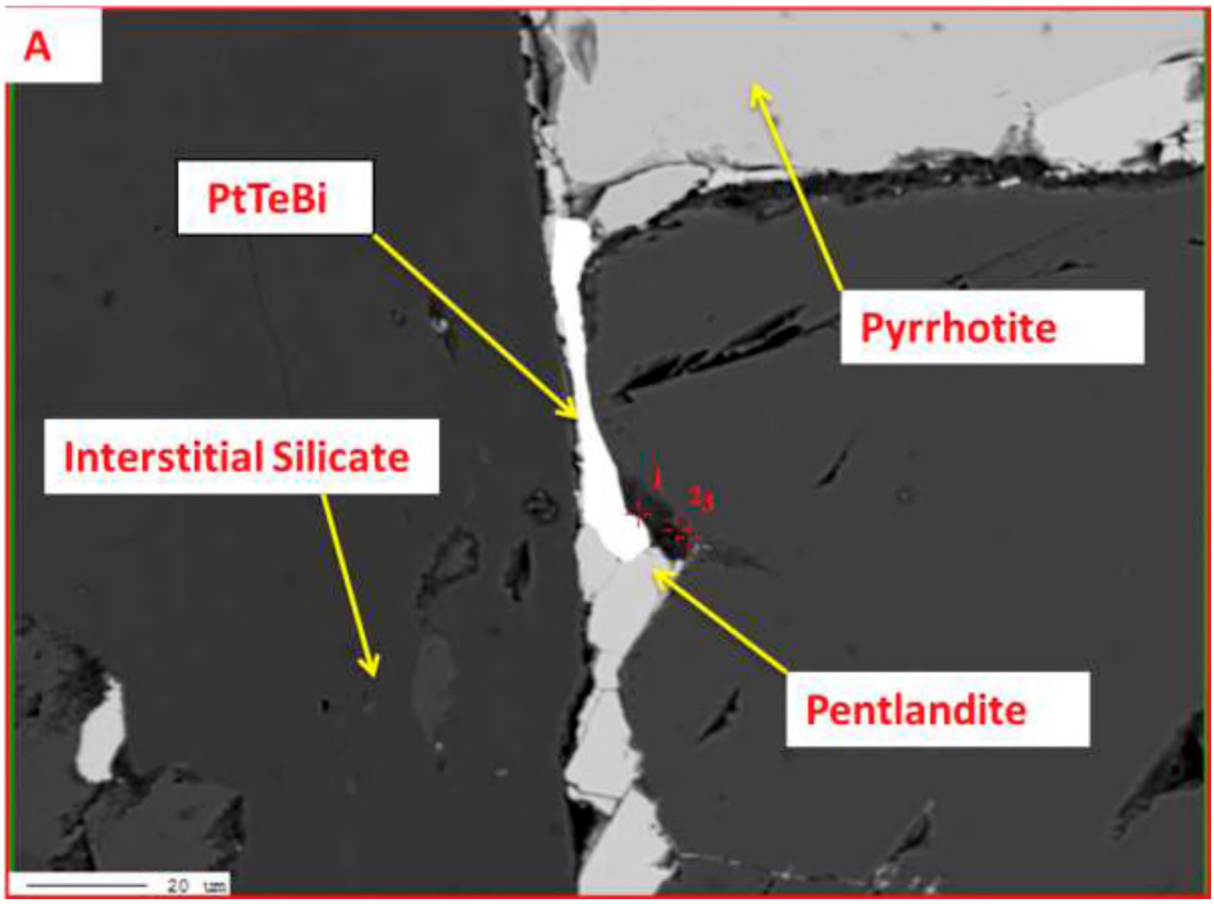

Figure 5.2: Back Scattered Electron (BSE) image illustrating elongated PGM maslovite (PtTeBi) located within both the sulphides and interstitial silicates near the top chromitite stringer.

Table 5.3: PGM and sulphides quantitative results at OV 777

Point	Sample no	Pt %	Ru %	Rh %	Os %	Te %	S %	Bi %	Fe %	Cu %	Ni %	Total %
1	777-2	37.07	0	0.135	2.328	39.59	0.107	18.6	0.682	0.23	0.184	98.92
2	777-2	37.54	0.004	0.096	3.124	37.17	0.072	20.12	0.606	0.04	0.34	99.11

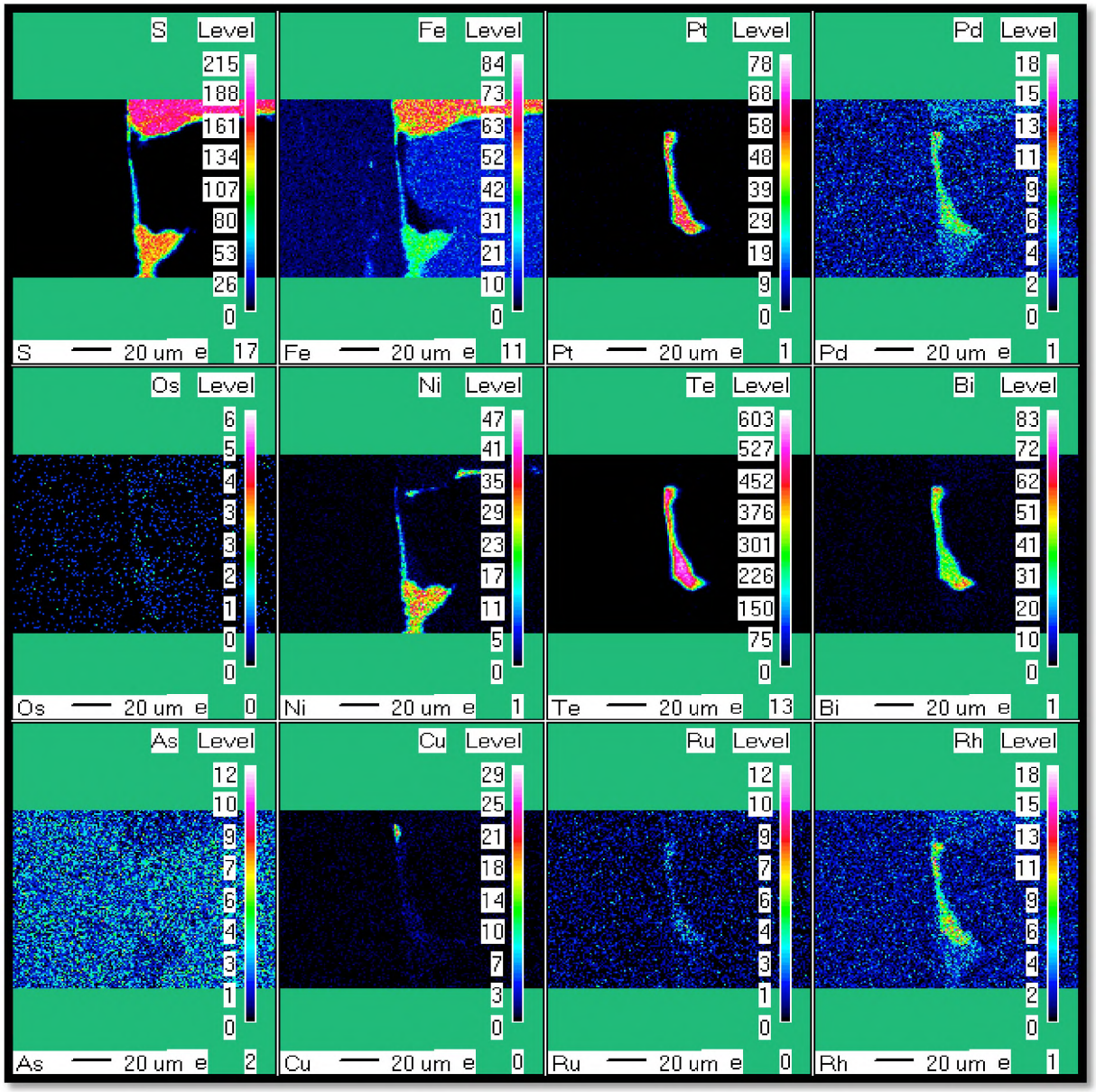

Figure 5.3: EPMA map analysis of S, Fe, Cu, Ni and other trace elements including platinum group elements within sulphides. Sulphides are distinguished by the S, Ni, Fe and Cu contents. Chalcopyrite is distinguished by the high Cu content and pentlandite by high Ni contents. The colour coded bar indicates the relative concentration of each element in reducing order downwards. (Drill core OV 777, sample777-2, Modikwa).

5.1.2.2. PGE-arsenides and sulphoarsenides

These form the second most abundant PGM group at Modikwa, comprising minerals such as sperrylite (PtAs) and platarsite (PtAsS) and form about 47 % modal abundance at Modikwa. The arsenides show intermediate to fine grain size distributions, anhedral or subhedral shapes and range from 10 to 20 microns in length. These various shapes could be linked to their formation in different conditions during ore forming processes.

Sperrylite at Modikwa was analysed by SEM and occurs in sulphide veins and is thought to form in the final stage of PGE mineralization as it appears to be associated with alteration associated with later stage fluids (SEM Image 6 Sample OV 778-3 attached as Appendix F1). Compositional variations are apparent, including variations of possible hollingworthite [(Rh, Pt) AsS)] and or (OsAsS) phases which are commonly associated with sperrylite.

5.1.2.3. PGE-sulphides

PGE sulphides are the third abundant PGM type at Modikwa, predominantly comprises cooperite (PtS), laurite (RuS) and braggite (PtPdS). They form about 38 % of the PGM modal occurrence at Modikwa, with cooperite being the most dominant. This PGM occurs in various shapes, anhedral to subhedral shapes and range from 5-80 microns in length. The PGM analysed at point 27 is identified as braggite (PtPdS) with grain size reaches up to 10 microns in length. The anhedral braggite shows association to pyrrhotite, pentlandite and strongly with chalcopyrite phases (Figure 5.4). Table 5.4 displays the compositional variation of the PGM. The fact that the PGM grain appear bigger, anhedral and complex in texture, and shows preferential to sulphide boundaries, points to a distinct primary magmatic origin. The qualitative elemental map analysis of braggite show the grain to be more enriched in platinum, and appear homogeneously distributed along the grain while palladium is enriched only in certain parts of the PGM grain (Figure 5.5). Minor enrichments of tellurium and arsenic along PGM tips were noted, also some deceleration radiation with rhodium and bismuth were recorded.

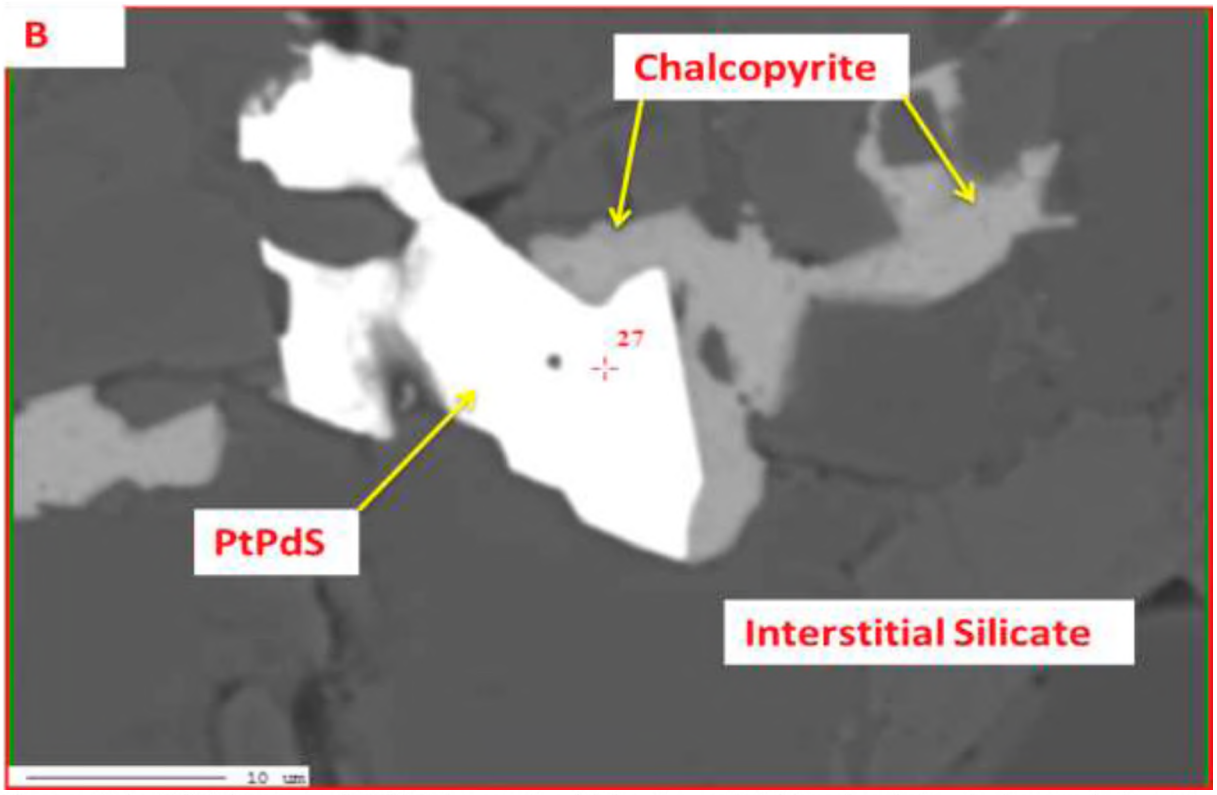

Figure 5.4: BSE image of PGM located within the sulphides (mainly chalcopyrite) and silicates. Sample lies just at the bottom chromitite stringer.

Table 5.4: PGM and sulphides quantitative results at OV 778

Point	Sample no	Pt%	Pd%	Rh%	Os%	S%	Fe%	Cu%	Ni%	Total%
27	778-9	49.84	24.17	0.205	2.017	18.66	0.102	4.181	0.414	99.59

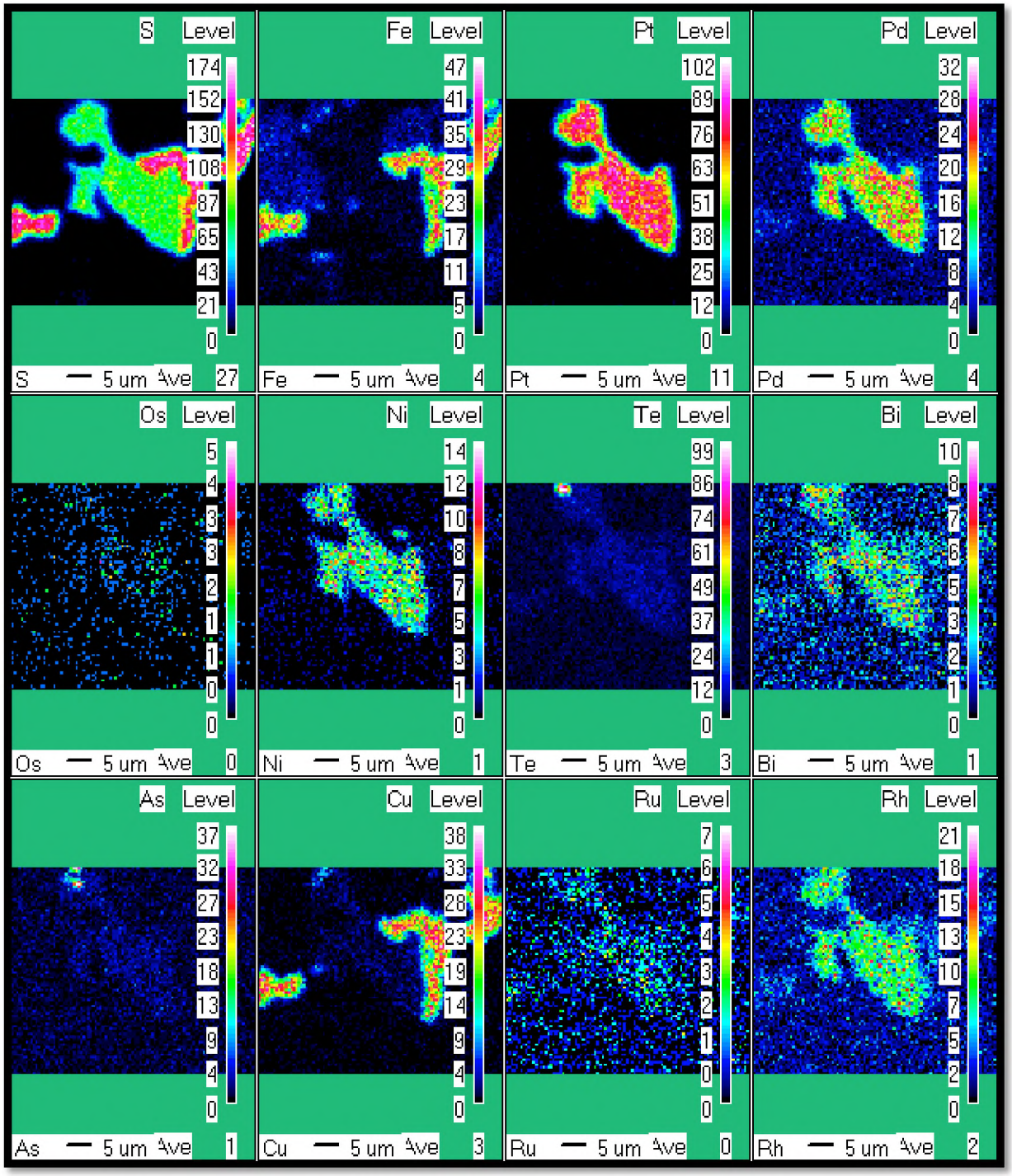

Figure 5.5: EPMA map analysis map of S, Fe, Cu, Ni and other trace elements including platinum group elements within sulphides. Sulphides are distinguished by the S, Ni, Fe and Cu contents. Chalcopyrite is distinguished by the high Cu content and pentlandite by high Ni contents. The colour coded bar indicates the relative concentration of each element in reducing order downwards. (Drill core OV 778, sample 778-9 Modikwa).

5.1.2.4. Gold

Gold grains at Modikwa occur as electrum, showing strong association with silver (AuAg) compound and form about 13 % of the total PGM occurrence at Modikwa. It also revealed high associations with silicates and lower association with BMS suggesting that it might have been hydrothermally redistributed and does not occur enclosed with sulphides like the PGM does. Gold grain occur as fine, sub-angular to angular in shapes and ranging from about 5-20 microns in length. See SEM images attached as Appendix FI Image 3 (Sample OV 777-8) and Image 5 (Sample OV 778-1).

5.2.1.1 PGE-alloys

This group includes palladium and platinum alloys and forms about 17 % of PGM modal abundance at Modikwa. They show greater association with secondary silicates and most likely are late or secondary in nature. Other rare combinations of platinum, palladium with bismuth, tin and lead are grouped also under "Other PGE-alloys". The data for the grain distribution of PGE-alloys was limited but where observed they occur as fine, anhedral to subhedral grains, ranging from 5-30 microns in length. See SEM images attached as Appendix FI and FII (Image 4, Sample - OV 777-8).

5.2.2 ***Platinum Group Mineral Distribution within the Merensky Reef at Two Rivers***

5.2.2.1 PGE Tellurides and Bismuthotellurides

As with Modikwa, this group forms the most dominant PGMs encountered forming about 97 % of the PGM population at Two Rivers. These include PGM such as maslovite (PtBiTe) and michenerite (PdBiTe). The occurrence of the PGE-tellurides at Two Rivers exhibits various shapes, subhedral to euhedral shapes and ranging from 10 to 80 microns in grain sizes. There are variants of palladium present within this group comprising of michenerite (PdBiTe), unknown (PtPdTeBi) and merenskite (PdTe). All these occur in varying proportions of bismuth and tellurium, and the EDS-based classification presented in Table 5.5 provides a rough estimate of the composition. A PGM identified as michenerite (PdBiTe) is shown in Figure 5.6. Michenerite is anhedral to euhedral in crystal habit and reaching up to 10 microns in length. The PGM grain is large, well-developed along the sulphide boundaries/margins in between the interstitial silicate showing association with only one phase of sulphide, chalcopyrite.

The elemental qualitative map analysis of the PGM show homogenous distribution in tellurium, bismuth and palladium, and trace concentration of rhodium in Figure 5.7.

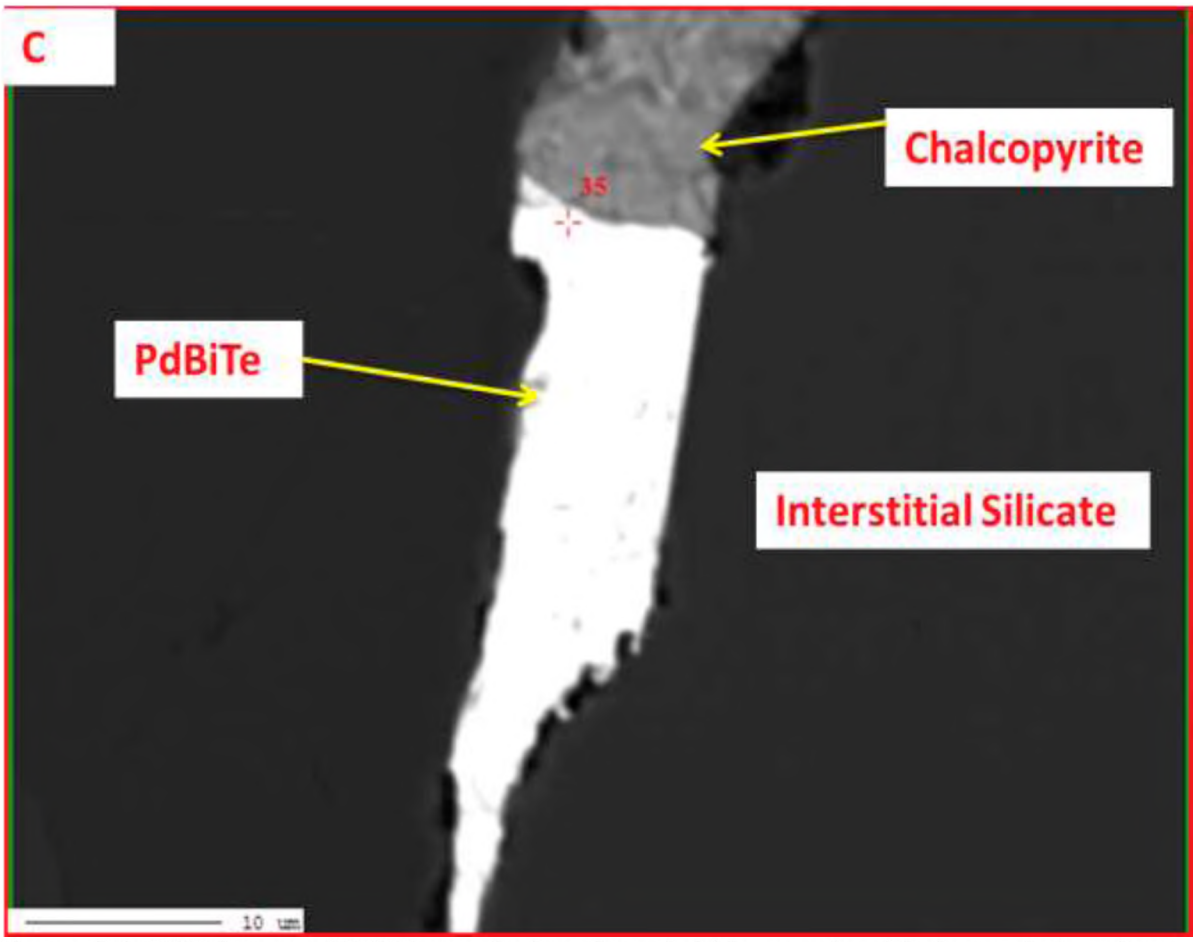

Figure 5.6: BSE image of PGM attached to the sulphide margins (chalcopyrite) and to the silicate. This sample is located within the pyroxenite.

Table 5.5: PGM and sulphides quantitative results at TRP 260

Point	Sample no	Pt %	Pd %	Ru %	Os %	Au %	Te %	S %	Bi %	Fe %	Cu %	Total %
35	260-6-5	0.094	37.11	0.044	2.601	0.025	29.26	0.069	27.7	0.827	0.338	98.07

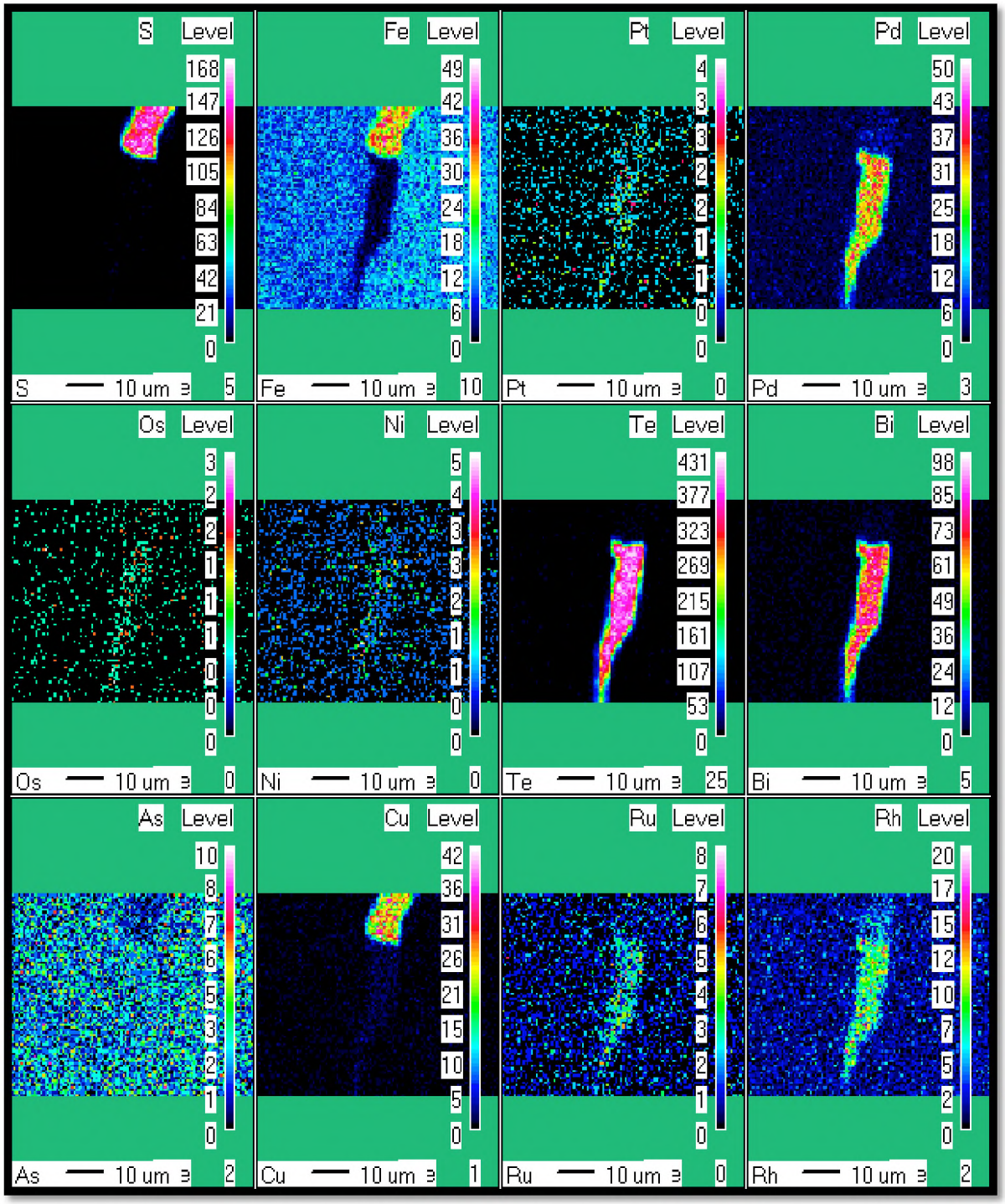

Figure 5.7: EPMA map analysis of sulphur, iron, copper, nickel and other trace elements including platinum group elements within sulphides. Sulphides are distinguished by the sulphur, nickel, iron and copper contents. Chalcopyrite is distinguished by the high copper content and pentlandite by high nickel contents. The colour coded bar indicates the relative concentration of each element in reducing order downwards. (Drill core TRP 260, sample 260-6-5 Two Rivers).

5.2.2.2 PGE-sulphides

This group is the second most abundant at two Rivers, with both cooperite (PtS) and braggite (PtPdS) being the most dominant PGMs. PGE-tellurides form about 90 % modal abundance at Two Rivers, occurring as anhedral to subhedral in shape and appearing as composite or free grains with sulphides and silicates. Grain sizes range from 5-100 microns in length. SEM images attached as Appendix FI Image 8 (Sample 260-4-4) and Image 13 (Sample 271-15B). A PGM grain analysed at point 29 is identified as cooperite (PtS). The PGM grain is anhedral in shape and reaching up to 10 microns in length. It shows association with only chalcopyrite phase (Figure 5.8). Cooperite composition varies as shown in Table 5.6 and containing about (83 %) Pt and (17 %) S and other minor and trace elements. The irregular shaped cooperite grain is located at the margins of chalcopyrite in between the interstitial silicate and appear attached to the chalcopyrite. The elemental qualitative map analysis revealed the PGM to be more enriched in platinum with minor traces of tellurium and palladium. Rhodium appearing enriched only in certain spots along the PGM tips (Figure 5.9).

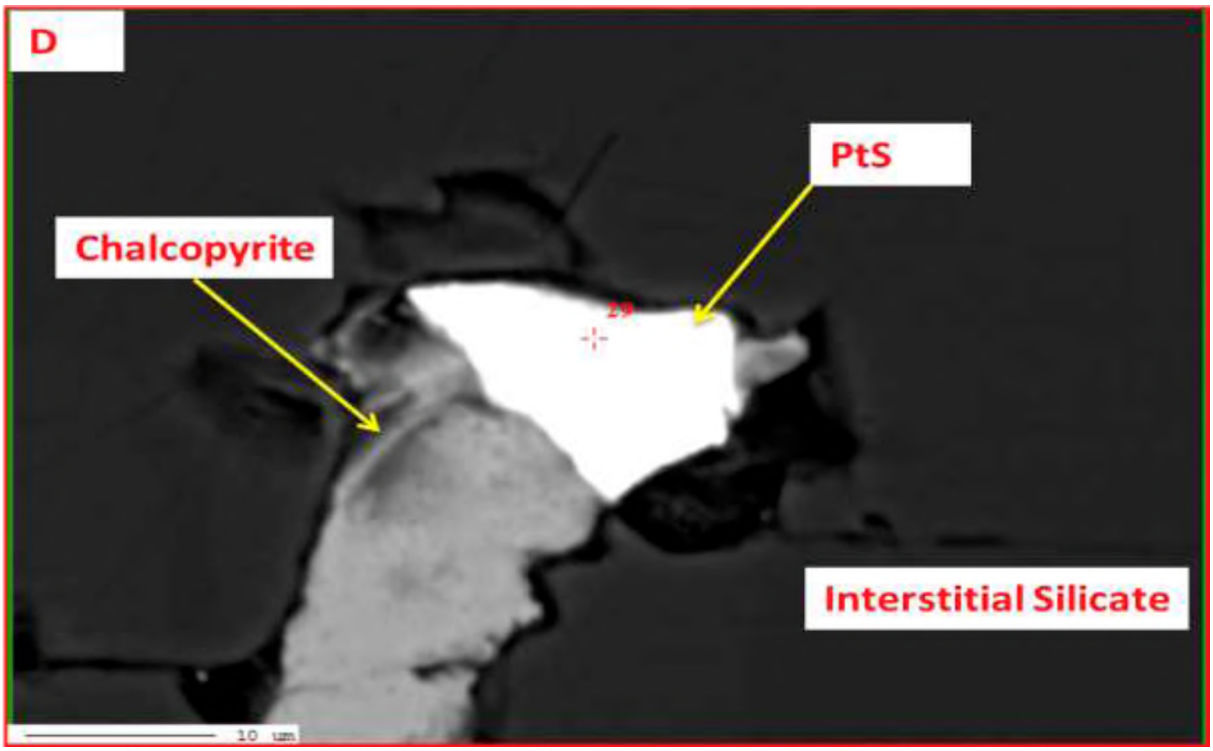

Figure 5.8 A: BSE image of PGM located within the boundaries of chalcopyrite. This sample is in close proximity to the bottom chromitite stringer.

Table 5.6: PGM and sulphides quantitative results at TRP 271

Point	Sample no	Pt %	Pd %	Rh %	Os %	Te %	S %	Fe %	Cu %	Ni %	Total %
29	271-15A	83.92	2.26	0.268	3.906	0.034	17.69	0.395	0.585	0.132	109.2

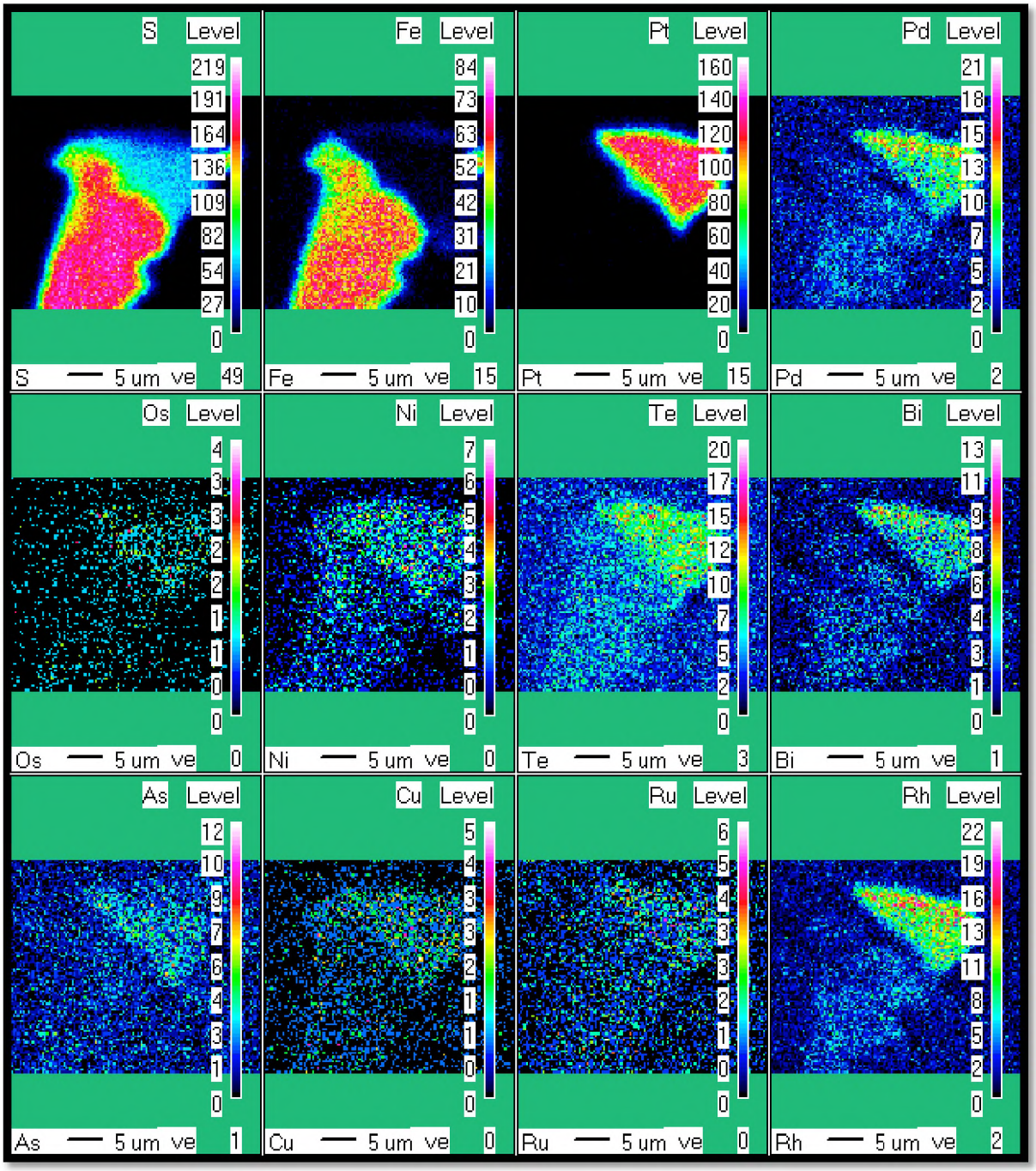

Figure 5.9: EPMA map analysis of sulphur, iron, copper, nickel and other trace elements including platinum group elements within sulphides. Sulphides are distinguished by the sulphur, nickel, iron and copper contents. Chalcopyrite is distinguished by the high copper content and pentlandite by high nickel contents. The colour coded bar indicates the relative concentration of each element in reducing order downwards. (Drill core TRP 271, sample 271-15A_1 Two Rivers).

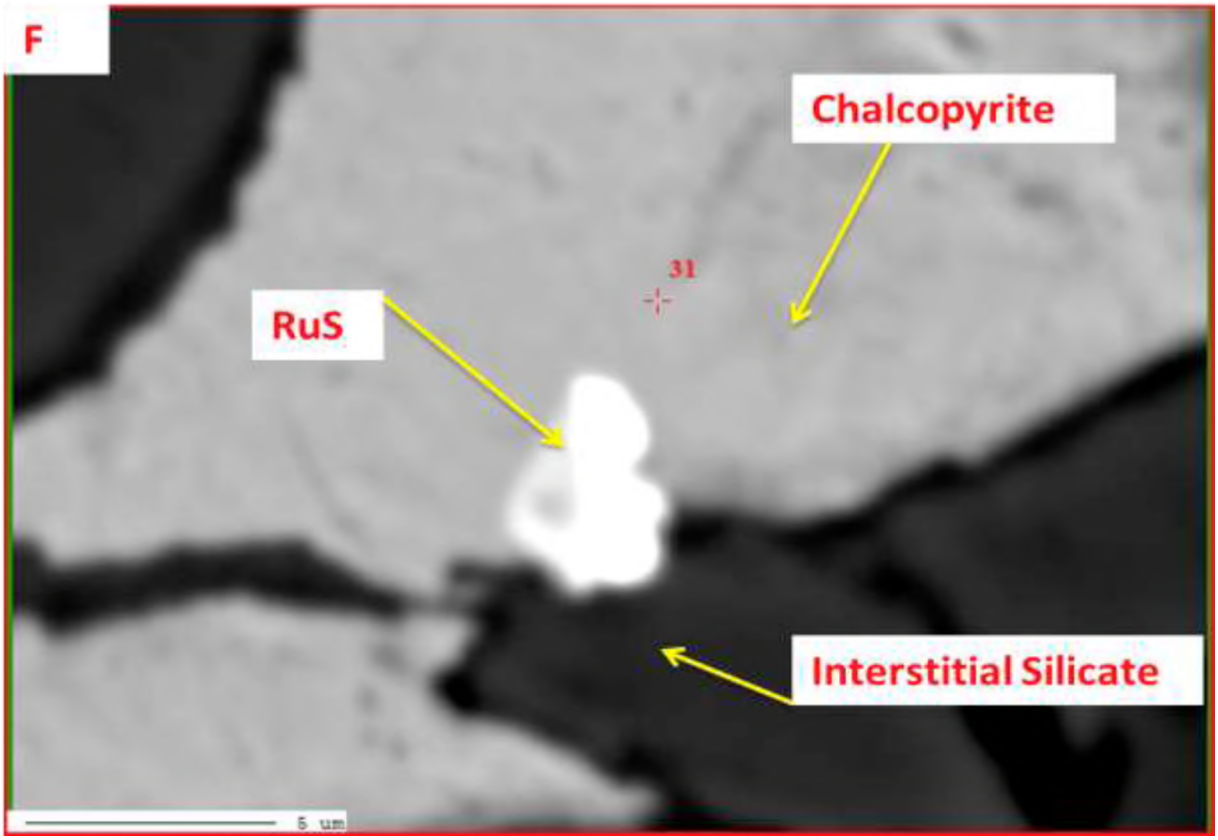

Figure 5.10: BSE image of PGE-sulphide, laurite (RuS_2) occurring in and at the margins of sulphide, sample located near the bottom chromitite stringer.

Table 5.7: PGM and sulphides quantitative results at TRP 271

Point	Sample no	Pt %	Pd %	Ru %	Rh %	Os %	Au %	Te %	As %	S %	Fe %	Cu %	Ni %	Total %
31	271-15A	3.23	2.307	31.59	2.456	3.449	0.535	0.858	2.217	38.38	10.93	0.099	1.093	97.16

From the table above the composition of laurite shows a relatively wide elemental composition. The elemental qualitative map analysis shows the PGM to be homogeneous in platinum, arsenic, ruthenium and with rhodium enriched in certain spots and suggesting that the PGM shows a bimodal composition. The second phase appears to be platarsite (Pt, Rh, Ru) AsS or irarsite (Ir, Pt, Rh, Ru, Pt) AsS. Tellurium, bismuth and palladium appear as minor traces and enriched only in certain spots (Figure 5.11). It has been observed common of laurite to occur intergrown with sulphides and particularly at the margins of sulphides as seen in Sample TRP 271-15B attached as Image 13 on Appendix FI.

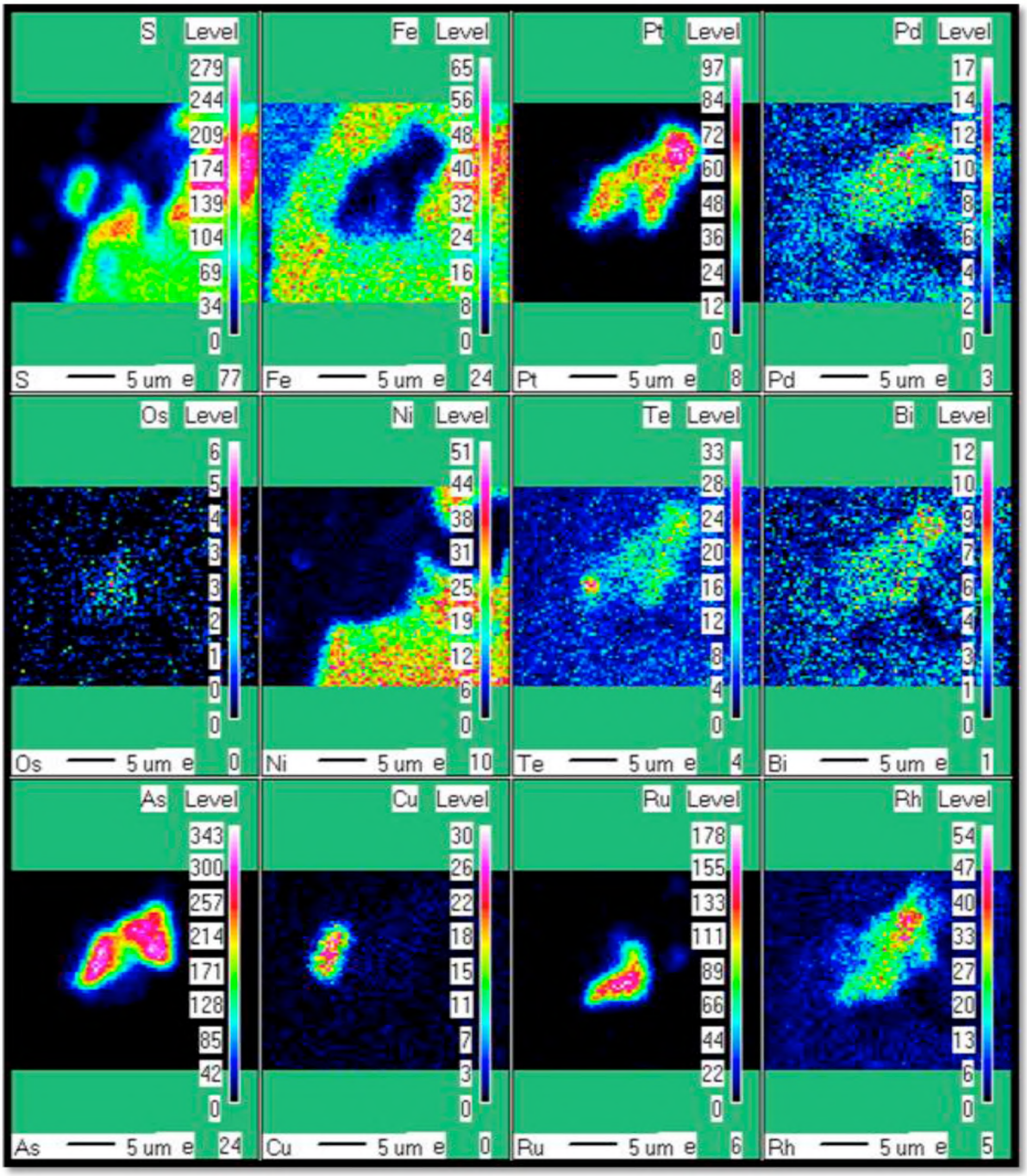

Figure 5.11: EPMA map analysis of sulphur, iron, copper, nickel and other trace elements including platinum group elements within sulphides. Sulphides are distinguished by the sulphur, nickel, iron and copper contents. Chalcopyrite is distinguished by the high copper content and pentlandite by high nickel contents. The colour coded bar indicates the relative concentration of each element in reducing order downwards. (Drill core TRP 271, sample 271-15A_3, Two Rivers).

5.2.2.3 PGE-arsenides and sulphoarsenides

This group is the third dominant type of PGMs occurring at Two Rivers and forms about 14 % of the total PGMs. They occur in various shapes of subhedral to anhedral and ranging from 10 to 20 microns in length. A PGM grain analysed with SEM and identified as sperrylite (PtAs), the reader is referred to the SEM images attached as Appendix FI Image 12 (Sample TRP 271-15A). Arsenides show intermediate grain size distributions, anhedral to subhedral shape and reach up to 100 microns in length. They occur interstitial with silicates and along sulphide margins.

5.2.2.4 Gold

Gold occurs in the form of native gold and forms about 13.17 % of the total PGM grains at Two Rivers. It shows close association with the silicates as shown in images in Appendix (SEM image attached as Appendix FI Image 11 (Sample TRP 271-4-2) and not with sulphides. The grains vary from about 5-50 microns in length with various shapes, angular to sub-angular shapes.

5.2.2.5 PGE-alloys

This group includes palladium and platinum alloys and indicated greater association with silicates forms about 8 % of the total PGM occurrence at Two Rivers. Other combinations that occur in this group include platinum, tin with iron. The grains show fine to intermediate grain size distributions, anhedral to subhedral in shape and reaching up to 20 microns in length. PGE alloys were analysed and are shown in the SEM images attached as Appendix FI Image 10 (Sample-TRP 271-3B). Pie charts illustrating the PGM types in the Merensky Reef at Modikwa and Two Rivers are shown in Figure 5.12 below.

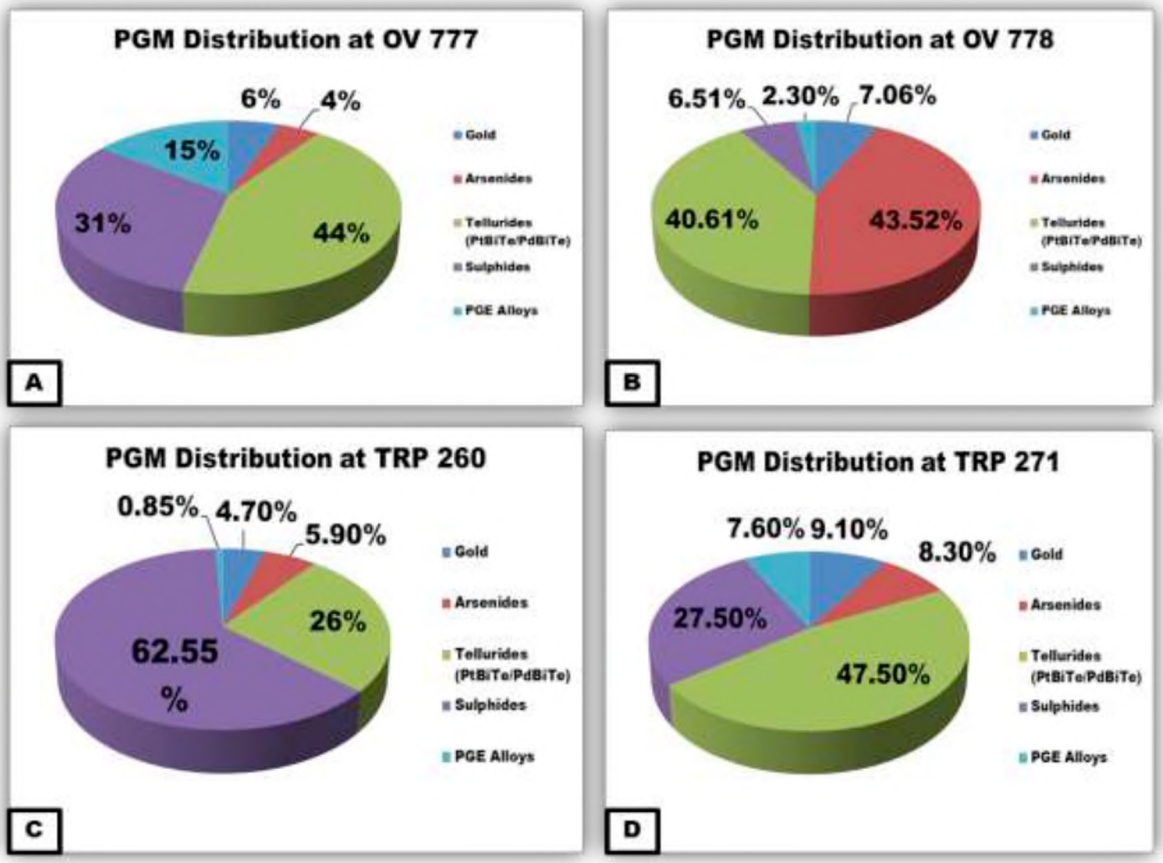

Figure 5.12: Pie chart showing the distribution of PGM at Modikwa (boreholes OV 777 and OV 778) and Two Rivers (boreholes TRP 260 and 271) Platinum Mines.

5.2.2.6 Platinum Group Mineral Grain Size Distributions

In assessing the grain size distribution of PGMs in the two mines, there is relatively minimal difference in the grain size distribution (Figure 5.13). The grain sizes (microns) plotted versus the cumulative frequency (in wt %) demonstrate that PGMs at Two Rivers are coarser in grain size relative to those at Modikwa. The total mineral in the sample pass different grain sizes in microns, therefore, the higher percentage passing at a given grain size, the higher the grain sizes (referred to as maximum passing) and the lower percentage passing at a given grain size, the lower grain sizes (referred to as minimum passing). The grain size distributions are generally similar in the two mines with maximum passing of PGM grain size ranging between 16 and 125 microns at Modikwa and ranging between 53 and 125 microns at Two Rivers. It has been noted that samples from drill cores OV 777 and TRP 271 demonstrate similarities in their PGM grain size distribution. Samples from drill cores OV 778 and TRP 260 also display a similar pattern.

Some PGMs occur as free grains or inclusions and attachments to sulphides and silicate minerals. Pillay *et al.* (2011) reported that the key mineralogical factors controlling the separation are the texture of the sulphides, grain size, particle density and particle shape. Generally, in the Merensky Reef the liberation size is coarse with most operations choosing a grind size between (P_{80}) 75 and 150 microns. To liberate the PGMs in the two mines, a minimum grinding size of 0.73 microns and a maximum grinding size of 125 microns are required. The average of the PGM grain sizes in both mines is 20 microns.

According to Penberthy *et al.* 2000, the recovery of liberated PGM is entirely dependent on the milling size and an associated mineral. In view of this, if the grain size has a dominant control on liberation degree of flotation then the PGE-tellurides should be recovered faster, next should be the PGE-sulphides followed by the PGE-arsenides and then lastly will be the PGE- alloys and gold (these have finer grain sizes). Wiese *et al.* (2006) interpreted the role of reagents in the flotation of platinum bearing Merensky ores and stated that the different BMS in the Merensky Reef respond differently to different reagents and operating conditions. This essentially indicates that the degree at which a mineral is presented to various chemical environments will adhere viably to flotation processes. Sulphides and tellurides both have reasonable floatability without any collector, whereas the arsenides are not amenable to floating. Arsenide and telluride minerals can be recovered in significant quantities using xanthate as the collector but small particle sizes are probably the result of low recoveries. PGM telluride would not cooperate with collectors the same way as the PGM sulphide, due to their distinctive crystal structures.

At Two Rivers, the larger PGM grains occur close to both the top and bottom chromitite stringers while at Modikwa, the trend slightly differs as larger PGM grains are associated to the top chromitite stringer compared to the bottom chromitite stringer. In view of this, Hiemstra (1979) and Tredoux *et al.* (1995) proposed that PGM were scavenged in as solid micro-nuggets or clusters that settled with either sulphide liquid or chromitite to account for the extreme oversaturation of sulphide in PGE that would be required otherwise. This could also suggest that probably the larger sulphide blebs scavenged larger PGM micro-nuggets. Intermediate to small PGM grains occurred within the pyroxenite. These observations show that PGMs tend to vary stratigraphically thus, the PGM type, lithology and stratigraphy appear to have an influence on the vertical distribution of the PGM grain size.

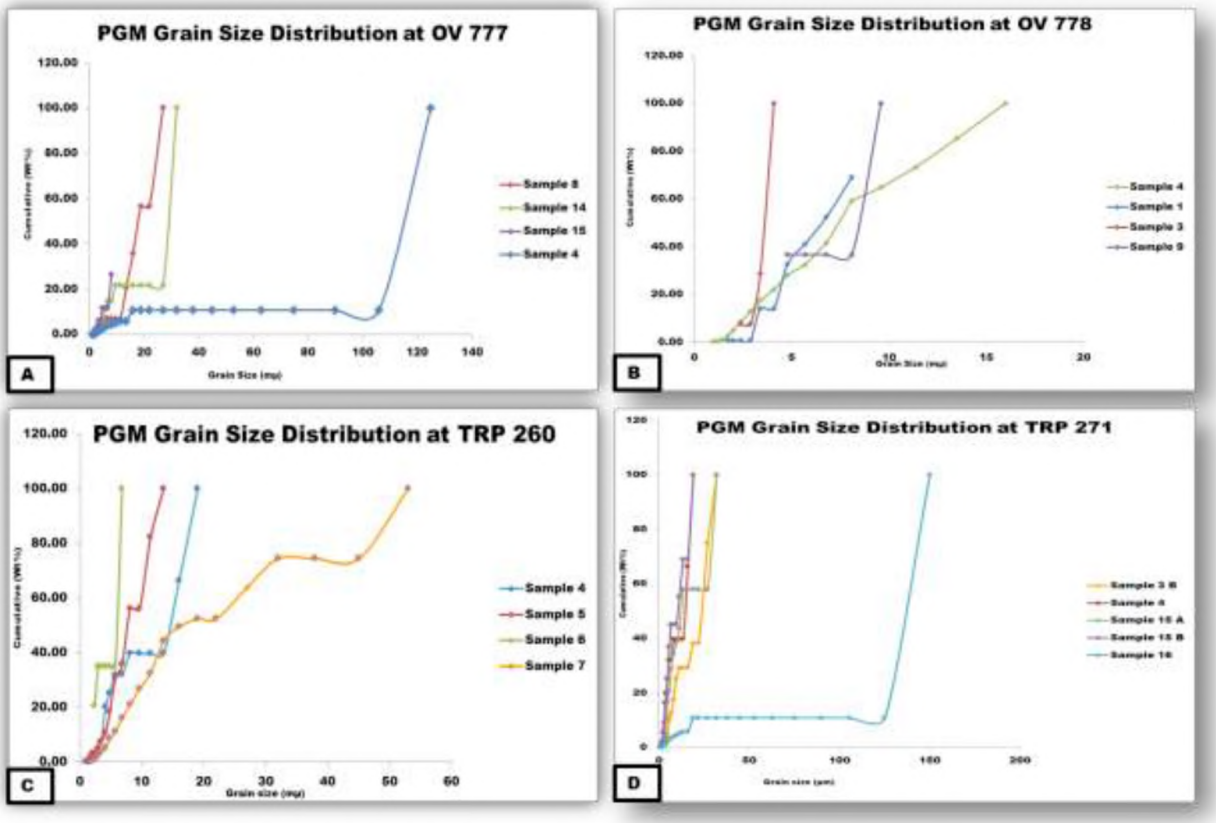

Figure 5.13: PGM grain size distribution at Modikwa (boreholes OV 777 and OV 778) and Two Rivers (boreholes TRP 260 and TRP 271) Platinum Mines.

5.2.3 *Discussion and Summary of the Platinum Group Mineral Distribution in the Merensky Reef*

The most prominent feature observed in the mineral association data of the PGMs at both Modikwa and Two Rivers Platinum Mines, is the strong association with sulphides. The PGMs found within the Merensky Reef pyroxenite sequence at Two Rivers and Modikwa are strongly associated with the BMS than with the chromite grains. The samples from both mines demonstrated that BMS including pyrrhotite, pentlandite, and chalcopyrite form the principal sulphides with pyrrhotite being the most dominant, and minor amounts of pyrite. Of the BMS association with PGMs, chalcopyrite revealed a strong association. These observations in the Merensky Reef agree with the work of Barnes *et al.* (2008) in the Western Bushveld Complex and the Great Dyke of Zimbabwe where it was noted that approximately 30-60 % of the siderophile elements are present in chalcopyrite, pentlandite and pyrrhotite.

The PGM quantitative mineralogical observations show that the most common mode of PGM occurrence observed in this study occur along the border or margins of the sulphide aggregates.

The preferred association of PGM with sulphides is well known, with other numerous studies of quantitative mineralogy in the Merensky Reef having observed the same by Vermaak and Hendriks (1976), Mostert *et al.* (1982), Schouwstra *et al.* (2000), Pritchard *et al.* (2004), Godel *et al.* (2007) and Rose *et al.* (2011). The higher affinity of PGM with chalcopyrite and pentlandite over pyrrhotite in the Merensky Reef is consistent with earlier studies by Rose *et al.* (2011). There is also an association of BMS with silicates as also confirmed by petrographic work in Chapter 4. The secondary/alteration silicates also revealed associations with the PGMs and this association is thought to represent redistribution of PGMs (Rose *et al.* 2011).

Similarly, to the study done by Junge *et al.* (2014), most of the PGMs identified in this study are primarily platinum bearing (see platinum element distribution maps attached as part of the Appendix). Platinum showed strong affinity with semimetals to form a PGM compared to palladium. The lesser amounts of palladium and rhodium within the PGMs presented may be since the PGEs are present as solid solution within sulphide minerals, pentlandite (Junge *et al.* 2014; Holwell and Macdonald 2010; Godel *et al.* 2007). This correlates to the trace element analysis findings conducted on the EPMA which revealed that, of the highest concentrations of palladium (ppm) measured are within pentlandite; these findings are reviewed and follow as a sub-section in this chapter.

There are PGMs that are extensively affected by alteration and therefore redistribution of PGMs by late magmatic fluids as suggested by Rose *et al.* (2011), is thus likely as shown in Figure 5.2 A and B, where maslovite had intruded as a vein into the silicate mush. The intruding of PGM into BMS directs to late magmatic processes.

The strong association of PGM with alteration silicates could be related to the two modes in which PGMs might have occurred from; (1) the occurrence of PGM at the border of sulphides where sulphides are commonly rimmed by a variety of alteration silicates that form at the edges of primary silicates (Pritchard *et al.* 2004); (2) the occurrence within the rim of secondary/alteration silicates surrounding sulphides (Figure 5.2 and Figure 5.3) and Image 3 attached on Appendix BI; Li *et al.* 2004). PGM occurrences along the borders/margins of sulphides were the most common in this present study.

Some other authors have found that PGM occurring at the borders of sulphides are more common than PGM enclosed by sulphides (e.g. Vermaak and Hendriks 1976; Schwellnus *et*

al. 1976; Mostert *et al.* 1982; Godel *et al.* 2007) while Penberthy and Merkle (1999) proposed that PGMs occurring with BMS at the grain boundaries or enclosed within BMS may be related to exsolution of PGMs from monosulphide solid solution. Furthermore, Yang *et al.* (1992) proposed that the PGMs occurring at the margins of sulphides could probably have been formed during the last crystallisation stage of the sulphide melt while PGMs that occur enclosed within sulphides represent primitive PGM formed during the sulphide crystallisation stage (Yang *et al.* 1992).

It has been observed that tellurides form the most abundant PGE group at both mines. Sperrylite is the abundant PGM in the Merensky Reef (based on the data sourced from the Western Platinum and Rusternburg Platinum Mines in the western limb) (Brynard *et al.* 1976). However, in this study sperrylite is more enriched at Modikwa relative to Two Rivers. This could be due to the increased arsenic activity during the late stage of PGE mineralization resulting in formation of superimposed sperrylite mineralization. Fluid alteration could be the factor controlling the PGE-arsenides as they were observed occurring in sulphide veins at Modikwa. Laurite is present within both Modikwa and Two Rivers as was documented in the previous work of Kinloch (1982) and Lee (1986) in the Merensky Reef. Currently, explanation of the PGM alteration processes by fluids is lacking. The Merensky Reef pyroxenite sequence revealed different PGM types with varying grain sizes distributions which may possibly influence the recovery of the PGE during flotation in situations where PGM are fully liberated. Coarser PGMs are associated with coarser sulphides suggesting a correlation between the grain size distribution of PGM and sulphides. BMS are strongly associated with PGM.

5.3 PGE Concentration Analyses in Sulphides

5.3.1 *Platinum Group Element concentration in BMS at Modikwa and Two Rivers*

Trace elements including platinum group elements (platinum, palladium, rhodium, ruthenium, iridium and osmium) in the base metal sulphides were carried out to determine the distribution of these elements in the sulphides. A total of 17 sulphide-rich samples were carefully selected and analysed for PGE concentrations. Only the Platinum group (PPGE), which includes palladium, rhodium and platinum concentrations were detected.

The Iridium-group (IPGE), which includes iridium, ruthenium and osmium, concentrations were mostly below detection limits. The concentrations of all points analysed for PGE in BMS are outlined in the tables below. The lower limit of detection is <10 ppm for all PGE.

Drill core OV 777

Pentlandite: Palladium in pentlandite shows lower concentrations ranging from a minimum of 3 to 67 ppm. Rhodium in pentlandite shows concentrations reaching up to 77 ppm. The high nickel concentrations are expected as they point to the presence of base metal sulphides, pentlandite. The results are depicted in Table 5.8 below.

Pyrrhotite: In sample OV 777-1, palladium concentrations in pyrrhotite range from 18 to 112 ppm with an average of about 67 ppm. The palladium content in pyrrhotite is even higher than that of pentlandite in this sample (OV 777-1). Rhodium concentrations in pyrrhotite reaches up to 67 ppm, platinum reaches up to 14 ppm in pyrrhotite.

In sample OV 777-10, pyrrhotite shows both rhodium and palladium concentrations decreasing down to 17 and 15 ppm, respectively. Sample OV 777-10 is within the range of the Merensky Reef pyroxenite while sample OV 777-1 is near the top chromitite stringer.

Chalcopyrite: In sample OV 777-1, chalcopyrite shows high rhodium concentrations ranging from 85 ppm to a maximum of 793 ppm. Platinum concentrations in the chalcopyrite reach up to 4 ppm (Table 5.8).

Drill core OV 778

Pentlandite: Sample OV 778-2 is near the top chromitite stringer. It contains the highest palladium concentrations varying from 45 to a maximum of 379 ppm. However, low palladium concentrations are observed in pyrrhotite (up to112 ppm) compared to pentlandite and none detected in chalcopyrite. Rhodium concentrations in pentlandite range between 32 and 122 ppm (Table 5.9 below).

In sample OV 778-4, also close to the top chromitite stringer, rhodium concentration ranges from 2 and 11 ppm in pentlandite. Palladium in pentlandite ranges between 44 and 122. Platinum reaches up to 53 ppm in pentlandite, increased concentrations were identified in chalcopyrite reaching up to 93 ppm.

Sample OV 778-9 (close to the bottom chromitite stringer), pentlandite contains varying palladium concentrations starting off at 33 and 49 ppm and then increasing up to 131 ppm at maximum. Rhodium contents in pentlandite in this sample reach up to 17 ppm.

Magnetite concentrations detected in this sample (OV 778-9) revealed extremely higher varying rhodium concentrations ranging between 916 and 982 ppm.

Pyrrhotite: Concentrations of platinum and palladium in pyrrhotite reach up to 9 and 112 ppm, respectively in sample OV 778-2, rhodium reaches up to 17 ppm in pyrrhotite while it reaches up to 122 ppm in pentlandite.

Pyrrhotite in sample 778-4 hardly contains any PGE. Analysis carried out on sample OV 778-9 shows palladium concentrations in pyrrhotite reaching up to 106 ppm (sample occurs correctly within the bottom chromitite stringer).

Chalcopyrite: Sample OV 778-2 show high rhodium concentrations in chalcopyrite and reaching up to 181 ppm.

Sample OV 778-4 occcurs near the top chromitite stringer and show higher rhodium concentrations in chalcopyrite, ranging between 552 and 579 ppm at maximum.

Sample OV 778-9, which is also near the top chromitite stringer show palladium concentrations in chalcopyrite reaching up to 59 ppm. It is worth noting that concentrations of all the PPGE in the analysed samples from Modikwa increase rapidly within or closer to the top chromite stringers.

Table 5.8: PGE concentration in base metal sulphides at Modikwa (All concentrations in ppm)

OV 777-1					OV 778-4				
Mineral	**Ni**	**Rh**	**Pd**	**Pt**	**Mineral**	**Ni**	**Rh**	**Pd**	**Pt**
Pyrrhotite	2717	n.d	n.d	n.d	Pyrrhotite	1552	n.d	n.d	n.d
Pyrrhotite	3086	67	n.d	n.d	Pentlandite	319200	n.d	44	n.d
Pyrrhotite	2605	n.d	112	14	Pentlandite	312000	2	n.d	n.d
Pyrrhotite	2674	n.d	18	n.d	Pentlandite	314800	11	122	n.d
Pentlandite	312200	n.d	67	n.d	Pentlandite	321300	n.d	78	53
Pentlandite	323400	77	3	n.d	Chalcopyrite	n.d	577	n.d	n.d
Chalcopyrite	n.d	85	n.d	n.d	Chalcopyrite	n.d	359	n.d	93
Chalcopyrite	n.d	793	n.d	4	Chalcopyrite	n.d	n.d	17	n.d
OV 777-10					Chalcopyrite	n.d	579	n.d	n.d
Pyrrhotite	n.d	n.d	15	n.d					
Pyrrhotite	n.d	17	n.d	n.d					
OV 778-2					**OV 778-9**				
Pyrrhotite	562	n.d	112	9	Chalcopyrite	n.d	552	n.d	n.d
Chalcopyrite	n.d	181	n.d	n.d	Pyrrhotite	331	n.d	106	n.d
Pentlandite	257200	122	178	n.d	Pentlandite	336800	17	33	n.d
Pentlandite	246000	n.d	379	n.d	Pentlandite	339600	n.d	49	n.d
Pentlandite	288500	37	309	n.d	Pentlandite	306900	n.d	131	n.d
Pentlandite	243900	32	45	n.d	Pentlandite	310600	n.d	n.d	n.d
Pentlandite	218100	111	229	n.d	Chalcopyrite	30	n.d	59	n.d
					Magnetite*	676	916	n.d	n.d
					Magnetite*	1267	941	n.d	n.d
					Magnetite*	1097	982	n.d	n.d

*Magnetite detected by microprobe with high Rh contents
n.d – not detected

Drill core TRP 260

Pentlandite: Pentlandite contains high palladium concentrations of about 62 ppm in sample TRP 260-2-2, which occurs near the top chromitite stringer. Rhodium concentrations in pentlandite reach up to 19 ppm in this sample.

In sample TRP 260-4-4, palladium concentrations in pentlandite range between 30 and 79 ppm. Rhodium concentrations range from 19 to 39 ppm.

Pyrrhotite: In sample TRP 260-2-2, pyrrhotite show significant concentrations of platinum varying between 8 and 283 ppm. Rhodium in pyrrhotite ranges from 35 to 49 ppm. Palladium concentrations reached up to 30 ppm.

In sample TRP 260-4-4, pyrrhotite shows rhodium concentrations reaching up to 30 ppm while palladium concentrations reach up to 46 ppm.

Chalcopyrite: A chalcopyrite grain in sample TRP 260-4-4 indicated platinum concentrations reaching up to 52 ppm, while palladium concentrations range between 12 and 50 ppm in pentlandite.

Pyrite: Rhodium concentrations in pyrite range between of 9 and 76 ppm in sample TRP 260-2-2.

Magnetite: Sample TRP 260-4-4 indicated rhodium concentrations reaching up to 930 ppm.

Drill core TRP 271

Pentlandite: Samples TRP 271-15A and TRP 271-15B were taken close to the bottom chromitite stringer. Pentlandite shows palladium concentrations ranging from 207 and 300 ppm in TRP 271-15A and relatively higher palladium concentration (from 257 to 695 ppm) in sample TRP 271-15B. Rhodium shows relatively high concentrations in pentlandite in this sample reaching up to 240 ppm in sample TRP 271-15A compared to TRP 271-15B (up to 17 ppm).

Pyrrhotite: Platinum concentrations in pyrrhotite range between 24 ppm (Sample TRP 271-5A) and 159 ppm (Sample TRP 271-15B). Rhodium concentrations in pyrrhotite vary from 41, 48 and up to 59 ppm. Palladium concentrations in pyrrhotite also vary between from 24, 50 and 70 ppm.

Pentlandite: Sample TRP 271-15A shows palladium concentrations in pentlandite ranging between 207 and 300 ppm. Rhodium shows relatively high concentrations in pentlandite in this sample reaching up to 240 ppm. The sample is close to the bottom chromitite stringer.

Sample TRP 271-15B, is like the previous sample 271-15A, where pentlandite shows varying significant high concentrations of palladium, but the concentrations are slightly increased in TRP 271- 15B. Rhodium concentration in pentlandite reaches up to 17 ppm.

Pyrrhotite: Platinum concentrations are contained in pyrrhotite, ranging between 24 ppm (in sample TRP 271-5A) and 159 ppm (in sample TRP 271-15B). The rhodium concentrations are also contained in pyrrhotite varying between 41, 48 and reaching up to a maximum of 59

ppm. Palladium concentrations contained in pyrrhotite also vary between from 24, 50 and 70 ppm. All concentrations are presented in Table 5.13 below.

Table 5.9: PGE concentration in base metal sulphides at Two Rivers (All concentrations in ppm)

TRP 260-2-2					TRP 271-15A				
Mineral	Ni	Rh	Pd	Pt	Mineral	Ni	Rh	Pd	Pt
Pyrrhotite	4201	35	n.d	283	Pyrrhotite	4863	n.d	n.d	n.d
Pyrrhotite	1652	49	n.d	n.d	Pyrrhotite	5572	n.d	8	159
Pyrrhotite	2128	n.d	n.d	n.d	Pyrrhotite	5592	n.d	n.d	n.d
Pyrrhotite	2118	n.d	n.d	n.d	Pyrrhotite	6685	n.d	n.d	n.d
Pyrrhotite	4049	n.d	n.d	n.d	Pyrrhotite	7119	n.d	n.d	n.d
Pentlandite	344200	n.d	n.d	n.d	Pyrrhotite	331900	n.d	n.d	n.d
Pentlandite	347300	19	n.d	n.d	Pyrrhotite	6089	n.d	24	n.d
Pentlandite	346400	n.d	n.d	n.d	Pentlandite	353200	n.d	207	n.d
Pyrite	1030	9	n.d	n.d	Pentlandite	353700	240	300	n.d
Pyrite	397	76	n.d	n.d					
TRP 260-4-4					**TRP 271-15B**				
Pyrrhotite	1585	30	46	n.d	Pyrrhotite	6057	59	n.d	24
Pyrrhotite	1778	n.d	n.d	n.d	Pyrrhotite	5697	n.d	24	n.d
Pentlandite	345200	n.d	n.d	n.d	Pyrrhotite	5409	n.d	n.d	n.d
Pentlandite	342000	39	79	n.d	Pyrrhotite	5452	48	n.d	n.d
Pentlandite	339100	19	30	n.d	Pyrrhotite	6323	n.d	70	n.d
Pentlandite	344900	n.d	79	n.d	Pyrrhotite	6386	n.d	23	n.d
Chalcopyrite	n.d	n.d	12	n.d	Pyrrhotite	6687	41	n.d	n.d
Chalcopyrite	n.d	n.d	50	n.d	Pyrrhotite	6167	n.d	50	n.d
Pyrite	218	23	23	n.d	Pentlandite	350500	17	695	n.d
Pyrite	9	n.d	n.d	n.d	Pentlandite	331300	n.d	257	n.d
Magnetite*	614	930	n.d	n.d					

*Magnetite detected by microprobe with high Rh contents
n.d – not detected

5.3.2 *Discussion*

The PGE concentrations in BMS showed similar distribution patterns (particularly the PPGE-group) in the Merensky Reef sequence at Modikwa and Two Rivers. Based on Knight (2014), the PGE may bond together as PGE alloys or with base metals (e.g. nickel and copper) and semimetals (arsenic, bismuth, antimony, selenium, and tellurium) forming PGM. Alternatively, PGE may occur as trace elements in solid solution in BMS (Naldrett 2004). The distribution of the PGE in BMS in both mines revealed highest palladium concentrations in pentlandite, with lesser amounts in pyrrhotite and barely any in chalcopyrite. Pentlandite is the principal host of palladium at both Modikwa and Two Rivers with palladium concentration reaching up to 379 ppm and 695 ppm respectively.

In all the four studied drill cores (TRP 260; TRP 271; OV 777 and OV 778) it has been found out that palladium is enriched in pentlandite. Previous studies in the Merensky and Platreef on EPMA and LA-ICP-MS indicated higher concentrations of palladium and rhodium in pentlandite (e.g. Cabri 1984; Oberthür *et al.* 2003; Godel *et al.* 2007; Holwell and McDonald 2010; Osbahr *et al.* 2013, 2014; Junge *et al.* 2014).

Other researchers (e.g. Ballhaus 2001; Fleet 1993; Mungall *et al.* 2005; Li *et al.* 1996) used experiments to determine how PGE and gold behave in terms of partitioning between MSS and a sulphide liquid and concluded that copper, platinum, palladium and gold are all strongly incompatible with MSS whereas iridium and rhodium are strongly compatible.

In this study, PGEs are mostly present in pyrrhotite and pentlandite with chalcopyrite hosting a larger amount of rhodium at Modikwa. This is the principal difference observed between the two mines where significant rhodium concentrations are contained in chalcopyrite at Modikwa with concentrations reaching up to a maximum of 793 ppm, while at Two Rivers rhodium concentrations are more enriched in pentlandite; reaching up to a maximum of 240 ppm. The enrichment of rhodium in chalcopyrite might suggest that rhodium readily substitutes for copper. There is little research into the remobilisation of rhodium in chalcopyrite as most of the investigations concentrated on platinum and palladium. Other researchers (e.g. Ballhaus and Sylvester 2000; Barnes *et al.* 2008 and Godel *et al.* 2007) of the Merensky Reef have observed differently and found chalcopyrite containing the lowest PGE values including rhodium. At Two Rivers, rhodium values are contained in pentlandite which is consistent with the work of Rose *et al.* (2011) and Junge *et al.* (2014) who also reported high rhodium values in pentlandite in the same mine.

Two Rivers show high platinum concentrations (up to 283 ppm) relative to Modikwa (up to 93 ppm) with platinum concentrations identified at both mines contained in pyrrhotite compared to other sulphides. This is somehow surprising as accordingly, pyrrhotite and pentlandite should be enriched in osmium, iridium, ruthenium and rhodium and chalcopyrite in palladium, platinum, silver and gold, however, this effect was not observed in previous studies of different nickel-copper-PGE deposits (Barnes *et al.* 2006; Dare *et al.* 2010; Godel *et al.* 2007). There seem to be variation in precious metals and PGE in different sulphide phases due to fractionation of the sulphide liquid containing these elements.

Additional studies by Peregoedova (1998) indicated that platinum and palladium are not only incompatible with MSS, but also incompatible with ISS.

Individual PGE behaves differently, and this behaviour changes because of different magma compositions, cooling rates and post magmatic alteration. In this study, platinum show strong affinity with semimetals to form PGM than palladium.

Helmy *et al.* (2007) studied the effects of tellurium on the partition coefficients of platinum and palladium in MSS and found that platinum also showed strong affinity with semimetals to form PGM than palladium.

He concluded that with limited semimetals available, excess palladium would be accommodated by pentlandite rather than competing with platinum to form a PGM with the semimetals (Helmy *et al.* 2007). Further studies by Helmy *et al.* (2010) show arsenic behaving more complex and dependant on the proportions of platinum and palladium present. If platinum is dominant, sperrylite may crystallise, whereas if palladium is dominant, an immiscible palladium-arsenic liquid may separate from the sulphide melt; both these processes occur early before the crystallisation of MSS.

Campbell and Naldrett (1979) suggested that sulphides that formed from a very large volume of magma (large R) would have low copper/platinum ratios, reflecting the effect of the high partition coefficient for platinum into sulphide. Where there is less volume of magma (small R), the effect of depleting the magma in platinum becomes dominant and higher copper/platinum values are predicted Campbell and Naldrett (1979). The PGE are predominantly affected by variants in R due to their high partition coefficients into sulphide liquids.

Another noteworthy difference observed in this study is the high concentrations of rhodium in magnetite in both mines, with concentrations reaching up to 982 ppm at Modikwa and up to 930 ppm Two Rivers. Published information on the PGE distribution in magnetite is scarce. However, Barnes *et al.* (2004) and Page *et al.* (1982) investigated the PGE composition of magnetite layers in the Bushveld and concluded that magnetite contained very little PGEs (including rhodium) implying to a virtual absence of sulphide minerals presumably because of the unsaturation of sulphur in the magma. The high PGE concentrations in parts enriched by magnetite (while these zones do not contain sulphur) suggest desulphurisation and the formation of secondary magnetite.

As magma cools, instabilities generated partial desulphurisation of the sulphides (Knight 2014). It is a thought that fluids altered the BMS to secondary magnetite and deposited rhodium but a possible explanation for the processes involved in the deposition of rhodium in magnetite is lacking at present.

Generally, the PGE distribution patterns throughout the Merensky Reef pyroxenite in all the four studied drill cores show maximum PGE concentrations at the top and bottom chromitite stringers. These observations at Modikwa were also reported by Mitchell and Scoon (2007) at Winnaarshoek property in the central sector of the eastern Bushveld. They observed high PGE concentrations associated to the top chromitite stringer. Rose *et al.* (2011) observed high PGE concentrations in both the top and bottom chromitite stringers in the southern sector at Two Rivers.

Even though the processes involved in PGE collection remains indistinct, it has been observed that the PGE in the reefs are in many cases found associated with BMS or occur in PGM that are associated with these BMS (Kinloch, 1982; Ballhaus and Sylvester 2000; Zientek *et al.* 2002; Pritchard *et al.* 2004).

Naldrett and Lehmann (1988) suggested that the BMS that were initially in the chromitite layer had interacted with the chromite resulting in the loss of sulphur, copper and palladium from the chromitite layer. Sulphide saturation is most likely responsible for the formation of BMS and the scavenging of PGE in the Merensky Reef in both the Eastern limb and in the Western limb (Teigler and Eales 1993 and Rose *et al.* 2011). Maier (2005) reported that extensive degrees of partial melting are required to allow PGEs to separate from the mantle and become incorporated into the melt. The crystallization of these iron-rich minerals lowers the oxygen fugacity allowing for sulphur saturation (Maier 2005 and Cawthorn 2010). Then the interaction of sulphides with large volume of magma makes greater chance to scavenge the PGEs. However, sulphides maybe reworked as magma rises while pressure is reduced and allowing for more sulphide saturation (Maier 2005).

It is concluded that at Two Rivers the behaviour of the PGE during magmatic conditions causes rhodium to prefer pentlandite whereas at Modikwa rhodium tends to partition in chalcopyrite.

Therefore, high rhodium concentrations in the Merensky Reef at both Modikwa and Two Rivers cannot be generalized that pentlandite is the host 100 % of both palladium and rhodium, as observed in this study that significant rhodium contents are also contained in chalcopyrite at Modikwa.

The association of PGEs with sulphides generally points to the fact that PGEs were originally concentrated by an immiscible sulphide liquid (e.g. Naldrett *et al.* 1979; Naldrett 2004).

Barnes and Maier (2002) specified that the partition coefficients between sulphide and silicate liquids for PGE, Au, Ni, and Cu are all high suggesting that the principal phase that collected the metals was a sulphide liquid. Furthermore Li *et al.* (2004) and Hutchison and McDonald, (2008) stated that if PGE are present in solid solution in BMS, hydrothermal fluids may liberate PGE from their BMS host resulting in the formation of PGM within and at the edges of sulphides. This sulphide liquid could have settled onto the cumulate pile along with other cumulate phases (Naldrett 1989; Campbell 1983).

5.4 Fire Assay-Analytical Results

The assay data for the two drill cores (TRP 260 and TRP 271) from Dwarsriver farm was provided by Two Rivers Platinum Mine (not all the assay data is attached to the appendix due to confidentiality). The data was unavailable for the other two drill cores from Onverwacht farm at Modikwa; hence the assay analysis was conducted at Mintek. The mineralization in the Merensky Reef show close relationship with the chromitite stringers. Highest PGE concentration is contained within the top chromitite stringer and bottom chromitite stringers and referred to as top and bottom loaded respectively. Grade profiles of the mineralization are attached in Appendix H, Images 26-29. These profiles are only reported based on the Platinum group (PPGE), which includes platinum, palladium and rhodium.

The grade profiles for drill cores OV 777 and OV 778 from Modikwa commonly show relatively higher platinum, palladium and rhodium concentration in the top chromitite stringer and decreasing within the pyroxenite then slightly increase again within the bottom chromitite stringer. Platinum shows a concentration of 6.8 ppm within the top chromitite stringer at OV 777, it increases and decreases within the pyroxenite to 0.2 ppm and then increases rapidly to 5.9 ppm in the bottom chromitite stringer.

Palladium reaches up to 2.0 ppm in the top chromitite stringer and decreases to 0.24 ppm right through in the pyroxenite and then increase to 1.55 ppm in the bottom chromitite stringer. Rhodium reaches up to 0.39 in top chromitite stringer and then slightly decreases to 0.29 in bottom chromitite stringer. The mineralization in this drill core is thus referred to as top loaded given the higher PPGE (platinum, palladium and rhodium) concentration within the top chromitite stringer (See appendix H, Image 26).

Platinum shows a high concentration of 6.6 ppm within the top chromitite stringer at OV 778, it then decreases within the pyroxenite to 2.4 ppm and then increases slightly to 3.2 ppm in the bottom chromitite stringer.

Palladium reaches up to 1.9 ppm in the top chromitite stringer and decreases right through in the pyroxenite and reaching up to 1.1 ppm in the bottom chromitite stringer. Rh reaches up to 0.39 in top chromitite stringer and then slightly decreases to 0.29 in bottom chromitite stringer. The mineralization in this drill core is thus referred to as top loaded given the higher PPGE (platinum, palladium and rhodium) concentration within the top chromitite stringer (See Appendix H, Image 27).

The grade profiles of drill cores TRP 260 and TRP 271 from Two Rivers generally shows an increased PPGE along the bottom chromitite stringers compared to the top chromitite stringers with rapid decrease in the pyroxenite. Platinum shows a concentration of 5.1 ppm within the top chromitite stringer at TRP 260, it decreases within the pyroxenite and increases to 6.5 ppm in the bottom chromitite stringer.

Palladium starts off at 1.2 ppm in the top chromitite stringer and then remains constant in the pyroxenite and then increases rapidly to 4.3 ppm in the bottom chromitite stringer. Rhodium reaches up to 0.3 ppm in top chromitite stringer and then slightly decreases in the pyroxenite and then slightly increases again in the bottom chromitite stringer reaching a minimum of 0.34 ppm. Platinum and rhodium reveal the same pattern. The mineralization in this drill core is thus indicated as bottom loaded given the higher PPGE (platinum, palladium and rhodium) concentration within the bottom chromitite stringer (See Appendix H, Image 28).

Platinum shows a concentration of 3.3 ppm within the top chromitite stringer at drill core TRP 271. It remains constant within the pyroxenite at 3.3 ppm and then later increases to a maximum of 5.3 ppm in the bottom chromitite stringer.

Palladium reaches up to 0.10 ppm in the top chromitite stringer; it increases within the pyroxenite to 3 ppm and reaches up to 4.7 ppm in the bottom chromitite stringer. Rhodium reaches up to 0.26 ppm in the top chromitite stringer, remains constant in the pyroxenite and later increases to 0.39 ppm in the bottom chromitite stringer. Platinum, palladium and rhodium reveal the same pattern in the bottom chromitite stringer. The mineralization in this drill core exhibit complex patterns.

Platinum concentrations are higher in the top chromitite while palladium and rhodium only start off to increase within the pyroxenite but considering the higher PPGE (platinum, palladium and rhodium) concentration within the bottom chromitite stringer, this drill core referred to bottom loaded (See Appendix H, Image 29).

Barnes and Maier (2002) concluded three possibilities which can be considered regarding the PGE paradox; (1) the affinity of chromitites to bond with PGEs than silicate rocks could arise since the conditions favouring chromite crystallisation also favour PGM crystallisation or as chromitites nucleate on the PGM and then settle them out of the silicate liquid;

(2) PGEs are concentrated by the MSS that crystallised from a sulphide liquid but this does not address the enrichment of platinum in chromitites which has been observed in this study; (3) the PGE enrichment in chromitite layers is due to the interaction between trapped sulphides liquid and chromitite resulting in loss of sulphur from the sulphide liquid. During reheating the sulphides may have reacted with chromites leading to low sulphur contents in the sulphide liquid and some of the fractionated liquid is squeezed out from the chromitite during compaction.

Tredoux *et al.* (1995) indicated that the relative proportion of the six PGEs in the magmas depends largely on the temperatures reached during the melting event and that they are carried in the magmas, not in true solution but as tiny clusters of 500-100 metal atoms. This would suggest that, magmas generated at lower temperatures are relatively enriched in the metals of lower melting points (platinum, palladium and rhodium), while magmas formed at higher temperatures would bear high proportions of the metals of higher melting points (ruthenium, iridium and osmium).

Additionally, the PGE mineralization has also been observed in this study associated with compositional variations within the host pyroxenite, this relationship could suggest that controls on PGE mineralization are essentially primary magmatic as proposed by Scoon and Mitchell (2007). Scoon and Teigler (1994) interpreted height related trends in the PGE-bearing, sulphide poor, chromitites of the Bushveld Complex (LG-1 through UG-1) as differentiating magma chamber. The formation of both chromitite layers and PGE mineralization is ascribed to magma mixing due to repeated replenishment (Scoon and Mitchell 2007).

Summary

Contrary to what was documented by Lee (1996) that in most of the Merensky Reef facies the economic PGE mineralization is concentrated in the pegmatoidal feldspathic pyroxenite. It has been observed in all the four drill cores that, significant PPGE concentrations occur within the chromitite stringers however a slight decrease within the pyroxenite range was also recorded. The PGE distribution pattern observed in the two mines differ, exhibiting a top loaded PGE mineralization in drill cores from the central sector (Modikwa) while drill cores from the southern sector (Two Rivers) represent a bottom loaded PGE mineralization. The comparatively high PGE grades at Modikwa in the top chromitite stringer and high PGE grades in the bottom chromitite stringer at Two Rivers is probably reflecting sulphur saturation which resulted in high PGE grades.

This could suggest different injections of magma, each producing a chromitite and pyroxenite, the absence or lesser number of PGEs in the top/bottom chromitite stringers is presumably attributed to the unsaturation of sulphur in the magma. Cameron (1982) suggested that these different events of magma injections might have been enriched or depleted in sulphur or mixing with the residual magma and might have caused a change in the oxygen (fO_2), sulphur (fS_2) fugacity and a change in total pressure. These ideas imply that the processes that triggered the S removal and the platinum and/or palladium enrichment or remobilisation are complex and most likely distinct. However, after all these factual evidences there remain uncertainties about the precise deposition of these ore.

5.5 Theories relating to the origin of the ore

As previously mentioned from Chapter 1 of this study, the boundary between the Main and Critical zones is of interest here, as the Merensky Reef occurs within this vicinity. From this study, two PGE peaks were observed in each of the four drill cores from the two mines. The PGE contents are analogous to a profile described by Rose *et al.* (2011) from Two Rivers and from near Atok by Scoon and Mitchell (2002), with both mines reaviling the lower and the upper peak associated with BMS within the chromitite stringers. This trend clearly suggests there are two separate mineralization events which appear to have contributed to the PGE content of the Merensky Reef, one associated with sulphide mineralization and the other associated with chromitite layer. As observed in this study, PGMs occur as microscopic inclusions within sulphide grains (Figures 4.2 - 4.4), at the margins of sulphide grains and to a lesser extent as inclusions in silicate minerals. A significant proportion of them occur as invisible solid solutions of PGEs within sulphide grains (as shown in section 5.2 under PGE concentration). There is no uniquely convincing answer as the facts are open and interpreted in different ways and include:

Sulphide as a collector

Several models based on the mixing of magmas in a stratified sequence of liquid layers and scavenging of PGEs have been formulated, one of them is that of Naldrett *et al.* (1987), where he theorised that turbulent plumes of hot, ultramafic liquid rose through a stratified sequence of liquids overlying the crystal line floor until they reached a level where their relatively required low density required them to spread laterally as a new, vigorously convecting, intrusive layer. As this layer, lost heat to the cooler environment, crystallisation of orthopyroxene and separation of sulphides liquid droplets would have begun within the layer.

In time, dense slurry of orthopyroxene plus sulphide plus entrained liquid would have broken through the interface with the underlying liquid layer and plunged downwards to the crystallisation floor which would have been the Meensky Reef. Viljoen (1999) attributed the Merensky Reef as regional unconformity. If this is the case, then how is it possible that the emplacement of slurry from which both orthopyroxene and sulphides were already separating would can erode the Merensky Reef footwall at depths of tens of meters.

Chromite as a collector

In contrast, it is not possible to explain the PGE content by considering only the model of collection of PGE by sulphide liquid stated above. Contradictions arose with this model since it does not address the association of chromitite with the PGE. Cawthorn (2010) suggested that a layer of chromitite was later deposited followed by pyroxenite, with each chromitite layer associated with mineralization of sulphide liquid carrying PGEs. Hiemstra (1979) at the South African National Institute for Metallurgy pointed out that PGEs in the Bushveld ores occur as such small particles that they could not have settled sufficiently rapidly to become concentrated together with the much larger chromite grains. He further highlighted that sulphide droplets are capable of wetting chromites crystals and thus adhering to, and sinking with them through the liquid.

The effects of auxiliary or reactions

Other researchers have pointed out high degree of alteration of silicates minerals of the Merensky Reef by water-rich fluids. Ballhaus and Stumpfl (1986) at the Mining University, Leoben, Australia interpreted this to mean that when sulphur in the melt reacted to form sulphides, water was formed in the magma as a separate fluid. The PGEs were then concentrated in this fluid as complex chlorides and then precipitated around the sulphide grains. Other workers maintained that the separation of chromite depletes the magma in iron and that this causes the sulphur in the melt to become less soluble and thus to form sulphides with which the PGEs are associated.

Sulphide layers as traps

It has also been popularly documented that as unconsolidated crystal mushes became compacted, residual fluids were expelled from them and driven upwards through the crystal pile.

When they encountered the sulphide-rich Merensky Reef, the PGEs they carried were trapped. There are sulphide bearing layers beneath the Merensky Reef which are not economically mineralised, thus this view can be discounted.

Deposition by primary (orthomagmatic) processes

The nature of the Merensky Reef at Winnaarshoek property in the central sector of the Eastern limb has provided similar trends to what was observed in the current study.

The PGE mineralization in this area is concentrated within the two chromitite layers hosted by a Merensky pyroxenite. Pegmatoidal units are developed but rather weakly mineralised and lie outside the mineralised zone.

Arguments based on chalcophile properties of the PGEs have led Naldrett (2008) to the view that mantle processes and the emplacement of mantle-derived magmas into one or more staging chambers beneath the presently exposed Bushveld, may have been more effective in yielding PGE-enriched magmas. Traditional views that have no more than ultra-trace levels of PGEs characterising basaltic liquids elsewhere are questioned, the view expressed that, levels approaching 200 ppb could have been generated in magmas specifically parental to the Merensky Reef. Emplacement of such magmas in more than a single pulse could imply an orthomagmatic origin for the ore. Additionally, it was suggested during the development of the concept of enrichment in PGEs with a staging chamber beneath the Bushveld that, sulphur unsaturated magma reacted with early-formed sulphide in the staging chamber by dissolving iron sulphide and thus enriching the remaining sulphide in PGEs (Naldrett *et al.* 2009).

Studies by Seabrook *et al.* (2005) have shed a light on complexities that were not unravelled in the earlier years which could be considered. These studies were focused on the geochemical and isotopic differences between the Critical and Main zones and have shown that these two units are end-products of processes of mixing of gravitationally settled cumulus crystals of orthopyroxene and plagioclase, rather than of mixing of their parent liquids. The different geochemical and isotopic signatures of the two minerals present in the cumulus rock point to their derivation from different parent magmas where orthopyroxene grains have been derived from Critical zone magmas while plagioclase grains in the same layer were from Main zone.

Proposed model for the current study

It is well known and supported by the data of the current study that sulphide saturation was caused by magma mixing which led to the formation of the immiscible sulphide liquid into which PGE partitioned (Campbell and Naldrett 1979; Campbell *et al.* 1983; Naldrett 2010). The strong association observed in quantitative mineralogy between PGM and sulphides in this study is confirmed by other numerous studies (e.g. Vermaak and Hendriks 1976; Schwellnus *et al.* 1976; Mostert *et al.* 1982; Schouwstra *et al.* 2000; Pritchard *et al.* 2004; Godel *et al.* 2007; Rose *et al.* 2011).

Thus, the sulphide liquid has been identified as the major collector of PGE in the genetic models proposed for the Merensky Reef. As this leaves little doubt that the PGE was emplaced in the Merensky Reef with a sulphide liquid.

In addition, Naldrett and Lehmann (1988) suggested that the iron sulphide could react with chromite producing an iron rich chromite and removing sulphur from the system, thereby triggering PGM crystallisation by lowering the fS_2. This suggestion could explain the fact that BMS in the chromitite layers have high PGE/s ratios and are generally rich in copper and nickel.

The current study has revealed that PGEs may occur as trace elements in solid solution in BMS as documented by Naldrett (2004). This view would mean common economic PGE occurrences are often linked to magmatic sulphide ore deposits.

Hence, understanding the genesis of these types of deposits requires the knowledge of the physical and chemical processes involved. Pressure, temperature, composition and oxidation state of the magma are important factors controlling the solubility of iron sulphide in magmas and therefore potentially affecting the point at which sulphide saturation is achieved.

However, the view of Tredoux *et al.* (1995) is that the relative proportions of the six PGEs in the magma depend largely on the temperatures reached during the melting event, and that they are carried in the magma and not in the solution but as tiny clusters. This proposal would then suggest that magmas generated at lower temperatures are relatively enriched in the metals of lower melting points (platinum, palladium and rhodium), while magmas formed at higher temperatures would bear higher proportions of the metals of a lower melting point (ruthenium, iridium and osmium).

The briefly summarised ideas stated above reveal a lack of consensus in accounting for PGE as some models are suggest the association of PGM with chromite while some argue for sulphides as collectors. These ideas point to the necessity of continued detailed research to eventually uncover the convincing models.

5.6 Summary and Conclusions

The sequence of the Merensky Reef at the two sectors of the Eastern Bushveld showed a remarkable similarity in their mineralogy suggesting that these two sectors (central and southern) might have formed from the same liquid or formed simultaneously within a single magma chamber. The mode of occurrence of the PGM is of importance, not only from a genetic point of view but also for the recovery of PGE values. Three mineralogical PGM occurrence are shown by the current study and these are with chromite, base metal sulphide and silicates. The association of PGM with the base metal sulphide is identified as a remarkable one (Rose *et al.* 2011). The close association of PGM with BMS and at the margins of sulphide indicate that the PGM were derived from the sulphide melt.

From the quantitative mineralogical data acquired the following conclusions at Modikwa and TRP Mines are drawn.

- At Two Rivers, the pegmatoidal feldspathic pyroxenite is literally absent while at Modikwa it is found sandwiched in between the normal pyroxenite close to the top chromitite stringer.
- In both Modikwa and Two Rivers, the most abundant silicate minerals include orthopyroxene, clinopyroxene and plagioclase.
- In both mines samples of the Merensky Reef, show pyrrhotite as the most abundant sulphide mineral followed by pentlandite, chalcopyrite and pyrite.
- Relative proportions of dominant PGMs differed between the two mines, with tellurides and bismuthotellurides being the most dominant PGE group. At Modikwa 85 % of the PGMs were PGE-tellurides and bismuthotellurides while Two Rivers indicated 97 %. PGE-sulphides, tellurides and laurite are the earliest or primary PGM assemblage to form, whereas PGE-alloys, arsenides and sulpharsenides are related to late or post magmatic alteration effects.
- To maximise PGE recovery, the recovery of all the BMS needs to be optimised. Reagents are added to perform specific roles that manipulate the pulp chemistry and enhance the differences in mineral surface hydrophobicity to facilitate the separation. Due to the higher liberation and recovery potential of coarser PGMs, PGE-sulphides are recovered first, next will be PGE-tellurides and PGE-arsenides, and later PGE-alloys and gold (as these are usually finer in grain sizes).

- Sulphides and tellurides are both sensibly floatable without any collector while the arsenides are not amendable to floating due to their distinctive crystal structures. Flotation is beyond the scope of this work.
- The PGMs grain size varies between the two mines ranging from less than a micron to about 125 microns with an average of 20 microns.
- In all the four investigated drill cores, the PGE concentrations occur within the top and bottom chromitite stringers.
- Most of the PGEs in the two mines are hosted by PGMs and lesser amounts of PGE occur in solid solution within BMS.
- PGE distribution in the sulphides at Modikwa showed pentlandite containing the highest concentrations of palladium (up to 379 ppm) while the highest rhodium concentrations (up to 793 ppm) were contained in chalcopyrite. Samples from Two Rivers indicated pentlandite to be the principal host of both palladium and rhodium, with concentrations reaching up to 695 and 930 ppm respectively.
- Magnetite contains major amounts of Rh reaching up to a maximum of 982 at Modikwa while increased Rh amounts reach up to 930 ppm at Two Rivers.
- At both Modikwa and Two Rivers, the pyrrhotite compared to other sulphides contained all the elements found in the Platinum group (PPGE), namely, platinum, palladium, and rhodium, with all the platinum identified found in the pyrrhotite. The PGE mineralization varies within each mine. The mineralization revealed top loaded in the central sector and bottom loaded in the southern sector.
- Commonly occurring alteration silicates associated with the PGMs at both Modikwa and Two Rivers include talc, amphibole and serpentine. The mode of occurrence of these alteration silicates is commonly along the rims of primary silicates and sulphides and makes it difficult to predict liberation of the PGMs.
- The PGM mineralogy of the Merensky Reef pointedly diverse to that of the UG-2, based on the mineralogical investigation by Penberthy *et al.* (2000), the most commonly found PGM group are PGE sulphide minerals (e.g. laurite, cooperate, and braggite) in the UG-2 chromitites while the Merensky contains more of PGE-tellurides (e.g. maslovite and michenerite) and PGE-arsenides (e.g. sperrylite and platarsite) therefore, the concentrator plant requires customization to accommodate the distinctive challenges of floating the PGE minerals concentrated within the Merensky Reef.

Recommendations

The remobilisation of PGE requires much further research particularly the presence of PGE in magnetite and chalcopyrite to understand the behaviour of individual PGE and PGM as the chemistry classification of these minerals proved to be highly complex, based on the EDS analysis, and it is highly recommended that follow-up studies should be undertaken to challenge these aspects.

6 References

African Rainbow Minerals. Annual Report (2007).

Anglo Platinum Business Report (2003).

Arndt, N.T., Lesher, C.N., Czamanske, G.K., (2005). Mantle-derived magmas and magmatic Ni-Cu-(PGE) deposits. *Economic Geology, 100th Anniversary*. 5-25, pp.

Ballhaus, C., Tredoux, M., and Spath, A., (2001). Phase relations in the Fe-Ni-Cu-PGE-S system at magmatic temperature and application to massive sulphide ores of the Sudbury Igneous Complex. *Journal of Petrology*. **42:** 1911-1926, pp.

Ballhaus, C., and Sylvester, P. (2000). Noble Metal Enrichment Processes in the Merensky Reef: evidence from hydrous silicates and fluid inclusions. *Contributions to Mineralogy and Petrology*. **41:** 545-561, pp.

Ballhaus, C., and Ryan, C.G. (1995). Platinum-group elements in the Merensky Reef. I. PGE in solid solution in base metal sulphides and the down-temperature equilibration history of Merensky ores. *Contributions to Mineralogy and Petrology.***122:** 241-251, pp.

Ballhaus, C., and Stumpfl, E.F., (1986). Sulphides and platinum mineralization in the Merensky Reef: evidence from hydrous silicates and fluid inclusions. *Contributions to Mineralogy and Petrology.* **94:** 193-204, pp.

Barnes, S.J., Pritchard, H.M., Cox, R.A., Fisher, P.C, and Godel, B., (2008). The location of the chalcophile and siderophile elements in platinum group element ore deposits (a textural, microbeam and whole rock geochemical study): Implications for the formation the deposits. *Chemical Geology.* **248:** 295-317, pp.

Barnes, S.J., Cox, R.A., and Zientek, M.L., (2006). Platinum group element, Gold, Silver, and Base metal distribution in compositionally zoned sulphide droplets from the Medvezky Creek Mine, Noril'sk, Russia. *Contributions to mineral Petrology.* **152:** 187-200, pp.

Barnes, S. J. and Maier, W. D., (2002). Platinum-group element distributions in the Rustenburg Layered Suite of the Bushveld Complex, South Africa. In the Geology, Geochemistry, Mineralogy and Mineral Beneficiation of Platinum-Group Elements. Edited by L.J. Cabri, *Canadian Institute of Mining, Metallurgy and Petroleum, Special Volume* **54:** 431-458, pp.

Barnes, S.J., and Roeder, P.L., (2001). The range of spinel compositions in terrestrial mafic and ultramafic rocks. *Journal of Petrology*. **42**(12): 2279-2302, pp.

Barnes, S.J., van Achterbergh, E., Makovicky, M., Rose-Hansen, J., and Karup-Moller, S., (1997). Partition coefficient for Ni, Cu, Pd, Pt, Rh and Ir between monosulphide solid solution and sulphide liquid and the formation of compositionally zoned Ni-Cu sulphide bodies by fractional crystallization of sulphide liquid. *Canadian Journal, Earth Scienc*e. **34:** 366-374, pp.

Barnes, S.J., (1993). Partitioning of the platinum group elements and gold between silicate and sulphide magmas in the Munni Munni Complex, Western Australia. *Geochima Cosmochemica Acta*. **57:** 1277-1290, pp.

Barnes, S.J., Naldrett, A.J., Gorton, M.P., (1985). The origin of the fractionation of platinum group elements in terrestrial magmas. *Chemical Geolology*. **53:** 303-323, pp.

Becker, M., Harris, P.J., Wiese, J.G. and Bradshaw, D.J. (2009). Mineralogical characterisation of naturally floatable gangue in the Merensky Reef ore floatation. *International Journal of Mineral Processing*. **93:** 246-255, pp.

Beniscelli, J., (2011). Geometallurgy-Fifteen Years of Developments in Codelco: Pedro Carrasco Contributions. In: *The First AusIMMInternational Geometallurgy Conference* 2011, 5 - 7 September 2011, Brismane, Australia, 3-7, pp.

Bezmen, N.I., Asif, M., Brugmann, G.E., Romanenko, I.M., and Naldrett, A.J., (1994). Distribution of Pd, Rh, Ru, Ir, Os and Au between sulphide and silicate metals. *Geochima Cosmochemica Acta*. **58:** 1251-1260, pp.

Boissonnas, J., and Omenetto, P., (1998). Mineral Deposits within the European Community. Berlin Heidelberg New York: *Springer Verelag*. 120-200, pp.

Boudreau, A.E., and McCallum, I.S., (1992). Infiltration metasomatism in layered intrusions – An example from the Stillwater Complex, Montana. *Journal Volcanology and Geothermal Research*. **52:** 171-183, pp.

Boudreau, A.E., Meurer, W.P., (1999). Chromatographic separation of the platinum group elements, gold, base metals and sulphur during degassing of a compacting and solidifying igneous crystal pile. *Contributions to Mineral Petrology*. **134:** 174-185, pp.

Boudreau, A.E., (1992). Volatile fluid over pressure in layered intrusions and formation of potholes. *Australian Journal of Earth Sciences*. **39:** 277-287, pp.

Boudreau, A.E., Mathez, E.A., and McCallum, I.S., (1986). Halogen geochemistry of the Stillwater and Bushveld Complexes: evidence for transport of the platinum-group elements by Cl-rich fluids. *Journal of Petrology*. **27:** 967-986, pp.

Bradshaw, D. J., Buswell, A.M., Harrison, P.J., and Ekmekci. Z., (2006). Interactive effects of the type of milling media and copper sulphate addition on the flotation performance of sulphide minerals from the ore part 1: Pulp chemistry. *International Journal of Mineral Processing*. **78:** 153-163, pp.

Brenan, J.M., (2008). The platinum-group elements: Admirably adapted for science and industry. *Platinum-Group Elements*.**4:** 227-232 pp.

Brynard, H.J., De Villiers, J.P., and Viljoen, E.A., (1976). A mineralogical investigation of the Merensky Reef at the Western Platinum Mine, near Marikana, South Africa. *Economic Geology*.**71:** 1299-1307, pp.

Buchanan, D.L., (1988). *Platinum-group-element exploration*. Elsevier Science Publisher B.V., Amsterdam, 185, pp.

Buswell, A.M., and Nicol, M.J., (2002). Some aspects of the electrochemistry of the flotation of pyrrhotite. *Journal of Applied Electrochemistry*. **32:** 1321-1329, pp.

Cabri, L.J., Kojonen, K., Gervilla, F., Oberthur, T., Weiser, T., Jahanson, B., Sie, S.H., Campbell, J.L., Teesdale, W.J., and Laflamme, J.H.G., (2002). Comparison of Platinum group element trace analyses of pentlandite and some arsenides and sulpharsenides by *EPMA and Micro-PIXE; 9th International Platinum Symposium*, Billings, Montana, 21-25 July 2002, 73-80, pp.

Cabri, L.J., Balnk, H., El Goresy, A., Laflamme, J.H.G., Nobiling, R., Sizgoric, M.B., and Traxel, K., (1984). Quantitative trace-element analyses of sulphides from Sudbury and Stillwater Complex by Proton Microprobe. *Canadian Mineralogist*. **22:** 521-542, pp.

Cabri, L.J., (1981). Platinum-group elements: Mineralogy, geology, recovery: Montreal, *Canadian Institute of Mining and Metallurgy Special Volume*. **23:** 267, pp.

Cabri, L.J., and Laflamme, J.H.G., (1981) Analyses of minerals containing platinum-group elements. In: Cabri, L.J., (ed.) Platinum-Group Elements: Mineralogy, Geology, Recovery. *Canadian Institute of Mining and Metallurgy Special Volume*. **23:** 151-173, pp.

Cameron, E.N., (1980). Evolution of the Lower Critical Zone, central sector, Eastern Bushveld Complex and its chromite deposits. *Economic Geology*. **75:** 845-871, pp.

Cameron, E.N., (1982). The Upper Critical Zone of the Eastern Bushveld Complex, precursor of the Merensky Reef. *Economic Geology*. **77:** 1307-1327, pp.

Campbell, I.H., Naldrett, A.J., and Barnes, S.J., (1983). A model for the origin of the platinum-rich sulphide horizons in the Bushveld and Stillwater Complexes. *Journal of Petrology*. **24:** 133-165, pp.

Campbell, I.H., and Barnes, S.J., (1984). A model for platinum-group elements in magmatic sulphides deposits. *Canadian Mineralogist*. **22:** 151-160, pp.

Campbell, I.H., and Naldrett, A.J., (1979). The influence of silicate: sulphide ratios on the geochemistry of magmatic sulphides. *Economic Geology*. **74:** 1503-1505, pp.

Cawthorn, R.G., (2015). A Review of the Bushveld Complex and its mineralization. In: Hammond, N.Q., and Hatton C., (Eds.). Platinum Group Element (PGE) mineralization and resources of the Bushveld Complex, South Africa. *Mineral Resources Series 2, Council for Geoscience.* Pretoria. 46-53, pp.

Cawthorn, R.G., (2010). The Platinum Group Element Deposits of the Bushveld Complex in South Africa. *Platinum Metals Reviews.* **54** (4): 205-215, pp.

Cawthorn, R.G., Barnes, S.J., Ballhaus, C., and Malitch, K.N., (2005). Platinum Group Element, Chromium, and Vanadium deposits in mafic and ultramafic rocks. *Economic Geology 100th Annivarsary Volume*: 215-249, pp.

Cawthorn, R.G., Eales, H.V., Walraven, F., Uken, R., and Watkeys, M.K., (2006b). The Bushveld Complex in the Geology of South Africa edited by Johnson, M.R., Anhaeusser, C.R., and Thomas, R.J. *Geological Society of South Africa.*

Cawthorn, R.G., and Boerst, K., (2006). Origin of the Pegmatitic Pyroxenite in the Merensky Unit, Bushveld Complex, South Africa. *Journal of Petrology.* **47**(8): 1509-1530, pp.

Cawthorn, R.G., Eales, H.V., Walraven, F., Uken, R. and Watkeys, M.K., (2006a). The Bushveld Complex. In: Johnson, M.R., Anhaeusser, C.R and Thomas, R.J. (Eds.). The Geology of South Africa. Geological Society of South Africa/Council for Geoscience Publication, 261-282, pp.

Cawthorn, R.G., Merkle, R.K.W., and Wiljoen, M.J., (2002b). Platinum Group Element deposits in the Bushveld Complex, South Africa. In: Cabri, L.J., (Ed), The Geology, Geochemistry, Mineralogy and Beneficiation of Platinum Group Elements. *Canadian Institute of Mining, Metallurgy and Petroleum, Special Volume.* **54:** 389-430, pp.

Cawthorn, R.G., Lee, C.A., Schouwstra, R.P., and Mellowship, P., (2002a). Relationship between Platinum Group Elements and Platinum Group Minerals in the Bushveld Complex. *Canadian Mineralogist.* **40:** 311-328, pp.

Cawthorn, R.G., (1999). The platinum group element mineralization in the Bushveld Complex- a critical reassessment of geochemical models. *South African Journal of Geology.* **102** (3): 268-281, pp.

Chetty, D., Gryffernberg, L., Lekgetho, T.B., and Molebale, I.J., (2009). Automated SEM study of PGM distribution across a UG-2 flotation concentrate bank: implications for understanding PGM floatability. *The Journal of the Southern African Institute of Mining and Metallurgy.***109:** 587-593, pp.

Cheney, E.S., Twist, D., (1991). The conformable emplacement of the Bushveld mafic rocks along a regional unconformity in the Transvaal succession of South Africa. *Precambrian Research.* **52:** 115-132, pp.

Coetzee, L.L., Theron, S.J., Martin, G.J., Vander Merwe, J.D., and Stanek, T.A., (2011). Modern gold Deportments and its Application to Industry. *Minerals Engineering.***24:** 565-575, pp.

Consultation in terms of section 40 of the Mineral and Petroleum Resources Development Act 2002, (Act 28 of 2002) For the Scoping Report in respect of the farm Onverwacht 292 KT, situated in the Magisterial District of Sekhukhune, Limpopo Region. Reference number, 6/2/477, 25 August 2008. [Accessed date: 14 May 2015].

Cousins, C.A., and Kinloch, E.D., (1976). Some observations on textures and inclusions in alluvial platinoids. *Economic Geology.***71:** 1377-1398, pp.

Craig, J. R., and Vaughan, D.J., (1994). Ore Microscopy and Ore Petrography. Second Edition. Wiley-Interscience. New York. 164-193, pp.

Cramer, L.A., (2001). The Extractive Metallurgy of South Africa's Platinum Ores. *Journal of Mineralogy.* **53** (10), 14-18, pp.

Crocket, J.H., Teruta, Y. And Garth, J., (1976). The relative importance of Sulphides, Spinels and Platinoid Minerals as Carriers of Pt, Pd, Ir and Au in the Merensky Reef Western Platinum Limited, near Marikana, South Africa. *Economic Geology.* **71:** 1308-1323, pp.

Dare, S.A.S., Barnes, S.J., Pritchard, H.M., Fisher, P.C., (2010b). The timing and formation of platinum group minerals from the Creighton NI-Cu-PGE sulphide deposit. Sudbury, Canada – early crystallization of PGE-rich sulpharsenides. *Economic Geology.* **105:** 1071-1096.

Dare, S.A.S., Barnes, S.J., Pritchard, H.M., (2010a). The distribution of platinum group elements and other chalcophile elements among sulphides from Creighton Ni-Cu-PGE sulphide deposit. Sudbury and the origin of palladium in pentlandite. *Mineral Deposita.* **45:** 765-793, pp.

Davey, S.R., (1992). Lateral variations within the Upper Critical Zone of the Bushveld Complex on the farm Rooikoppies 297 JQ, Marikana, South Africa. *South African Journal of Geology*. **95:** 141-149, pp.

De Beer, J.H., Meyer, R., Hattingh, P.J., (1987). *Geoelectrical and Paleomagnetic studies of the Bushveld Complex.* In: Proterozoic Lithosphere Evolution American Geophysical Union Geodynamics. Edited by A Kroner, 191-205, pp.

Du Plessis, A., and Kleywegt, R.J., (1987). A dipping sheet model for the mafic lobes of the Bushveld Complex. *South African Journal of Geology.* **90:** 1-6, pp.

Dzvinamurungu, T., Viljoen, K.S., Knoper, M.W. and Mulaba-Bafubiandi, A., (2013). Geometallurgical characterization of Merensky Reef and UG-2 at the Marikana Mine, Bushveld Complex, South Africa. *Minerals Engineering.* **52:** 74-81, pp.

Eales H.V., and Cawthorn R.G., (1996). The Bushveld Complex. In: Cawthorn, R.G., (Ed). Layered Intrusions. Elsevier, Amsterdam.181-229, pp.

Eales, H.V., and Reynolds, I.M., (1986). Cryptic Variations within Chromitite of the Upper Critical Zone, North western Bushveld Complex. *Economic Geology*. **81:** 1056-1066, pp.

Eales, H.V., Teigler, B., and Maier, W.D., (1993). Cryptic variations of minor elements Al, Cr, Ti, and Mn in the Lower and Critical Zone orthopyroxenes of the Western Bushveld Complex. *Mineralogical Magazine*. **57:** 257-264, pp.

Fandrich, R., Gu, Y., Burrows, D. and Moeller, K., (2007). Modern SEM-based mineral liberation analysis. *International Journal of Mineral Processing.* **84:** 310-320, pp.

Fleet, M.E., Chryssoulis, S.L., Stone, W.E., and Weiisner, C.G., (1993). Partitioning of platinum group elements and Au in the Fe-Ni-Cu-S system: Experiments on the fractional crystallization of the sulphide melt. *Contributions to Mineralogy and Petrology.* **115:** 36-44, pp.

Godel, B., (2015). *Platinum Group Element Deposits: Recent Advances in the Understanding of the Ore Forming Processes.* In: Charlier, C., Namur, O., Latypov, R., and Tegner, C., (Eds.). Layered Intrusions. Springer Science + Business Media Dordrecht. 379-342, pp.

Godel, B., Barnes, S.J., and Maier, W.D., (2007). Platinum-Group Elements in Sulphide Minerals, Platinum-Group Minerals, and Whole-Rocks of the Merensky Reef (Bushveld Complex, South Africa): Implications for the Formation of the Reef. *Journal of Petrology*: **48** (8): 1569-1604, pp.

Goodall, W.R., Scales, P.J., and Butcher, A.R., (2005). The use of QEMSCAN and diagnostic leaching in the characterization of visible gold in complex ores. *Minerals Engineering.* **18:** 877-886, pp.

Gottlieb, P., Wilkie, G., Sutherland, D., Ho-Tun, E., Suthers, S., Perera, K., Jenkins, B., Spencer, S., Butcher, A. and Rayner, J., (2000). Using Qualitative Electron Microscopy for Process Mineralogy Applications. *Journal of Mineralogy.* **52** (4): 24-25, pp.

Gregory, M.J., Lang, J.R., Gilbert, S. and Hoal, K.O., (2013). Geometallurgy of the Pebble porphyry copper-gold-molybdenum of the deposit, Alaska: Implications for gold distribution and paragenesis. *Economic Geology*: **108:** 463-482, pp.

Gu, Y., (2003). Automated Scanning Electron Microscope Based Mineral Liberation Analysis. *Journal of Minerals and Materials Characterization and Engineering.* **2**(1): 33-41, pp.

Harmer, R.E., Armstrong, R. A., (2000). *Duration of Bushveld Complex (seno lato) magmatism: Constraints from new SHRIMP zircon chronology.* Abstracts and program, Workshop on the Bushveld Complex, Gethane Lodge, Burgersfort.

Harmer, R.E., and Farrow, D., (1995). An isotopic study on the volcanics of the Rooiberg Group: age implications and a potential exploration tool. *Mineralium Deposita.* **30:** 188-195, pp.

Harris, C., Pronost, J.J.M., Ashwal, L.D., and Cawthorn, G., (2005). Oxygen and hydrogen Isotope Stratigraphy of the Rustenburg Layered Suite, Bushveld Complex: Constraints on Crustal Contamination. *Journal of Petrology.* **46** (3): 579-601, pp.

Hatton, C.J., Schweitzer, J.K., (1995). Evidence for synchronous extrusive and intrusive Bushveld Complex. *Canadian Mineralogist.* **17:** 579-594, pp.

Hatton, C.J., and Von Gruenewaldt, G., (1987). *The Geological setting and Petrogenesis of the Bushveld chromitite layers.* In Stowe, C.W., ed. Evolution of chromium ore fields: New York, van Nostrand Reinhold, 109-143, pp.

Hawley, J.E., (1965). Upside down zoning at Frood. Sudbury, Ontario. *Economic Geology.* **60:** 529-575, pp.

Helmy, H.A., Ballhaus, C., Wohlgemuth-Ueberwassar, C., Fonseca, R.O.C., and Laurenz, V., (2010). Partitioning of Se, As, Sb, Te, and Bi between monosulphide solid solution and sulphide melt-Application to magmatic sulphide deposits. *Geochimica. Cosmochimica Acta.* **74:** 6174-6179, pp.

Helmy, H.A., Ballhaus, C., Berndt, J., Bockrath, C., and Wohlgemuth-Ueberwassar, C., (2007). Formation of Pt, Pd and Ni tellurides: experiments sulphide-telluride systems. *Contributions to Mineralogy and Petrology.* **153:** 577-597, pp.

Hey, P.V., (1999). The effects of weathering on the UG-2 chromitite reef of the Bushveld Complex, with special reference to platinum group minerals. *South African Journal of Geology.* **102:** 251-260, pp.

Hiemstra, S.A., (1979). The Role of collectors in the formation of the platinum deposits of the Bushveld Complex. *Canadian Mineralogist.* **17:** 469-482, pp.

Hiemstra, S.A. (1976). The role of collectors in the formation of the platinum deposits in the Bushveld Complex. *The Canadian Mineralogist.* **17:** 469-482, pp.

Hoal, K.O., Appleby, S.K., Stammer. J.G., and Palmer, C., (2009). SEM-based quantitative mineralogical analysis of peridotite, kimberlite and concentrate. *Lithos.* **112S:** 41-46, pp.

Holwell, D.A., McDonald, I., and Butler, I.B., (2010). Precious metal enrichment in the Platreef, Bushveld Complex, South Africa: evidence from homogenized magmatic sulphide melt inclusions. *Contributions to Mineralogy and Petrology.* DOI 10.1007/s00410-010-0577-0.

Holwell, D.A. and McDonald, I., (2007). Distribution of platinum-group elements in the Patreef at Overysel, northern Bushveld Complex: a combined PGM and LA-ICP-MS study. *Contributions to Mineralogy and Petrology.* **154:** 171-190, pp.

Holwell, D.A., McDonald, I., and Armitage, P.E.B., (2006). Platinum-group mineral assemblages in the Platreef at the South-Central Pit, Sandsloot Mine, Northern Bushveld Complex, South Africa. *Mineralogical Magazine.***70:** 83-101, pp.

Hulbert, L.J., and von Gruenewaldt, G., (1982). Nickel, Copper, and Platinum mineralization in the lower zone of the Bushveld Complex, South of Potgietersrus. *Economic Geology*. **77:** 1296-1306, pp.

Hutchinson, D., and Kinnaird, J.A., (2005). Complex multistage genesis for the Ni-Cu-PGE mineralization in the southern region of the Platreef, Bushveld Complex, South Africa. *Applied Earth Science* (*Transactions of the Institute of Mining and Metallurgy B).***114:** B208-B224, pp.

Jasienak, M., and Smart, R.St.C., (2009). Collectorless flotation of pyroxene in Merensky ore: Residual layer identification using statistical ToF-SIMS analysis. *International Journal of Mineral Processing.* **92:** 169-176, pp.

Jeolusa.com, (n.d.). JEOL USA JXA-8530F HyperProbe Electron Probe Microanalyzer (EPMA). [online] Available at: http://www.jeolusa.com/PRODUCTS/Microprobe and Auger/JXA8530F/tabid/224/Default.aspx [Accessed 25 Feb. 2015].

Junge M., Oberthur, T., and Melcher, F., (2014). Cryptic variation of chromite chemistry, platinum group element and platinum group mineral distribution in the UG-2 chromite: an example from the Karee Mine, western Bushveld Complex, South Africa. *Economic Geology*. **109:** 795-810, pp.

Kingston, G.A., and E1-Dosuky, B.T., (1982). A Contribution on the Platinum Group mineralogy of the Merensky Reef at the Rustenburg Platinum Mine. *Economic Geology.* **77:** 1367-1384, pp.

Kinloch, E.D., and Peyerl, W., (1990). Platinum-Group Minerals in Various Rocks of the Merensky Reef: Genetic Implications. *Economic Geology.* **85:** 537-555, pp.

Kinloch, E.D., (1982). Regional Trends in the Platinum-Group Mineralogy of the Critical Zone of the Bushveld Complex, South Africa. *Economic Geology.***77:** 1328-1347, pp.

Kinnaird, J.A., (2005). The Bushveld Large Igneous Province. Available at: www.largeigneousprovinces.org/LOM.html [Accessed May 2015].

Kleemann, G.J., and Twist, D., (1989). The compositionally zone sheet-like granite pluton of the Bushveld Complex: Evidence bearing on the Nature of A-type magmatism. *Journal of Petrology.* **30:** 1383-1414, pp.

Knight, R., (2014). The primary magmatic concentration and secondary remobilisation of platinum-group elements in Ni-Cu sulphide ores. Doctoral dissertation, Cardiff University. Available online at: http://orca.cf.ac.uk/65680/2/Thesis.pdf [Accessed May 2015].

Kruger, F.J., (1990). The Stratigraphy of the Bushveld Complex: a reappraisal and the relocation of the Main Zone boundaries. *South African Journal of Geology.* **93:** 376-381, pp.

Kruger, F.J., and Marsh, J.S., (1985). The Mineralogy, Petrology and origin of the Merensky Cyclic Unit in the Bushveld Complex. *Economic Geology.* **80:** 958-974, pp.

Lee, C.A., (1996). *A review of Mineralization in the Bushveld Complex and some other layered intrusions.* In: Cawthorn, R.G., (Ed). Layered Intrusions. Elsevier, Amsterdam.103-145, pp.

Lee, C.A., and Sharpe, M.R., (1986). *The structural setting of the Bushveld Complex – An assessment aided by landsat imagery.* In: Anhaeusser, C.R., and Maske, S. (Eds), Mineral Deposits of Southern Africa. Geological Society of South Africa, Johannesburg. 1031-1038, pp.

Lee, C.A., (1983) Trace and platinum group element geochemistry and the development of the Merensky Unit of the western Bushveld Complex. *Mineral Deposit.***18:** 173-190, pp.

Li, C. and Ripley, E.M., (2005). Empirical equations to predict the sulphur content of mafic magmas at sulphide saturation and applications to magmatic sulphide deposits. *Mineralium Deposita.* **40:** 218-230, pp.

Li, C., Ripley, E.M., Merino, E., and Maier, W.D., (2004). Replacement of Base Metal SulphidesSulphidess by Actinolite, Epidote, Calcite and Magnetite in the UG-2 and Merensky Reef of the Bushveld Complex, South Africa. *Economic Geology.* **99:** 173-184, pp.

Li, C., Maier, W.D., and De Waal, S.A., (2001). The role of magma mixing in the genesis of platinum group element mineralization of the Bushveld Complex. Thermodynamic calculation and new interpretations. *Economic Geology.* **96:** 653-662, pp.

Lotter, N.O., (2011). Modern Process Mineralogy: An integrated multi-discipline approach to flowsheeting. *Minerals Engineering.***24:** 1229-1237, pp.

Lotter, N.O., Bradshaw, D.J., Becker, M., Parolis, M.A.S., and Kormos, L.J., (2008). A discussion of the occurrence and undesirable flotation behaviour of orthopyroxene and talc in the processing of mafic deposits. *Minerals Engineering.* **21:** 905-912, pp.

MacKenzie, W.S., Donaldson, C.H., and Guilford, C., (1982). *Atlas of igneous rocks and their textures.* Wiley MU Geology Research, New York, QE461. M219.

Maier, W.D., and Barnes, S.J., (1999). Platinum Group Elements in Silicate Rocks of the Lower, Critical and Main Zones at Union Section, Western Bushveld Complex. *Journal of Petrology.* **40** (11): 1647-1671, pp.

Mathez, E.A., Hunter, R.H, and Kinzler, R., (1997). Petrologic evolution of partially molten cumulate: the Atok section of the Bushveld Complex. *Contributions to Mineralogy and Petrology.* **129:** 20-34, pp.

Mathez, E.A., (1995). Magmatic metasomatism and formation of the Merensky reef, Bushveld Complex. *Contributions to Mineralogy and Petrology.***119:** 277-286, pp.

McLaren, C.H., and De Villiers, J.P.R., (1982). The Platinum Group Chemistry and Mineralogy of the UG-2 Chromitite layer of the Bushved Complex. *Economic Geology.* **77:** 1348-1366, pp.

Merkle, R.K.W., and McKenzie, A.D., (2002). The Mining and Beneficiation of South African PGE Ores - An overview. In: Cabri, L.J. (ed.), The Geology, Geochemistry, Mineralogy and Beneficiation of Platinum-Group Elements. *Canadian Institute of Mining, Metallurgy and Petroleum Special Volume.* **54:** 793-809, pp.

Merkle, R.K.W., (1992). Platinum Group Minerals in the middle group of chromitite layers at Marikana, western Bushveld Complex; Indications for collection mechanisms and postmagmatic modification. *Canadian Journal of Earth Science*. **29:** 209-221, pp.

Mining Technology, (n.d.). Modikwa Platinum Mine. [online] Available at:

http://www.mining-technology.com/projects/modikwa-platinum/ [Accessed April 2015].

Misra, K.C., (2000). *Understood Mineral Deposits.* Kluwer Academic Publishers, Netherlands, 864, pp.

Mitchell, A.A., and Scoon, R.N., (2007). The Merensky Reef at Winnaarshoek, Eastern Bushveld Complex: A Primary Magmatic Hypothesis Based on a wide Reef Facies. *Economic Geology*. **102:** 971-1009, pp.

Mitchell, A.A., (1990). The stratigraphy, petrography and mineralogy of the Main Zone of the north-western Bushveld Complex, South Africa. *Journal of Science*. **93:** 818-831, pp.

Molyneux, T.G., and Klinkert, P.S., (1978). A structural interpretation of parts of the eastern mafic lobe of the Bushveld Complex and its surroundings. *Trans Geological Society of South Africa*. **81:** 359-368, pp.

Molyneux, T.G., (1974). A geological investigation of the Bushveld Complex in Sekhukhuneland and part of the Steelpoort valley. *Transactions of the Geological Society of South Africa.***77:** 329-338, pp.

Mostert, A.B., Hofmeyer, P.K. and Potgieter, G.A., (1982). The Platinum-Group Mineralogy of the Merensky Reef at the Impala Platinum Mines, Bophuthatswana. *Economic Geology.***77:** 1385-1394, pp.

Mungall, J.E., (2005). Magmatic geochemistry of the platinum-group elements; Exploaration for PGE deposits, editor Mungall, J.E., *Mineralogical association of Canada, short coarse series volume*. 35, pp.

Naldrett, A.J., Kinnaird, J., Wilson, A., Chunnett, G., and Yudovskaya, M., (2015). Platinum Group Elements in the Critical Zone of the Bushveld Complex. In: Hammond, N.Q., and Hatton C., (Eds.). Platinum Group Element (PGE) mineralization and resources of the Bushveld Complex, South Africa. *Mineral Resources Series 2, Council for Geoscience.* Pretoria. 123-127, pp.

Naldrett, A.J., (2010). Secular variation of magmatic sulphide deposits and their source magmas. *Economic Geology*. **105**: 669-688, pp.

Naldrett, A.J., Wilson, A., Kinnaird, J., and Chunnett, G., (2009). PGE Tenor and Metal Ratios within and below the Merensky Reef, Bushveld Complex: Implications for its Genesis. *Journal of Petrology.* **50** (4): 625-659, pp.

Naldrett, A.J., Kinnaird, J., Wilson, A., and Chunnett, G., (2008). Concentration of PGE in the Earth's crust with special reference to the Bushveld Complex. *Earth Science Frontiers.***15** (5): 264-297, pp.

Naldrett, A.J., (2004). Magmatic sulphide deposits. Springer, Heidelberg, 728, pp.

Naldrett, A. J., and Lehmann, J., (1988). *Spinel non-stoichiometry as an explanation for Ni-Cu- and PGE-enriched sulphides in chromitites.* In: Pritchard, H. M., Potts, P.J., Bowels, J. F. W. and Cribb, S. J. (Eds.) Geo-Platinum 87. Elsevier, Amsterdam, 113-143, pp.

Naldrett, A.J., (1986). The behaviour of platinum group elements during fractional crystallization and partial melting with special reference to the composition of magmatic sulphide ores. *Forschritte der Mineralogie.* **74:** 113-133, pp

Naldrett, A.J., Innes, D.G., Sowa, J., and Gorton, M.P., (1982). Compositional variation within and between five Sudbury ore deposits. *Economic Geology*. **77:** 1519-1534, pp.

Naldrett, A.J., Hoffman, E.L., Green, AH., Chou, C.L., Naldrett, S.R., and Alcock, R.A., (1979). The composition of Ni-sulphide ores with particular reference to their content of PGE and Au. *Canadian Mineralogist*. **17:** 403-415, pp.

Naldrett, A.J., (1989). Stratiform PGE deposits in layered intrusions. In: Whitney, J.A., and Naldrett, A.J., (eds). Ore deposits associated with Magmas. *Society for Economic Geologists, Reviews in Economic Geology*. **4:** 135-165, pp.

Naldrett, A. J., and von Gruenewaldt, G., (1989). Association of platinum group elements with chromitite in the layered intrusions and ophiolite complexes. *Economic Geology, Vol.***84:** 180-187, pp.

Nex, P.A.M., Cawthorn, R.G., and Kinnaird, J.A., (2002). Geochemical effects of magma addition: compositional reversals and decoupling of trends in the Main Zone of the western Bushveld Complex. *Mineralogical Magazine.***66** (6): 833-856, pp.

Nex, P.A.M., Kinnaird, J.A., Ingle, L.J., Vander Vyver, B.A., and Cawthorn, R.G., (1998). A new stratigraphy for the Main Zone of the Bushveld Complex, in the Rustenburg area. *South African Journal of Science*. **101:** 215-223, pp.

Nicholson, D.M., and Mathez, E.A., (1991). Petrogenesis of the Merensky Reef in the Rusternburg section of the Bushveld Complex. *Contributions to Mineralogy and Petrology*. **107:** 293-309, pp.

Oberthür, T., Weiser, T. W., Gast, L. and Kojonen, K., (2003). Geochemistry and mineralogy of platinum-group elements at Hartley Mine, Zimbabwe. *Mineral Deposita.***38:** 327-343, pp.

Osbahr, I., Klemd, R., Oberthur, Y., Bratz, H. and Schouwstra, R., (2013). Platinum-Group Element Distribution in base-metal sulphides of the Merensky Reef from the eastern and western Bushveld Comlpex. South Africa. *Mineralium Deposita.* **48**(2): 211-232, pp.

Page, N.J., Von Gruenewaldt, G., Haffty, J., and Aruscavage, P.J., (1982). Comparison of platinum, palladium and rhodium distribution in some layered intrusions with special reference to the late differentiates (upper zone) of the Bushveld Complex, South Africa. *Economic Geology*. **77:** 1405-1418, pp.

Penberthy, C.J., Oosthuyzen, E.J., and Merkle, R.K.W., (2002). The Recovery of Platinum Group Elements from the UG-2 chromitite, Bushveld Complex – A mineralogical perspective. *Mineralogy and Petrology*. **68:** 213-222, pp.

Penberthy, C.J., Oosthuyzen, E.J., and Merkle, R.K.W. (2000). The Recovery of Platinum Group Elements from the UG-2 chromitite, Bushveld Complex – A mineralogical perspective. *Mineralogy and Petrology*. **68:** 213-222, pp.

Penberthy, C.J., and Merkle, R.K.W., (1999). Lateral variations in the Platinum group element and mineralogy of the UG-2 chromitite layer, Bushveld Complex Complex. *South African Journal of Geology*. **102**: 240-250, pp.

Peregoedova, A., Barnes, S.-J., Barker. D.R., (2004). The formation of Pt-Ir-alloys and Cu-Pdrich sulphide melts by partial desulphurization of Fe-Ni-Cu sulphide: results of experiments and implications for natural system. *Chemical Geology*. **208**: 247-264, pp.

Petruk, W. (2000). *Applied mineralogy in the mining industry*. Elsevier, Amsterdam, 268, pp.

Philander, C., and Rozendaal, A., (2011). The contributions of geometallurgy to recovery of lithified heavy mineral resources at the Namaqua Sands Mines, West Coast of South Africa. *Minerals Engineering.***24:** 1357-1364, pp.

Pillay, K., Becker, M., Chetty, D., and Thiele, H., (2011). *The effect of gangue mineralogy on the density separation of low grade nickel ore.* Southern African Base Metals Conference, Mintek. The Southern African Institute of Mining and Metallurgy, 493-510, pp.

Pritchard, H.M., Barnes, S.J., Maier, W.D., and Fisher, P.C., (2004). Variations in the Nature of the Platinum –Group Minerals in a Cross-Section through the Merensky Reef at Impala Platinum: Implications for the Mode of Formation of the Reef. *The Canadian Mineralogist.* **42:** 423-437, pp.

Rose, D., Viljoen, F., Knoper, M. and Rajesh, H., (2011). Detailed assessment of platinum-group minerals associated with chromitite stringers in the Merensky Reef of the eastern Bushveld Complex, South Africa. *The Canadian Mineralogist.* **49:** 1385-1396, pp.

SACS (South African Committee for Stratigraphy)., (1980). Stratigraphy of South Africa. Part 1 (Kent, L.E., Comp) Lithostratigraphy of the Republic of South Africa, Southwest Africa/Namibia, and the Republics of Bophuthatswana, Trankie and Venda. *Handbook of the Geological Survey of South Africa.* 8, pp.

Seabrook, C.L., Cawthorn, R.G. and Kruger, F.J., 2005. The Merensky, Bushveld Complex: mixing of minerals, not mixing magma. *Economic Geology*, **100:** 1191-1206, pp.

Schouwstra, R. P., and Smit, A. J., (2011). Developments in Mineralogical Techniques-What about Mineralogists? *Minerals Engineering.* **24:** 1224-1228, pp.

Schouwstra, R. P., De Vaux, D., Hey, P., Malysiak, V., Shackleton, N. and Bramdeo, S. (2010). Understanding Gamsberg- A geometallurgical Study of a Large Stratifom Zinc Deposit. *Minerals Engineering.* **23** (11-13): 960-967, pp.

Schouwstra, R.P., Lee, C.A., and Kinloch, E.D., (2000). A short Geological Review of the Bushveld Complex. *Platinum Metals review*. **44** (1): 33-39, pp.

Schwellnus, J.S.I., Hiemstra, S.A. and Gasparrin, E. (1976). The Merensky Reef at Atok Platinum Mine and its Environs. *Economic Geology.***71:** 249-260, pp.

Scoon, R.N., and Mitchell, A.A., (2004b). Petrogenesis of discordant magnesian dunites from the central sector of the eastern Bushveld Complex with emphasis on the Winnaarshoek pipe and disruption of the Merensky Reef. *Economic Geology.* **99:** 517-541, pp.

Scoon R.N., and Mitchell A.A., (2004a). The platiniferous dunite pipes in the eastern limb of the Bushveld Complex: review and comparison with unmineralised discordant ultramafic bodies. *South African Journal of Geology.* **107:** 505-520, pp.

Scoon, R.N., and Teigler, B., (1994). Platinum Group Element mineralization in the Critical Zone of the Bushveld Complex. I. Sulphide-poor chromitites below the UG-2. *Economic Geology.* **89:** 1094-1121, pp.

Scoon, R.N., and De Klerk, W.J., (1987). The relationship of olivine cumulates and mineralization to cyclic units in parts of the Upper Critical Zone of the western Bushveld Complex. *The Canadian Mineralogist.* **25:** 51-77, pp.

SGS Minerals Services, Technical Paper 2002-03.

Sharpe, M.R., and Hulbert, L.J., (1985). Ultramafic Sills beneath the eastern Bushveld Complex: Mobilized suspensions of early Lower Zone Cumulates in a parental Magama with boninitic Affinities. *Economic Geology.* **80:** 849-871, pp.

Smith, A.J.B., (2013) The Geometallurgical characterization of the Merensky Reef at Bafokeng Rasimone Platinum Mine, South Africa. PhD (Geology) University of Johannesburg. Available at: https://ujdigispace.uj.ac.za [Accessed May 2015].

Spry, P.G., and Gedlinske, B.L., (1987), Tables for the determination of common opaque minerals, *Economic Geology Pub*.

Teigler, B., and Eales, H.V., (1993). Correlation between chromite composition and PGE mineralization in the Critical Zone of the Bushveld Complex. *Mineralium Deposita.***28:** 291-302, pp.

Tredoux, M., Lindsay, N.M., Davies, G., and McDonald, I., (1995). The fractionation of platinum-group elements in magmatic systems, with the suggestion of a novel casual mechanism. *South African Journal of Geology.* **98:**157-167, pp.

Two Rivers Trial Mining Report., (2003). Unpublished Company Report.

Van de Merwe, M.J., (2007). The occurrence of the critical zone along the exposed southern sector of the Eastern Bushveld Complex. *South African Journal of Geology.* **110:** 617-630, pp.

Van der Merwe, M.J., (1978). The geology of the basic and ultramafic rocks of the Potgietersrus limb of the Bushveld Complex. Phd Thesis, University of the Witwatersrand, Johannesburg, unpublished.

Van der Merwe, M.J., (1976). The Layered sequence of the Potgietersrus limb of the Bushveld Complex. *Economic Geology.***71:** 1337-1351, pp.

Vermaak, C.F., (1995). The Platinum group metals - a global perspective. *Council for Mineral Technology*. Randburg, 118, pp.

Vermaak, C.F., (1985). The UG-2 layer-South Africa's slumbering chromitite giant. *Chromium Review*. **5:** 9-23, pp.

Vermaak, C.F., and Hendriks, L.P., (1976). A Review of the Mineralogy of the Merensky Reef with Specific references to New Data on the Precious Metal Mineralogy. *Economic Geology.***71:** 1244-1269, pp.

Viljoen, F., Knoper, M., Rajesh, H., Rose D., and Geef, T., (2012). Application of a field emission mineral liberation analyser to the in-situ study of Platinum Group Element mineralization in the Merensky Reef of the Bushveld Complex, South Africa. *Proceedings of the 10th International Congress for Applied Mineralogy (ICAM)*. 757-764, pp. Springer Berlin Heidelber.

Viljoen, M.J, Schurmann L.W., (1998). Platinum group metals. In: Wilson MGC, Anhaeusser C.R., (eds) The Mineral Resources of South Africa. *Council for Geoscience*, Pretoria, 532-568, pp.

Viljoen, M.J., and Scoon, R.N., (1985). The Distribution and Main Geologic Features of Discordant Bodies of Iron-Rich Ultramafic Pegmatite in the Bushveld Complex. *Economic Geology*. **80:** 1109-1128, pp.

Von Gruenewaldt, G., Dicks, D., de Wet, J., and Horsch, H., (1990). PGE mineralization in the Western Sector of the Eastern Bushveld Complex. *Mineralogy and Petrology*.**42:** 71-95, pp.

Von Gruenewaldt, G., Hulbert, L.J. and Naldrett, A.J., (1989). Contrasting Platinum group element concentration patterns in cumulates of the Bushveld Complex. *Mineralium Deposita*. **24:** 219-229, pp.

Von Gruenewaldt, G., Hatton, C.J., Merkle, R.K.W., and Gain, S.B., (1986). Platinum-Group Elements-Chromitite Associations in the Bushveld complex. *Economic Geology*. **81:** 1067-1079, pp.

Von Gruenewaldt, G., Sharpe, M.R., and Hatton, C.J., (1985). The Bushveld Complex: Introduction and Review. *Economic Geology*. **80:** 803-812, pp.

Von Gruenewaldt, G., (1979). A Review of Some Recent Concepts of the Bushveld Complex, with Particular reference to Sulphide Mineralization. *The Canadian Mineralogist*. **17:** 233-256, pp.

Von Gruenewaldt, G., (1977). The mineral resources of the Bushveld Complex. *Mineral Science Engineering*. **9:** 83-95, pp.

Wagner, L.R., and Brown, G.M., (1968). *Layered Igneous Rocks*. Oliver and Boyd, Edinburgh, 588, pp.

Wagner, P.A., (1929). *Platinum Deposits and Mines of South Africa*. Strulk, Cape Town, 383, pp.

Walraven, F., (1997). Geochronology of the Rooiberg Group, Transvaal Supergroup, South Africa: University of Witwatersrand, *Economic Geology Research Unit Information Circular, number* **316:** 21, pp.

White, J.A., (1994). The Potgietersrus prospect geology and exploration history. In: Anhaeusser, C.R. (ed.), Proceedings XVth CMMI Congress. Geology. *Southern African Institute of Mining and Metallurgy*. **3:** 173-181, pp.

Willmore, C.C., Boudreau, A.E., and Kruger, F.J., (2000). The halogen geochemistry of the Bushveld Complex, Republic of South Africa: Implications for chalcophile element distribution in the Lower and Critical Zones. *Journal of Petrology*. **41:** 1517-1539, pp.

Willemse, J., (1969). The Geology of the Bushveld Complex, the Largest Repository of Magmatic Ore Deposits in the World. *Economic Geology Monograph.***4:** 1-22, pp.

Wilson, A.H., and Chunnett, G., (2006). Trace Element and Platinum Group Element Distributions and the Genesis of the Merensky Reef, western Bushveld Complex, South Africa. *Journal of Petrology*. **47:** 2369-2403, pp.

Wilson, A. H., Jermy, C.A., Ridgeway, M., and Chunnett, G., (2005). Rock-strength and physical properties of norites of the Merensky Reef and Bastard unit, western Bushveld Complex. South African. *Journal of Geology*. **708:** 525-540, pp.

Wilson, A.H., Lee, C.A., and Brown, R.T., (1999). Geochemistry of the Merensky Reef, Rustenburg section, Bushveld Complex: controls on the silicate framework and distribution of trace elements. *Mineralium Deposita*. **34:** 657-672, pp.

Wiese, J. G., Becker, M., Bradshaw, D.J., and P. J., Harris (2006). Interpreting the role of reagents in the floatation of platinum bearing Merensky ores. International Platinum Conference 'Platinum Surges Ahead', The Southern African Institute of Mining and Metallurgy, 175-180, pp.

Wiese, J., Harris, P. and Bradshaw, D., (2007a). The response of sulphide and gangue minerals in selected Merensky ores to increased depressant dosages. *Minerals Engineering*.**20:** 986-995, pp.

Wiese, J., Harris, P. and Bradshaw, D., (2005a). Investigation of the role and interactions of a dithiophosphate collector in the flotation of sulphides from the Merensky Reef. *Minerals Engineering*. **18:** 791-800, pp.

Xiao, Z and Laplante, A.R., (2004): Characterizing and recovering the platinum group minerals-a review. *Minerals Engineering*. **17:** 961-979, pp.

Yang, X. Z., Matsueda, H., Yui, S., and Dong, X.Y., (1992). Chemical Compositions and Paragenesis of the Platinum-group Element Minerals in the Jinchuan Sulfide Deposit, Gansu Province, China. *Journal of the Faculty of Science*, [online] Vol.XXIII (No. 2), pp.287-298. Available at: http://eprints.lib.hokudai.ac.jp/dspace/bitstream/2115/.../1/23-2_p287-299.pdf [Accessed February 2016].

Zientek, M. L., Cooper, R. W., Corson, S.R. and Geraghty, E.P., (2002). Platinum-group element mineralization in the Stillwater Complex, Montana. In: Cabri, L. J., (Ed.) Geology, Geochemistry, Mineralogy and Mineral Beneficiation of platinum-group element. *Canadian Institute of Mining, Metallurgy and Petroleum, Special Volume* **54:** 459-481, pp.